The influence of potassium and calcium species on the swelling and reactivity of a high-swelling South African coal

AC Collins

20271387

Dissertation submitted in partial fulfilment of the requirements for the degree *Magister Scientiae* in Chemistry at the Potchefstroom Campus of the North-West University

Supervisor: Prof CA Strydom

Co-supervisor: Prof JR Bunt

May 2014

It all starts here ™

NORTH-WEST UNIVERSITY
YUNIBESITI YA BOKONE-BOPHIRIMA
NOORDWES-UNIVERSITEIT ®

Abstract

Alkali compounds were added to a South African coal with a high swelling propensity and the behaviour of the blends were investigated. A vitrinite-rich bituminous coal from the Tshikondeni coal mine in the Limpopo province of South Africa was used. To reduce the influence of the minerals in the coal, the coal was partially demineralized by leaching with HCl and HF. The ash content of the coal sample was successfully reduced from 17.7% to 0.6%. KOH, KCl, K_2CO_3 and KCH_3CO_2 were then added to the demineralized coal in mass percentages of 1%, 4%, 5% and 10%. The free swelling indices (FSI) of the blends were determined and the samples were subjected to acquisition of TMA and TG-MS data. Addition of these potassium compounds to the demineralized coal reduced the swelling of the vitrinite-rich coal. From the free swelling indices of the various mixtures, it was concluded that the potassium compounds reduce the swelling of the coal in the following order of decreasing impact: KCH_3CO_2 > KOH > K_2CO_3 > KCl. From dilatometry experiments done on the blends with the 10% addition of potassium compounds, it was seen that with the addition of potassium compounds to the demineralized coal, a reduction in dilatation volume was obtained. The influence of the potassium compound in decreasing order: K_2CO_3> KOH> KCH_3CO_2> KCl. An increase in the softening temperature was observed for the demineralized coal-alkali blends. Thermogravimetric analyses were performed on the demineralized coal-potassium blended samples (<75 µm). These samples were pyrolyzed under a nitrogen atmosphere to a maximum temperature of 1200 °C using a heating rate of 10 °C/min. The relative reactivity for each of the blends with the different wt% addition was determined. From these results it was seen that KCH_3CO_2 increased the relative reactivity, whereas the KOH, KCl and K_2CO_3 showed an inhibiting influence. The attached mass spectrometer provided information on the low molecular mass gaseous products formed in the various temperature ranges as the thermal treatment proceeded. From the mass spectroscopy results, it was found that the potassium compounds decreased the temperature at which maximum evolution of H_2 takes place. Thermomechanical analyses were performed on the 10 wt% addition of the potassium compounds to the demineralized coal. During TMA analyses, the sample was heated to 1000 °C using a heating rate of 10 °C/min. From the TMA result obtained it was clear that the addition of KCl did not have an influence on the swelling of the demineralized coal. All results are discussed.

Keywords: South African coal, swelling, dilatometry, TMA, plastic properties, pyrolysis, potassium compounds

Uittreksel

Alkali verbindings is by ’n Suid-Afrikaanse steenkool met ’n hoë swelling geneigdheid gevoeg om die gedrag van die mengsels is ondersoek. ’n Vitriniet-ryke bitumineuse steenkool van die Tshikondeni steenkoolmyn in die Limpopo provinsie van Suid Afrika is gebruik. Om die invloed van minerale in die steenkool te verminder, is die steenkool gedemineraliseer met behulp van ’n uitlogingsproses met HCl en HF. Die mineraalinhoud van die steenkool is verminder van 17.7% na 0.6%. KOH, KCl, K_2CO_3 en KCH_3CO_2 is by die gedemineraliseerde steenkool in massapersentasies van 1%, 4%, 5% en 10% gevoeg. Die vry swellingsindeks (FSI) van die mengsels is bepaal en die monsters is onderwerp aan TMA en TG-MS eksperimente. Toevoeging van hierdie kaliumverbindings by die gedemineraliseerde steenkool, het ’n vermindering in die swelling van die vitriniet-ryke steenkool meegebring. Vanaf die vry swellingsindeks vir die verskillende mengsels, is daar tot die gevolgtrekking gekom dat die kaliumverbindings die swelling van die steenkool verminder in die volgende volgorde van dalende impak: KCH_3CO_2> KOH> K_2CO_3> KCl. Uit dilatometrie eksperimente gedoen op die mengsels met die 10% byvoeging van die kaliumverbindings, is gesien dat die byvoeging van hierdie verbindings tot die gedemineraliseerde steenkool ’n vermindering in die dilaterende volume laat plaasvind. Die invloed van die kaliumverbindings of die dilaterende volume in volgorde van dalende impak: K_2CO_3> KOH> KCH_3CO_2> KCl. ’n Verhoging in smeltings temperatuur is waargeneem vir die monsters met die kaliumverbindings teenwoordig. Termogravimetriese analises is uitgevoer op die gedemineraliseerde steenkool-kalium mengsels (<75 mm). Pirolise van die monsters het geskied onder ’n stikstof atmosfeer en die monsters is verhit tot ’n maksimum temperatuur van 1200 °C teen ’n verhittingstempo van 10 °C/min. Die relatiewe reaktiwiteit vir elk van die mengsels met die verskillende massa persentasie kalium byvoeging was bepaal. Vanuit die resultate kan gesien word dat die KCH_3CO_2 ’n verhoging veroorsaak, maar die KOH, KCl en K_2CO_3 ’n inhiberende invloed op die reaktiwiteit het. Die massaspektrometer gekoppel aan die termogravimetriese analiseerder verskaf inligting rakende die lae molekulêre massa gasprodukte wat gevorm word oor die temperatuur gebiede, gedurende die verhittingsproses. Vanuit die resultate verkry deur massa spektrometer, kan gesien word dat die ewolusie temperatuur van H_2 afneem met die toevoeging van die kaliumverbindings. Termomeganiese ontledings analises (TMA) is uitgevoer op die mengsels met die 10% kaliumverbinding byvoegings tot die gedemineraliseerde steenkool. Tydens die analise metode is die monsters verhit tot ’n temperatuur van 1000 °C teen ’n verhittingstempo van 10 °C/min. Vanuit die TMA resultate kan gesien word dat die KCl geen invloed op die swelling

van die steenkool gehad het nie, en dat die ander kaliumverbindings wel die swelling verlaag het. Alle resultate word bespreek.

Kernwoorde: Suid-Afrikaanse steenkool, swelling, dilatometrie, TMA, plastiese eienskappe, pirolise, kalium verbindings

Acknowledgements

I would like to acknowledge a few people who, in various ways contributed to the completion of this study.

- My heavenly Father for all of his blessings and the opportunity, courage, determination and strength throughout my studies;
- My project supervisors Prof CA Strydom and Prof JR Bunt for all their patience, guidance and assistance. Without their help this study would not have come to completion;
- The financial support I received from my supervisors;
- The North-West University, Sasol Technology (Pty) Ltd and the South African Research Chairs Initiative of the Department of Science and Technology and National Research Foundation of South Africa for financially supporting the research;
- Mr. Ernst Kleynhans and Mr. Lay Shoko for their assistance with the thermomechanical analysis.
- Mr. Gregory Okolo for his help and assistance with the BET CO_2 surface area experiments;
- Mr. Zach Sehume for his assistance and suggestions during the thermogravimetric experimentation;
- To all my friends, for their support and encouragement during the difficult times.
- And lastly my family, for their love, patience and support.

Index

Abstract	i
Uittreksel	ii
Acknowledgements	iv
Index	v
List of Figures	ix
List of Tables	xii
List of Abbreviations	xv
1. Introduction	1
1.1 Problem Statement and Substantiation	1
1.2 Hypothesis	3
1.3 Aims and Objectives	3
1.4 Method of Investigation	4
2. Literature Review	6
2.1 Introduction to coal	6
2.2 Coal processes	8
2.2.1 Pyrolysis	8
2.2.2 Gasification	11
2.2.3 Combustion	11
2.3 Important properties of coal	11
2.3.1 Swelling	11
2.3.2 Plasticity	12
2.3.3 Proposed Mechanisms during coal swelling	13
2.4 Swelling coals	15
2.5 Methods used to decrease swelling	15
2.5.1 Addition of Catalysts	15
2.5.2 Types of catalysts	16
2.5.3 Influence on coal reactivity	18
2.5.4 Catalytic mechanisms	18
3. Experimental Techniques	19
3.1 Free Swelling Index	20

3.2 Ultimate and Proximate Analysis 21
3.2.1 Ultimate Analysis 21
3.2.2 Proximate Analysis 21
3.3 Ash Fusion Temperature 22
3.4 X-Ray Diffraction and X-Ray Fluorescence 23
3.4.1 X-Ray Fluorescence (XRF) 23
3.4.2 X-Ray Diffraction (XRD) 24
3.5 CO_2 Surface area (BET) 24
3.6 Diffuse Reflectance Infrared Fourier Transform Spectrometry (DRIFT) 25
3.7 Thermomechanical Analysis (TMA) 26
3.8 Dilatometry 27
3.9 Thermogravimetric Analysis / DSC-Mass Spectroscopy (TG/DSC-MS) 29
3.9.1 TG 29
3.9.2 DSC 29
3.9.3 MS 29

4. Experimental Procedures 31
4.1 Raw materials 31
4.1.1 Coal 31
4.1.2 Materials 31
4.1.3 Alkali compounds 32
4.2 Demineralization of coal 32
4.3 Free Swelling Index 33
4.4 Tube Furnace Experiments 34
4.4.1 Sample Preparation 34
4.4.2 Heating procedure 34
4.5 Composition analyses of coal 35
4.6 Ash Fusion Temperature 36
4.6.1 Sample preparation 36
4.6.2 Method 36
4.7 X-Ray Fluorescence 36
4.8 X-Ray Diffraction 37
4.9 CO_2 Micropore surface area (BET) 37
4.9.1 Equipment 37
4.9.2 Method 37
4.10 Diffuse Reflectance Infrared Fourier Transform Spectroscopy 37

4.11 Thermomechanical Analysis 38
4.11.1 Sample Preparation 38
4.11.2 Heating Procedure 38
4.12 Dilatometry 39
4.13 TG / DSC-MS 39
4.13.1 Sample Preparation 39
4.13.2 Heating procedure 39

5. Results and Discussion – Coal Characterization 41
5.1 Free Swelling Index 42
5.2 Tube Furnace experiments 44
5.3 Ultimate and Proximate Analysis 46
5.3.1 Ultimate analysis 46
5.3.2 Proximate analysis 47
5.4 Ash Fusion Temperature 50
5.5 X-Ray Diffraction and X-Ray Fluorescence Analyses 50
5.5.1 X-Ray fluorescence (XRF) 50
5.5.2 X-Ray diffraction (XRD) 52
5.6 Micropore Surface Area (BET) 55
5.7 Diffuse Reflectance Infrared Fourier Transform Spectroscopy (DRIFT) 56

6. Results and Discussion – TMA and Dilatometry 62
6.1 Thermomechanical Analysis 62
6.2 Dilatometry 65

7. Results and Discussion – TGA-MS 71
7.1 Thermogravimetric Analysis 72
7.1.1 *TG Curves of the different samples* 72
7.1.1.1 Thermal analysis of the potassium compounds 72
7.1.1.2 Thermal analysis of the coal – alkali blends 76
7.1.1.3 Relative reactivity 80
7.1.2 Synergetic effect 81
7.2 Mass Spectroscopy (MS) 85
7.2.1 H_2 evolution 85
7.2.1.1 Raw and demineralized coal 85
7.2.1.2 Potassium hydroxide 86

7.2.1.3 Potassium chloride 87
7.2.1.4 Potassium carbonate 88
7.2.1.5 Potassium acetate 89
7.2.2 CH_3^+ evolution 91
7.2.2.1 Raw and demineralized coal 91
7.2.2.2 Potassium hydroxide 92
7.2.2.3 Potassium chloride 93
7.2.2.4 Potassium carbonate 94
7.2.2.5 Potassium acetate 95
7.2.3 CH_4 evolution 97
7.2.3.1 Raw and demineralized coal 97
7.2.3.2 Potassium hydroxide 98
7.2.3.3 Potassium chloride 99
7.2.3.4 Potassium carbonate 100
7.2.3.5 Potassium acetate 101
7.2.4 CO_2 evolution 103
7.2.4.1 Raw and demineralized coal 103
7.2.4.2 Potassium hydroxide 104
7.2.4.3 Potassium chloride 105
7.2.4.4 Potassium carbonate 105
7.2.4.5 Potassium acetate 107

8. Conclusions 111
8.1 Coal characterization 111
8.1.1 Demineralization of coal 111
8.1.2 Potassium additions 112
8.1.3 Free Swelling Indices 112
8.2 Thermomechanical analyses and Dilatometry 113
8.2.1 Thermomechanical analyses 113
8.2.2 Dilatometry 114
8.3 Thermogravimetric analyses and Mass Spectroscopy 114
8.3.1 Thermogravimetric analyses 114
8.3.2 Mass spectroscopy 115
8.4 Conclusion for TG, TMA, Dilatometry and MS 116
8.5 Recommendations 117

List of Figures

Figure 1:	Method of investigation schematic	5
Figure 2.1:	Different ranks of coal [web1]	6
Figure 2.2:	Pyrolysis of coal [Yu *et al*, 2007]	9
Figure 2.3:	Volatiles evolved during pyrolysis [Smith *et al*, 1994]	10
Figure 3.1:	Free swelling index profiles [Speight, 2005]	20
Figure 3.2:	Temperature points [Speight, 2005]	23
Figure 3.3:	DRIFT attachment for an FTIR spectrometer [WEB 2]	26
Figure 3.4:	Thermomechanical analysis setup	27
Figure 3.5:	Classes of plastic behaviour [Schobert, 2013]	28
Figure 3.6:	Pathway followed in as mass spectrometer	30
Figure 4.1:	Mill used to obtain good mixtures the coal and alkali salt samples	34
Figure 4.2:	Elite thermal system tube furnace	35
Figure 4.3:	DRIFT spectrometer	38
Figure 4.4:	TMA (SII Technology TMA/SS6100 with EXSTAR6000)	39
Figure 4.5:	TG/DSC-MS instrument	40
Figure 5.1:	Schematic representation of the free swelling indices	43
Figure 5.2:	Samples after heat treatment in tube furnace: a) Raw Coal, top view on the left and from below on the right; b) Demineralized Coal, top view on the left and from below on the right; c) 10% KCl + Demineralized Coal, top view on the left and from below on the right; d) 10% KOH + Demineralized Coal; e) 10% K_2CO_3 + Demineralized Coal; f) 10% KCH_3CO_2 + Demineralized Coal	45
Figure 5.3:	XRD diffractograms for the demineralized coal-alkali blend char: a) Raw coal char; b) Demineralized coal char; c) 10% KCl + Demineralized Coal; d) 10% KOH + Demineralized Coal; e) 10% K_2CO_3 + Demineralized Coal; f) 10% KCH_3CO_2 + Demineralized Coal	53
Figure 5.4:	DRIFT spectra for Raw coal (untreated, heat treated and char samples)	58
Figure 5.5:	DRIFT spectra for Demineralized coal (untreated, heat treated, and char samples)	59

Figure 5.6: DRIFT spectra for 10 K-wt% KOH blend (untreated, heat treated and char samples) 59
Figure 5.7: DRIFT spectra for 10 K-wt% KCl blend (untreated, heat treated and char samples) 60
Figure 5.8: DRIFT spectra for 10 K-wt% K_2CO_3 blend (untreated, heat treated and char samples) 60
Figure 5.9: DRIFT spectra for 10 K-wt% KCH_3CO_2 blend (untreated, heat treated and char samples) 61

Figure 6.1: Thermomechanical analysis curves for the potassium-coal blends up to 1000°C 63
Figure 6.2: Thermomechanical analysis curves for the potassium-coal blends up to 450°C 64
Figure 6.3: Typical dilatation curve for a swelling coal [Hang *et al*, 1987] 66
Figure 6.4: Dilatation curves for the coal and potassium-coal blends; a) Raw coal, b) Demineralized coal, c) KOH-coal blend, d) KCl-coal blend, e) K_2CO_3-coal blend and f), KCH_3CO_2-coal blend 67
Figure 6.5: Dilatation curves for the coal-alkali blends 68

Figure 7.1.1: TG curves for the potassium hydroxide during heat treatment in N_2 73
Figure 7.1.2: TG curves for the potassium chloride during heat treatment in N_2 74
Figure 7.1.3: TG curves for the potassium carbonate during heat treatment in N_2 75
Figure 7.1.4: TG curves for the potassium acetate during heat treatment in N_2 76
Figure 7.1.5: TG graphs for the a) raw and demineralized coal and the demineralized coal-alkali blends: b) KOH, c) KCl, d) K_2CO_3 and e) KCH_3CO_2 77
Figure 7.1.6: The coal mass loss for the demineralized coal and alkali-coal blends for temperatures up to 1200°C 81
Figure 7.1.7: Theoretical TG curves for the demineralized coal-alkali blends: a) coal-KOH blend, b) coal-KCl blend, c) coal-K_2CO_3 blend, d) coal-KCH_3CO_2 blend 82

Figure 7.2.1.1: Mass spectra of H_2 for a) the raw coal and b) the demineralized coal 86
Figure 7.2.1.2: Mass spectra of H_2 for the demineralized coal-alkali blended samples: a) 1% b) 4% c) 5% and d) 10% KOH compound loading 87
Figure 7.2.1.3: Mass spectra of H_2 for the demineralized coal-alkali blended samples: a) 1% b) 4% c) 5% and d) 10% KCl compound loading 88
Figure 7.2.1.4: Mass spectra of H_2 for the demineralized coal-alkali blended samples: a) 1% b) 4% c) 5% and d) 10% K_2CO_3 compound loading 89

Figure 7.2.1.5: Mass spectra of H_2 for the demineralized coal-alkali blended samples: a) 1% b) 4% c) 5% and d) 10% KCH_3CO_2 compound loading 90

Figure 7.2.2.1: Mass spectra of CH_3^+ for a) the raw coal and b) the demineralized coal 91
Figure 7.2.2.2: Mass spectra of CH_3^+ for the demineralized coal-alkali blended samples: a) 1% b) 4% c) 5% and d) 10% KOH compound loading 93
Figure 7.2.2.3: Mass spectra of CH_3^+ for the demineralized coal-alkali blended samples: a) 1% b) 4% c) 5% and d) 10% KCl compound loading 94
Figure 7.2.2.4: Mass spectra of CH_3^+ for the demineralized coal-alkali blended samples: a) 1% b) 4% c) 5% and d) 10% K_2CO_3 compound loading 95
Figure 7.2.2.5: Mass spectra of CH_3^+ for the demineralized coal-alkali blended samples: a) 1% b) 4% c) 5% and d) 10% KCH_3CO_2 compound loading 96
Figure 7.2.2.6: Mass spectra of CH_3^+ for the KCH_3CO_2 compound 97

Figure 7.2.3.1: Mass spectra of CH_4 for a) the raw coal and b) the demineralized coal 98
Figure 7.2.3.2: Mass spectra of CH_4 for the demineralized coal-alkali blended samples: a) 1% b) 4% c) 5% and d) 10% KOH compound loading 99
Figure 7.2.3.3: Mass spectra of CH_4 for the demineralized coal-alkali blended samples: a) 1% b) 4% c) 5% and d) 10% KCl compound loading 100
Figure 7.2.3.4: Mass spectra of CH_4 for the demineralized coal-alkali blended samples: a) 1% b) 4% c) 5% and d) 10% K_2CO_3 compound loading 101
Figure 7.2.3.5: Mass spectra of CH_4 for the demineralized coal-alkali blended samples: a) 1% b) 4% c) 5% and d) 10% KCH_3CO_2 compound loading 102
Figure 7.2.3.6: Mass spectra of CH_4 for KCH_3CO_2 103

Figure 7.2.4.1: Mass spectra of CO_2 for a) the raw coal and b) the demineralized coal 104
Figure 7.2.4.2: Mass spectra of CO_2 for the demineralized coal-alkali blended samples: a) 1% b) 4% c) 5% and d) 10% KOH compound loading 104
Figure 7.2.4.3: Mass spectra of CO_2 for the demineralized coal-alkali blended samples: a) 1% b) 4% c) 5% and d) 10% KCl compound loading 105
Figure 7.2.4.4: Mass spectra of CO_2 for the demineralized coal-alkali blended samples: a) 1% b) 4% c) 5% and d) 10% K_2CO_3 compound loading 106
Figure 7.2.4.5: Mass spectra of CO_2 evolution for K_2CO_3 107
Figure 7.2.4.6: Mass spectra of CO_2 for the demineralized coal-alkali blended samples: a) 1% b) 4% c) 5% and d) 10% KCH_3CO_2 compound loading 108
Figure 7.2.4.7: Mass spectra of CO_2 evolution for the KCH_3CO_2 109

List of Tables

Table 2.1:	Potassium compounds used in previous studies	16
Table 2.2:	Calcium compounds used in previous studies	16
Table 4.1:	Chemicals and gases used during experiments	32
Table 4.2:	Inorganic compounds used during this study	32
Table 4.3:	Methods used to characterize the samples	36
Table 5.1:	Free swelling indices for the following samples; raw coal, demineralized coal, five potassium compound blends and five calcium compound blends to demineralized coal	42
Table 5.2:	Ultimate analysis of the raw coal and demineralized coal samples	46
Table 5.3:	Ultimate analyses of the chars prepared from the raw coal, demineralized coal and the four demineralized coal-alkali blends with 10 K-wt% addition	47
Table 5.4:	Proximate analysis of the raw coal and demineralized coal samples	48
Table 5.5:	Proximate analysis of the chars prepared from the raw coal, demineralized coal and the four demineralized-alkali blends with the 10 K-wt% additions	49
Table 5.6:	Ash fusion temperatures of the chars prepared form raw coal and demineralized coal	50
Table 5.7:	XRF results of raw and demineralized coal and chars prepared from the raw coal, demineralized coal and the four demineralized coal-alkali blends with the 10 K-wt% addition	51
Table 5.8:	XRD results of chars prepared from the raw coal, demineralized coal and the four demineralized coal-alkali blends with 10 K-wt% addition. (Percentages reported as total of crystalline matter)	53
Table 5.9:	Micropore surface area for the raw coal and the demineralized coal	55
Table 5.10:	Micropore surface areas for the chars prepared from the raw coal, demineralized coal and the four demineralized coal-alkali blends with 10 K-wt% addition	56
Table 6.1:	Values determined from dilatation curves	70

Table 7.1.1: Total coal mass loss up to 1200°C for the demineralized coal and potassium – coal blended samples 80
Table 7.1.2: Deviation percentages determined for the alkali blend samples 84

Table 7.2.1.1: Maximum H_2 evolution temperatures for the samples derived from the raw and demineralized coal 85
Table 7.2.1.2: Maximum H_2 evolution temperatures for the char samples derived from the demineralized coal-alkali blends with KOH addition 86
Table 7.2.1.3: Maximum H_2 evolution temperatures for the char samples derived from the demineralized coal-alkali blends with KCl addition 88
Table 7.2.1.4: Maximum H_2 evolution temperatures for the char samples derived from the demineralized coal-alkali blends with K_2CO_3 addition 89
Table 7.2.1.5: Maximum H_2 evolution temperatures for the char samples derived from the demineralized coal-alkali blends with KCH_3CO_2 addition 90

Table 7.2.2.1: Maximum CH_3^+ evolution temperatures for the samples derived from the raw and demineralized coal 91
Table 7.2.2.2: Maximum CH_3^+ evolution temperatures for the char samples derived from the demineralized coal-alkali blends with KOH addition 92
Table 7.2.2.3: Maximum CH_3^+ evolution temperatures for the char samples derived from the demineralized coal-alkali blends with KCl addition 93
Table 7.2.2.4: Maximum CH_3^+ evolution temperatures for the char samples derived from the demineralized coal-alkali blends with K_2CO_3 addition 95
Table 7.2.2.5: Maximum CH_3^+ evolution temperatures for the char samples derived from the demineralized coal-alkali blends with KCH_3CO_2 addition 96

Table 7.2.3.1: Maximum CH_4 evolution temperatures for the samples derived from the raw and demineralized coal 97
Table 7.2.3.2: Maximum CH_4 evolution temperatures for the char samples derived from the demineralized coal-alkali blends with KOH addition 98
Table 7.2.3.3: Maximum CH_4 evolution temperatures for the char samples derived from the demineralized coal-alkali blends with KCl addition 99
Table 7.2.3.4: Maximum CH_4 evolution temperatures for the char samples derived from the demineralized coal-alkali blends with K_2CO_3 addition 100
Table 7.2.3.5: Maximum CH_4 evolution temperatures for the char samples derived from the demineralized coal-alkali blends with KCH_3CO_2 addition 102

Table 7.2.4.1: Maximum CO_2 evolution temperatures for the char samples derived from the demineralized coal-alkali blends with K_2CO_3 addition 106
Table 7.2.4.2: Maximum CO_2 evolution temperatures for the char samples derived from the demineralized coal-alkali blends with KCH_3CO_2 addition 108

List of Abbreviations

AFT	Ash Fusion Temperature
ASTM	American Society for Testing and Materials
BET	Brunauer, Emmett and Teller
daf	Dry and Ash free
Demin	Demineralized
DRIFT	Diffuse Reflectance Infrared Fourier Transform Spectroscopy
FSI	Free Swelling Index
FT	Fluid Temperature
FTIR	Fourier Transform Infra-red
HT	Hemispherical temperature
ISO	International Organization for Standards
IT	Initial Deformation Temperature
K/Ca-wt%	Potassium or calcium metal weight percentage
LOI	Loss on Ignition
MS	Mass Spectrometry
SABS	South African Bureau of Standards
SANS	South African National Standards
ST	Softening Temperature
T_c	Contraction temperature
T_e	Maximum swelling temperature
TG	Thermogravimetric
TMA	Thermomechanical Analysis
T_r	Resolidification temperature
T_s	Softening temperature
V_c	Contraction volume
V_e	Dilatation volume
V_r	Volume after resolidification
V_s	Swelling volume
W_{blend}	Sum of the components within the sample
w_{coal}	Weight loss of the coal in the sample
$w_{compound}$	Weight loss of the alkali compound
x_1/x_2	Mass fractions of components making up the sample
XRD	X-ray Diffraction
XRF	X-ray Fluorescence

Chapter 1

Problem statement and Hypothesis

In this chapter, a brief overview on the literature regarding this study will be given, along with the aim and objectives and the investigation method used.

1.1 Problem Statement and Substantiation

Potassium and calcium species and other minerals that are found in coal usually occur in the clay that forms part of the coal. The mineral matter occurring in coal is divided into three different groups. The first of these are the inorganic elements and salts dissolved in the water present in pores. The second group comprises of the inorganic elements that form part of organic macerals present in the coal structure. The third group relates to the inorganic particles that represent true minerals in the coal [Ward, 2002; Bolat *et al*, 1998]. Various methods to remove minerals from the coal have been developed. Grinding and removing of these minerals based on differences in physical properties such as density separation, have been found to inadequately remove minerals bound to the coal structure [Bolat *et al*, 1998]. Acid leaching methods have been developed to more effectively remove these minerals that are bound to the coal organic structure [Bolat *et al*, 1998]. The leaching technique used on the coal will thus depend on which of the minerals present in the coal, needs to be removed [Bolat *et al*, 1998]. The hydrochloric and hydrofluoric acid treatment method has been found to remove most of the minerals present, except pyrite, from the coal sample with only very small changes to the coal structure [Formella *et al*, 1986]. However, the removal of the minerals may influence the reactivity of the coal because some of these minerals may act as catalysts during thermal processing [Liu and Zhu, 1986].

Pyrolysis is the process where the coal is exposed to high temperatures in an inert atmosphere. During pyrolysis two products form; coal char and a volatile portion consisting of vapour, tar and other gases [Öztaş and Yürüm, 2000]. The more severe the pyrolyzing conditions the coal is exposed to, the lower the reactivity of the resultant char [Radovic *et al*, 1984; Radovic *et al*, 1985]. The duration and conditions of pyrolysis may also influence the swelling propensity of the coal. The swelling of coal during pyrolysis has been found to influence the reactivity and density of the coal char [Gale *et al*, 1995]. The swelling of coal is generally considered to be associated with the plastic properties of the coal. Coal that does not show any plastic properties during heat treatment will show no free swelling. It is believed that the swelling of coal is caused by released gas trapped within the coal during the plastic phase [Speight, 2005]. Also, the number of cross-links formed in the coal structure increases as the pyrolysis temperature increases [Öztaş and Yürüm, 2000]. Also, during pyrolysis the number of cross-links within the coal structure increases with an increase in the temperature.

The reactivity of coal during steam gasification has been found to increase in the presence of alkali and alkaline earth metals [Liu and Zhu, 1986]. All of the alkali metals have some degree of catalytic activity and the activity of a compound seems to increase with alkalinity [Nahas, 1983]. The most effective catalysts for coal gasification are alkali metal salts and the anion that is bound to the alkali metal plays a significant role in the reactivity [Veraa and Bell, 1978]. The anion will thus determine the effectiveness of the alkali compounds as a catalyst [Khan and Jenkins, 1986]. Studies have shown that alkali metals can also reduce the thermoplastic behaviour of the coal during the heating process [Khan and Jenkins, 1986; Öztaş and Yürüm, 2000].

Potassium based catalysts have been used in steam gasification reactions and it was observed that these species decrease the swelling and agglomeration propensity of the studied coal samples. Potassium has been found to react with the clay minerals in the coal, thus the more minerals present in the coal; the more catalyst is needed to affect the reactivity [Formella *et al*, 1986]. Some studies on different types of coal indicated that KCl has almost no activity when used as a catalyst [Yuh and Wolf, 1983]. Veraa and Bell [1978] found that KOH and K_2CO_3 have the same catalytic activity when added to the coal in the same loading percentages. This may be because the KOH is converted to K_2CO_3 upon exposure to CO_2 [Veraa and Bell, 1978].

In previous studies, it has been found that a good calcium catalysts distribution throughout the coal must be obtained for the catalyst to have an effect on the reactivity of the coal.

Distribution of calcium catalyst requires more effort than that of potassium catalysts. [Lang and Neavel, 1981]. The distribution of the catalysts on the surface of the coal depends on the nature of the catalyst, the amount added to the coal and the method by which the catalyst is added to the coal. Studies indicated that the method and conditions of loading has no effect on the potassium catalysts' activity, but the effectiveness of calcium catalysts depended on the method and conditions of loading [Liu and Zhu, 1986]. The coal reactivity rate thus does not depend on the calcium compound used, but on the loading method of the catalyst [Ohtsuka and Tomita, 1986]. Khan and Jenkins [1986] found that calcium and potassium species used as catalysts have reduced the swelling of coal at low pressures. It is suggested that a combination of potassium and calcium as catalysts may reduce the swelling of the coal under high temperature experimental conditions [Khan and Jenkins, 1986].

1.2 Hypothesis

Potassium and calcium compounds have an influence on the swelling behaviour of the coal and the volatile species evolved during the pyrolysis processes. These compounds have been known to increase the reactivity of the coal by acting as catalysts. The reactivity of the coal sample may depend on the compound present.

1.3 Aims and Objectives

The aims and objectives of this study

- to determine the influence of demineralization of the coal;
- to select a number of potassium and/or calcium compounds;
- to determine the influence the selected potassium and/or calcium compounds have on the swelling properties and behaviour of a high swelling South African coal;
- to determine the influence the selected potassium and/or calcium compounds have on the reactivity of a high swelling South African coal;
- to determine the influence of the potassium and/or calcium compounds have on the evolution of certain gas species during pyrolysis of the samples;
- and to compare the results obtained for the different alkali compounds.

1.4 Method of Investigation

In the first part of this study a high swelling coal will be demineralized using a hydrochloric and hydrofluoric acid leaching method. After the leaching process, the coal will be washed with distilled water until neutral pH. The demineralized coal will be dried and stored under nitrogen to decrease the extent of oxidation of the coal sample.

The alkali compounds will then be added to the demineralized coal in different weight percentages. Free swelling index (FSI) experiments will be done on the raw coal, demineralized coal and on the coal with the added alkali compounds (demineralized coal-alkali blends). Results from the FSI experiments will be used to select the alkali compounds to be investigated in this study.

The raw coal, demineralized coal and demineralized coal-alkali blends will be charred and subjected to further analyses. XRF, XRD, CO_2 BET, DRIFT, ultimate and proximate analysis will be done on the raw and demineralized coal, the raw and demineralized chars and on the demineralized coal-alkali blend char samples. Ash fusion temperature analysis will be done on the raw coal and the demineralized char.

Thermogravimetric analyses (TG) with mass spectrometry for the vapour phases (MS) will determine the reactivity and the gas species evolved during heat treatment of the raw coal, the demineralized coal, and the samples with the added alkali compounds (demineralized coal-alkali blends). These experiments will be performed under nitrogen.

Dilatometry analysis on the samples with 10 K-wt% added alkali compound will be measured. Thermomechanical analyses (TMA) will also be done on the samples with the 10 K-wt% alkali addition samples. Figure 1.1 represents the method of investigation in a schematic format.

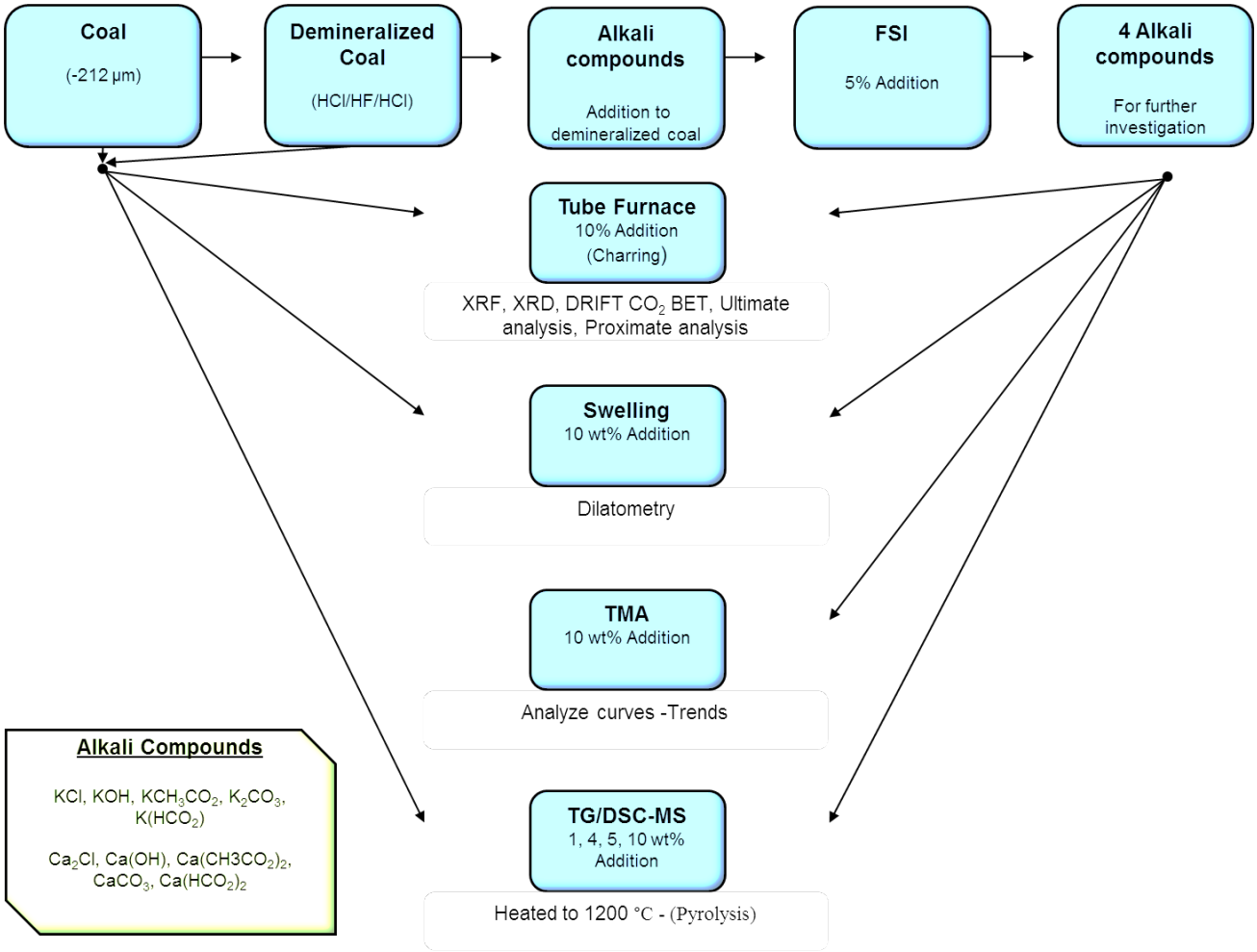

Figure 1: Method of investigation schematic

Chapter 2

Literature Review

In this chapter a brief review on coal, coal properties and the different reactions that may take place during the devolatilization process of coal will be discussed. The influence of specific alkali compounds on the swelling behaviour of the coal and the proposed mechanisms will also be discussed along with the influence of these compounds on the reactivity of the coal.

2.1 Introduction to coal

Coal is a heterogeneous material of which the physical and chemical properties depend on the age of the coal and the geological setting of the coal seam. By using these properties, a rank can then be assigned to the coal [Yu *et al*, 2007; Bolat *et al*, 1998]. Coal can be classified into six different ranks depending on the carbon content and the reflectance of the macerals [Ward, 2002]. The six coal ranks are: peat, lignite, sub-bituminous, bituminous, anthracite and graphite. Figure 2.1 is a visual representation of the different ranks of coal.

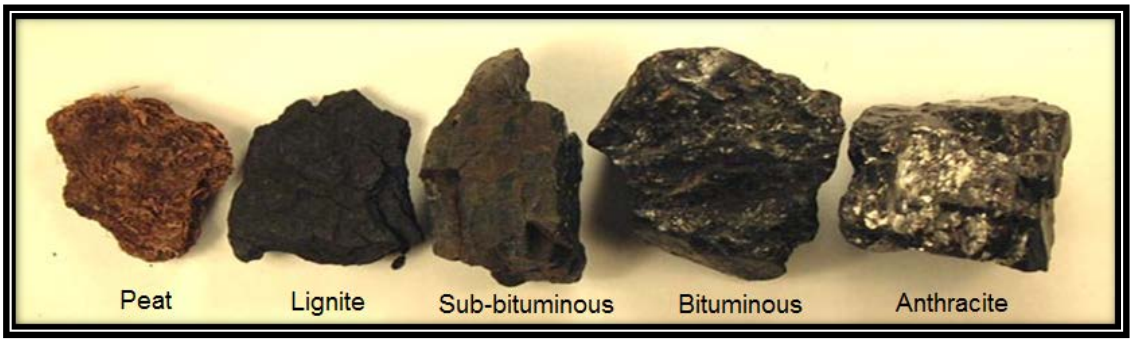

Figure 2.1: Different ranks of coal [WEB1]

With the increase in the coal rank, the following observations can be made;

i. a decrease in the water molecules and oxygen content in the structure,
ii. increase in the aromaticity of the carbon structure,
iii. decrease in the volatile matter,
iv. and a decrease in the hydrogen present in the structure [Yu *et al*,2007].

Changes in the properties of the different coal ranks will influence the behaviour of the coal during heat treatments [Yu *et al*, 2007].

Within this heterogeneous structure of the coal, organic and inorganic components are found. The organic components are referred to as macerals. Macerals can be divided into three main groups; liptinite, vitrinite and inertinite. The chemical and physical properties for each of these maceral groups differ from one another since they are derived from different plant materials. The coalification process also plays an important role in the formation of these macerals and their properties [Yu *et al*, 2007]. These maceral groups are used to define the nature of a coal, into a rank and type and also how best to utilize the coal [Ward, 2002]. These main groups of macerals can then be subdivided into other classification groups.

The inorganic components in the coal are referred to as mineral matter. Three types of minerals are found within the coal;

i. mineral salts dissolved in the water found within the coal pore structure,
ii. inorganic components that are bound to the organic compounds,
iii. and inherent mineral matter that is part of the coal structure [Ward, 2002; Tomeczek and Palugniok, 2002].

The mineral matter in the coal is responsible for a large portion of the ash formed during heat treatment of the coal. This is especially true for lower rank coals where about one third of the formed ash originates from the mineral matter in the coal [Ward, 2002]. Some of these minerals found in the coal may have a catalytic influence on the reactions taking place during coal processing. The catalytic influence of the minerals will depend on the nature of the minerals, the concentration of the minerals in the coal, the form in which they are present and how well these minerals are distributed throughout the coal sample [Samaras *et al*, 1996]. Concentration and composition of the mineral matter within the coal will depend on the rank of the coal and the conditions under which the coal deposit was formed [Samaras *et al*, 1996; Waugh, 1984]. The reactivity of the coal may be influenced by the alkali metal compounds found within coals with high mineral matter content [Samaras *et al*, 1996; Sentorun and Kücükbyrak, 1996]. Minerals that do not take part in any chemical reactions during heat treatment, may act as dilutent since they only serve to separate the coal

particles from one another. This may reduce some of the coal properties observed during the heating processes [Khan and Jenkins, 1986].

Removal of the minerals through sequential acid leaching will erase the catalytic- and diluting effect the minerals may have had on the coal. The amount of minerals removed from the coal will depend on the leaching steps, the types of acid used and also the concentration of the acid [Samaras *et al*, 1996].

2.2 Coal processes

2.2.1 Pyrolysis

Pyrolysis is the process where a solid is subjected to heat treatment in an inert atmosphere, to prevent any reactions with oxygen, where decomposition of the material will take place to form volatile products [WEB 3].

Figure 2.2 is a representation of the pathway generally followed by high ranking coals during pyrolysis. The structural properties of the coal will determine the behaviour of the coal during the pyrolysis process [Smith *et al*, 1994]. According to Yu *et al* [2007] and Smith *et al* [1994], the pyrolysis process consists of three stages.

- Stage I: A reduction in the hydrogen bonding and bond breaking within the coal structure, resulting in the formation of liquid components that are referred to as the metaplast. Bond breaking and bond stabilization compete with one another in this stage to form the initial char. Light molecular mass gases (primary gases) are released during the stage.
- Stage II: Further bond breaking occurs with the release of more primary gases and low molecular weight species are evolved as tar. By cross-linking reactions, the remaining high molecular species found in the metaplast reattach to the char structure.
- Stage III: In the last stage of pyrolysis, CO_2 and H_2 gases are evolved from the formed char with cross-linking reactions still taking place. Secondary gases and soot form as a result of further reactions of the tars that were evolved [Yu *et al* 2007; Smith *et al*, 1994].

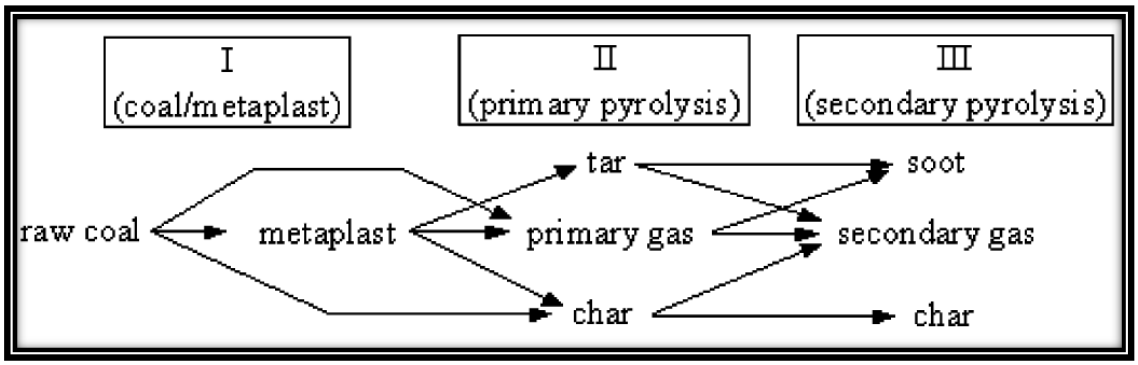

Figure 2.2: Pyrolysis of coal [Yu *et al*, 2007]

Char is the solid remaining after devolatilization has occurred and it is composed of the unreleased carbon molecules and mineral matter [Solomon *et al,* 1983; Alonso *et al*, 1999]. Cross-linking reactions during heat treatment will determine the rate of volatiles formed and more importantly the properties of the char [Smith *et al*, 1994]. The cross-linking reactions taking place during the heat treatment will be influenced by the properties of the parent coal, which is the rank and mineral composition [Alonso *et al*, 1999]. The structural changes undergone by the minerals during the heating process will influence the formation of the char [Oboirien *et al*, 2010]. Procedure conditions such as the heating rate, the maximum temperature of pyrolysis, oxygen levels in the atmosphere during pyrolysis and pyrolysis time will also play an important role in the char formation [Alonso *et al*, 1999; Tamhankar *et al* 1984]. Some of the following char properties may be influenced by some or all of these factors during pyrolysis;

- Porosity
- Surface areas
- Reactivity of the char [Alonso *et al*, 1999; van Heek and Mühlen, 1987].

The low- and high molecular weight species evolved during the pyrolysis process are known as volatiles (CO, CO_2, H_2O, and CH_4) [Solomon *et al*, 1993]. Tar, which is considered a low molecular weight component of the metaplast, is evolved during the second stage of pyrolysis and considered as a volatile product [Solomon *et al*, 1993; Smith *et al*, 1994]. Moisture is excluded and is not recognized as a volatile [Speight, 2005]. Figure 2.3 presents the primary and secondary pyrolysis stages, with the volatiles released during those stages.

Since coal is a heterogeneous solid the composition of the functional groups within the coal will depend on the rank of the coal. As the structure of the coal decomposes during the heat treatment, these functional groups will determine the amount of gas and the gas species being evolved [Smith *et al*, 1994]. Some of the gas species evolved during the heat

treatment may be related to the decomposition of functional groups present in the coal structure [Solomon *et al*, 1993]. It was found that the amount of volatile matter produced from South African coals may range from 5 to 60% [Slaghuis *et al*, 1991].

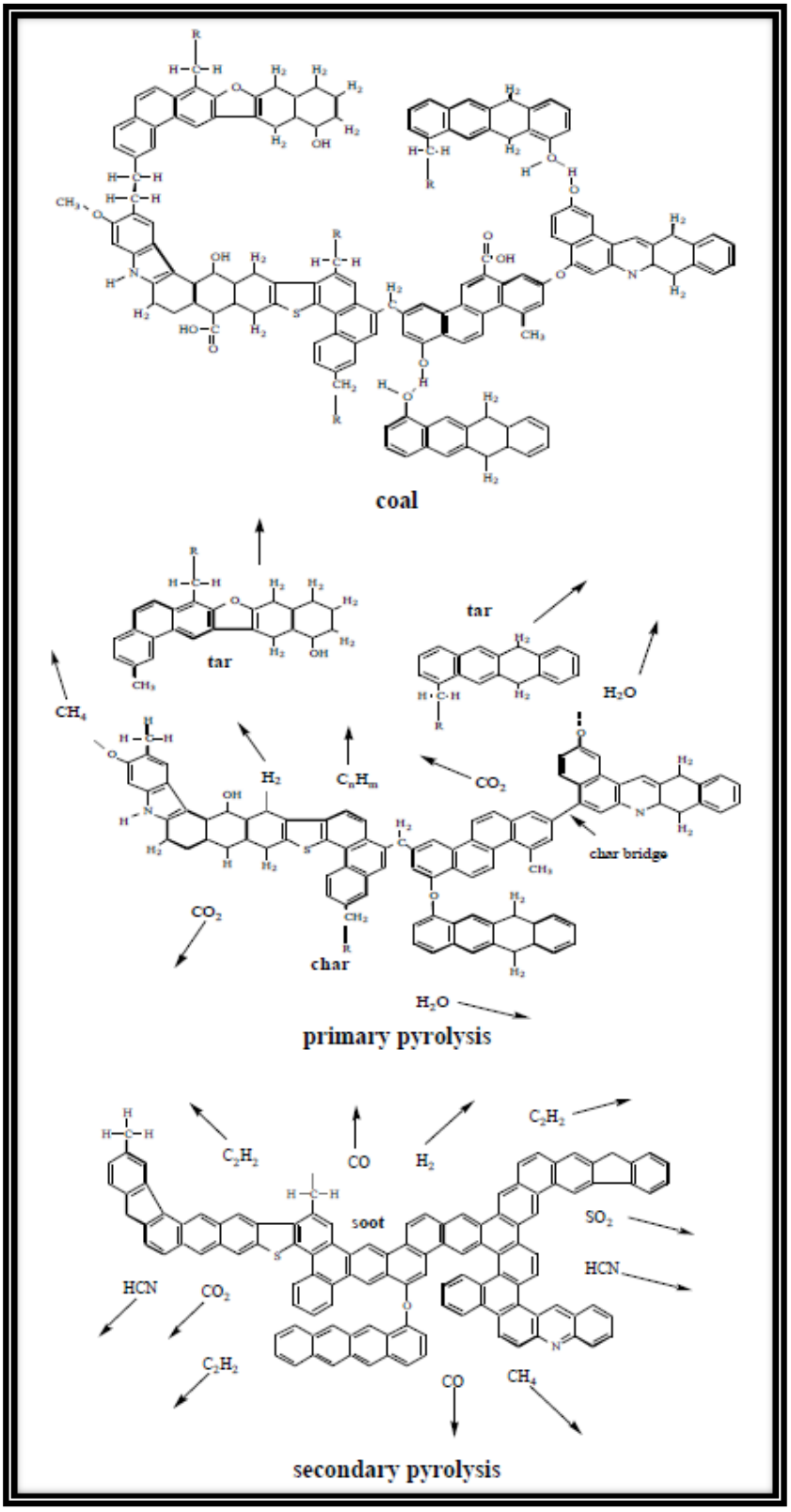

Figure 2.3: Volatiles evolved during pyrolysis [Smith *et al*, 1994]

2.2.2 Gasification

Chars formed during the pyrolysis process are used in the gasification process. The conditions under which the chars were prepared, will determine the gasification temperatures and the products that will form during this process [Solomon *et al*, 1993]. According to Radović *et al* [1983], the reactivity of a coal char will decrease during gasification if there was an increase in the pyrolysis temperature and residence time for the coal. The mineral composition of the char will have an influence on the reactivity of the char during gasification, since some minerals act as dilutents or catalyst [van Heek and Mühlen, 1987; Pan and Serageldin, 1987]. During the gasification process, the formed char is partially consumed into gases and thus a great change in the physical properties of the sample [van Heek and Mühlen, 1987].

According to McKee [1983], an increase in the rate that reactions take place or decreased operation temperatures may be observed when certain additives are added to the coal prior to gasification. As an example, the addition of K_2CO_3 reduces the production of CH_4 during the gasification process [McKee, 1983].

2.2.3 Combustion

Chars formed during the pyrolysis process are also used in the combustion process. During this process, partial or complete combustion of the chars may take place depending on the reactivity, the porosity, surface area and minerals present in the sample [van Heek and Mühlen, 1987].

Problems have been found to occur during combustion of coal. During the combustion process of coal, the minerals present in the coal may react at high temperatures to form deposits on the surface of the equipment. These deposits may be corrosive, cause abrasion and pollution [Ward, 2002; Tomeczek and Palugniok, 2002]. Pollutant substances such as nitrogen and sulphur containing gases are released into the atmosphere [Adánez *et al*, 1999].

2.3 Important properties of coal

2.3.1 Swelling

Some coals undergo physical changes and swell or contract during the heating process. This swelling behaviour of coal stems from chemical reactions within the coal which then lead to the physical changes [Bexley *et al*, 1986; Green *et al*, 1988; Barriocanal *et al*, 2003]. It is believed that the swelling of coal occurs when gases that are released during heat

treatment get trapped within the coal pores. Since the gases are trapped within the coal, a pressure build-up of the gases occurs causing the pores to expand within the coal structure and thus swelling of the coal is observed [Speight, 2005].

The swelling of coal is influenced by the pressure and atmosphere in which the sample is heated [van Heek and Mühlen, 1987]. According to van Heek and Mühlen [1987], the swelling of the coal was affected similarly by different inert gases at atmospheric pressure, but changed as the pressure changed.

According to Gale *et al* [1994], chars that have been prepared in a nitrogen rich atmosphere have a higher swelling propensity, a more porous structure and smaller internal surface areas than chars prepared in an atmosphere where high oxygen is present. Within the nitrogen atmosphere, less oxidation of the coal takes place which means a decrease in cross linking reactions [Gale *et al*, 1994].

It has been suggested that with an increase in the heating rate, that the swelling of the coal decreases during the heat treatment. The swelling is also influenced by the residence time and the maximum temperature of the pyrolysis procedure [Gale *et al*, 1994]. Hang *et al* [1987] found that the pores in the coal structure collapse when the coal is heated to its plastic state, thus trapping the gases within the coal. The coal will swell until high pressures are reached within the coal, thus causing the coal mass to break or crack to release the gases [Hang *et al*, 1987].

2.3.2 Plasticity

Coals undergo not only chemical changes, but also a number of physical changes during heat treatment. The physical change that some coals pass through is called the plastic properties of the coal, also known as the plasticity of the coal. The plastic range is the temperature range at which these changes take place [Speigh, 2005]. Coals that show these plastic properties are known as caking coals. The physical changes that can take place with caking coals are;

- Softening of the coal,
- Melting,
- Fusing of coal particles,
- Swelling of coal,
- And the resolidification of the coal [Speigh, 2005].

Fluidity is known as the degree of plasticity for a coal sample when it is heated in an inert atmosphere under controlled conditions [Speigh, 2005]. During heat treatment, the coal

passes through different stages as the temperature is increased. The first stage is the softening of the coal, the second the fluidity of the coal and the third is the resolidification of the coal [Barriocanal *et al*, 2003].

The fluidity of the coal will depend on the rank of the coal. The procedure used during pyrolysis will also have an influence on the structure of the coal and influence the fluidity [Solomon *et al*, 1993]. The heating rate will play an important role in the fluidity of the coal. An increase in the fluidity of the coal can be expected with an increase in the heating rate [Green *et al*, 1988]. Alonso *et al* [1999] found that more volatiles are released with the increase in the fluidity of the coal. Volatiles released during the heat treatment of the coal may also have a strong influence on the plasticity of the coal [Green *et al*, 1988]. A low micropore and surface area would suggest that the coal is very fluid during the heat treatment, when the results are compared to that of the parent coal [Audley, 1987].

High ranking coals have a smaller plastic range than low ranking coals. As suggested by Barriocanal *et al* [2003], with an increase in the coal rank, all the different stages of the plastic range will shift to higher temperatures. The reason for this change in the temperature values is because high ranking coals soften at higher temperatures than the low ranking coals [Barriocanal *et al*, 2003].

2.3.3 Proposed Mechanisms during coal swelling

Cross-linking reactions play an important role in determining the fluidity of the char, the reactivity, the surface area and the structure of the char [Solomon *et al*, 1990]. Cross-link density and the size of the molecules in the coal structure will determine the plastic behaviour of the coal [Barriocanal *et al*, 2003]. It has been suggested that cross-linking reactions will depend on the rank of the coal [Solomon *et al*, 1993]. As the rank of the coal increases the structure of the coal becomes more ordered and aromatic. With the increase in coal rank, higher temperatures will be required for these bonds to break and the coal to enter the softening stage. Thus with increase in coal rank, there will be a decrease in the fluidity of the coal and a decrease in the volatile matter released. Volatile matter released during the heat treatment will take place at higher temperatures. [Barriocanal *et al*, 2003].

Bond breakage between the polyaromatic rings in the structure during the pyrolysis process will cause the coal to soften and go into the metaplast state. Within the metaplast phase a variety of reactions occurs. Some of these reactions involve the release of volatile matter where as other reactions lead to the formation of new bonds. This new bond forming reactions will be responsible for the structure of the char that is formed [Alonso *et al*, 1999].

Fluidity of the coal during the plastic stage is determined by the amount of cross-links present in the coal structure. The surface area and the reactivity of the resulting char will be influenced by these cross-linking reactions and the repolimerazation of the metaplast. These reactions prevent further evolution of species from the coal [Solomon *et al*, 1993].

Another factor that will influence the cross-linking reactions is the presence of water in the coal. The water in the coal may participate in the reactions during pyrolysis [Suuberg *et al*, 1985].

$$\text{Coal} + H_2O \rightarrow CO + H_2 \text{ [Lang and Neavel, 1982]}$$

Cross-linking reactions in low-rank coals may suppress the fluidity of the coal during the metaplast stage. These reactions are related to the amount of oxygen present in the coal. It is assumed that during pyrolysis, carbon-carbon bonding is promoted by the removal of hydrogen through the oxygen present in the structure and atmosphere. According to Suuberg *et al* [1985], most cross-linking reactions occur when high concentrations of hydrogen are released. These reactions occur when other volatile matter releases are low and during the final stages of the pyrolysis process.

Solomon *et al* [1993] stated that low temperature cross-linking may be as a result of decomposing carboxylic groups. During this decomposition, CO_2 is formed. The amount of CO_2 formed will depend on the rank of the coal [Solomon *et al*, 1993; Solomon *et al*, 1990]. It was found that cross-linking reactions start during the evolution of CO_2 [Suuberg *et al*, 1985]. Methane (CH_4) evolution is a result of cross-linking reactions taking place at moderate temperatures [Solomon *et al*, 1993; Solomon *et al*, 1990]. Solomon *et al* [1993] also found that cross-linking reactions in bituminous coals occur during the evolution of methane [Solomon *et al*, 1993]. It was found by Solomon *et al* [1993] that coals that undergo low temperature cross-linking will produce low tar evolutions and low fluidity char.

The reduction of cross linking reactions can be accomplished by means of demineralization, which will remove the minerals and thus reduce the catalytic reactions in the coal. The demineralization process occurs in a hydrogen rich environment. Cross linking reactions increase as coal oxidizes, i.e. in an oxygen rich environment [Solomon *et al*, 1990].

2.4 Swelling coals

When bituminous coals are heated in the absence of oxygen, they undergo physical changes and pass through the plastic range [Khan and Jenkins, 1989].

As mentioned by Gale *et al* [1994], when the coal is heated and starts to melt, volatiles are released into the pores within the coal. The gases within the pores will expand as the temperature increases [Gale *et al*, 1994]. Swelling of coal is thus the formation of high pressure areas within the coal pore system which causes the coal to swell and then leads to the release of the volatiles [Khan and Jenkins, 1986]. The volatiles are released when cracks and ruptures occur on the coal surface [Gale *et al*, 1994].

Some problems experienced with the swelling behaviour of coal during thermal processing are the formation of large lumps. These formed lumps will disrupt the flow of the gas and create a non-uniform flow within the thermal reactor [Mulligan and Thomas, 1987].

2.5 Methods used to decrease swelling

2.5.1 Addition of Catalysts

Some minerals and inorganic compounds in small amounts found in coal have been known to change some of the properties of the coal during the gasification and pyrolysis processes. Some of the known changes these compounds can have on the coal are the following:

- They may have an catalytic effect;
- Bring about a change in the swelling behaviour of the coal;
- Change the spectrum of products formed during the processes
- And change the properties of the formed char [Bexley *et al*, 1986; Green *et al*, 1988].

The degree of catalytic activity of the alkali compounds added to the coal will depend on the alkalinity of the compound. By increasing the alkalinity of the compound, the activity during heat treatment may be increased [Nahas, 1983]. Other factors that may influence the catalytic activity:

- The method used to add the alkali compound to the coal;
- The nature of the anion bound to the alkali metal;
- And how well dispersed the alkali compound is through the coal [Audley, 1987; Liu and Zhu, 1986].

When the catalytic activity of an alkali compound is examined, the inherent minerals in the coal are removed through an acid leaching process. According to Ohtsuka and Tomita [1986], residual halogens left in the coal after leaching, may react with the alkali compound thus deactivating that compound. This has been found to happen with calcium compounds [Ohtsuka and Tomita, 1986].

2.5.2 Types of catalysts

A number of different potassium and calcium compounds have been used to investigate their influence on coal properties and their ability to act as catalyst during heat treatments [Wang *et al*, 2010]. The most effective of the alkali and alkaline compounds which act as catalysts have been found to be the alkali metal salts [Veraa and Bell, 1978]. Since the anion bound to the alkali metal will influence the reactions during heat treatment, it was found that alkali compounds considered the most catalytic active are the oxides, hydroxides, carbonates and bicarbonates [Veraa and Bell, 1978]. Potassium and calcium compounds that have been studied in the past are presented in Table 2.1 and Table 2.2

Table 2.1: Potassium compounds used in previous studies

Potassium Compound	Reference
Potassium carbonate	Formella *et al* [1986]
Potassium hydroxide	Formella *et al* [1986]
Potassium chloride	Yuh and Wolf [1983]
Potassium bicarbonate	Yuh and Wolf [1983]

Table 2.2: Calcium compounds used in previous studies

Calcium Compound	Reference
Calcium oxide	Köpsel and Zabawski [1990]
Calcium carbonate	Khan and Jenkins [1986]
Calcium acetate	Khan and Jenkins [1986]
Calcium hydroxide	Lang and Neavel [1982]
Calcium chloride	Liu and Zhu [1986]
Calcium nitrate	Ohtsuka and Tomita [1986]

During heat treatment, the potassium present in the coal sample may re-distribute itself through the coal and take part in the repolymerization reactions [Jibril *et al*, 2009]. As noted in previous studies, calcium compounds are not very mobile when subjected to heat

treatment [Lang and Neavel, 1982]. Because of this lack of mobility shown by the compound, Khan and Jenkins [1986] found that calcium crystallites form during heat treatment. Liu and Zhu [1986] found that the loading method for the potassium compounds to the coal did not influence their catalytic activity, but loading method did matter for the calcium compounds.

Some clay minerals like quartz, illite and kaolite have been found to react with the potassium compounds [Formella *et al*, 1986]. Most of these reactions between the potassium compound and the mineral matter in the coal may form insoluble compounds. Thus, these reactions deactivate the alkali compound that may act as a catalyst during heat treatment [Bruno *et al*, 1986; Liu and Zhu, 1986]. Using coal from which the mineral matter has been removed, thus subjecting the coal to a leaching process, the deactivation of the catalyst may be prevented [Wang *et al*, 2010].

According to Yuh and Wolf [1983], potassium bonds to the carbon surface during the heat treatment forming alkali salt complexes on the surface of the carbon. These complexes form when potassium bonds with -COOH and -OH groups in the structure of the coal [Liu *et al*, 2004]. These complexes act as catalytic sites and may come in the forms of C-O-K and C-K. Yuh and Wolf [1983] found that KCl does not form any of these complexes. The advantage of using potassium compounds during heat treatment is that active sites form continuously, whereas the calcium compounds lose activity [Lang and Neavel, 1982].

According to Bexley *et al* [1986], pyrolysis of a swelling coal mixed with a potassium compound will decrease or eliminate the swelling behaviour of the coal. With this decrease in swelling of the coal, a larger surface area for the char may be expected [Bexley *et al*, 1986]. This surface area will thus also depend on the conditions of the heat treatment, since high temperatures may cause collapsing of the pores [Hang *et al*, 1987]. Khan and Jenkins [1986] suggested that the calcium compounds reduce the plastic range the coal passes through when undergoing heat treatment.

Some studies have been done on coal by adding potassium and calcium compounds to the same sample. These studies showed that the reactivity of the coal and char was greater than that of singular addition of these compounds. A decrease in the swelling of the coal was also noticed [Khan and Jenkins, 1989]. As suggested by Khan and Jenkins [1989], the mobility of the potassium compounds may help to distribute the calcium compounds throughout the coal sample.

2.5.3 Influence on coal reactivity

Some factors are believed to play an important role in the reactivity of the coal. These factors are determined by the pyrolysis conditions and the rank of the coal. The active sites on the surface of the coal, the presence of catalysts in the coal and the ability for gases to gain access to these active sites are some of the factors [Samaras *et al*, 1996]. An increase in the reactivity may be observed with the addition of alkali compounds to the coal sample. This increase may be as a result of the formation of active sites caused by the addition of the alkali compound [Audley, 1987]. As suggested by Tamhankar *et al* [1984], the heating method used on the coal samples may also have an effect on the reactivity. Van Heek and Mühlen [1987] found that a decrease in the char reactivity can be seen when the sample is treated to temperatures above 1000°C, and thus rendering the coal "dead".

A loss of reactivity may be caused by the loss of active carbon sites; the loss of catalytic activity of the alkali compound and in some cases both of these reasons [Radović *et al*, 1983]. The decrease of the reactivity of the char may also be caused by incomplete devolatilization of the coal, meaning that there may be some hydrogen left in the char [Alonso *et al*, 1999]. It has also been found that the reactivity of the char decreases as the residence time increases. It is believed that the longer residence time destroys the active sites found in the structure.

2.5.4 Catalytic mechanisms

Green *et al* [1988] stated that the catalysts react chemically with the coal during the carbonization process and that the properties of the char will depend on the conditions of the process. It has been proposed that the mechanisms taking place between the catalytic compounds and the coal during heat treatment are electron-transfer or oxygen-transfer theories [McKee, 1983].

- During the electron-transfer theory, with the addition of the catalytic compound to the coal, electrons are transferred to or from the carbon, thus creating a redistribution of the electrons within the coal structure. This may cause weakening of the C-C bonds and increase the C-O bonds [McKee, 1983]. This theory has a yet not been proven.
- The oxygen-transfer theory states that the catalytic compound be regarded as an oxygen carrier that may influence and promote the transfer of oxygen groups to the carbon surface. This may be accomplished by the formation of a metal oxide intermediate on the carbon surface [McKee, 1983].

According to McKee, [1983], alkali metals may act as active sites on the carbon surface, weakening the C-C bonds by chemisorption of oxygen groups by the active sites.

Chapter 3

Experimental Techniques

Coal is a heterogeneous compound containing a mixture of organic and inorganic components. There is a difference in the coal composition when coals from different seams are compared. The same is true for coal removed from the same seam but from different locations [Leonard III and Hardinge, 1991]. Experimental techniques have been established to characterize coal to better understand its behaviour.

In this chapter a brief review is given on the background of the analytical techniques that were used during this study. These techniques include physical, chemical and mineralogy techniques namely:

- *Free swelling index (FSI);*
- *Ultimate analysis;*
- *Proximate analysis;*
- *X-Ray Diffraction (XRD);*
- *X-Ray Fluorescence (XRF);*
- *CO_2 Surface Area (BET);*
- *Diffuse Reflectance Infrared Fourier Transform Spectrometry (DRIFT);*
- *Thermomechanical Analysis (TMA).*
- *Dilatometry;*
- *Thermogravimetric Analysis / DSC-Mass Spectroscopy (TG/DSC-MS).*

3.1 Free Swelling Index

This is a crude method to determine the increase in volume of a coal sample when the sample is heated under specific conditions [Speight, 2005]. Figure 3.1 presents the standard index profiles for the coke buttons produced when using this method. After heating the sample to the specified conditions, the resulting coke button is compared to the standard index profiles to find the best fit. The coke button will then be assigned a swelling number according to this index. The high index numbers indicate a high swelling propensity for the coal, whereas the lower index numbers show less swelling. A coke button with index number 1 means that there was no swelling of the coal [Leonard III and Hardinge, 1991].

An increase in the coal sample volume may also be an indication of the plastic properties of the coal. Coals that do not swell do not exhibit any plastic properties. The amount of swelling for each coal sample will depend on the fluidity of the coal and the volatiles released during the heating and the tension between the solid particles still present and the fluid particles. Evolved gases trapped within the sample during the plastic stage are believed to cause the swelling of the coal [Speight, 2005; Strutzer and Noè, 1940].

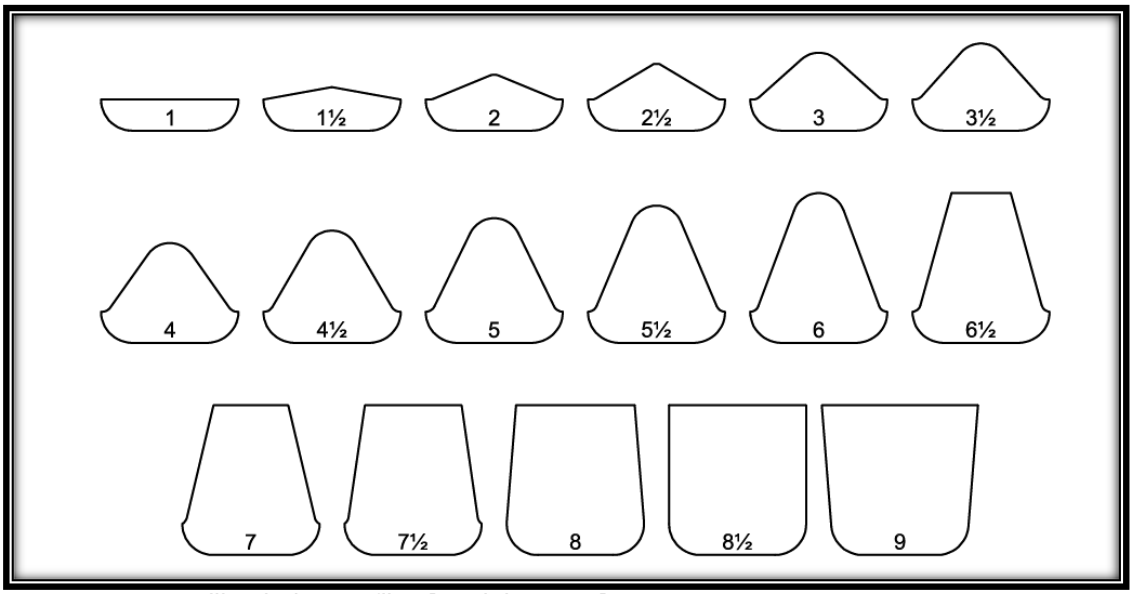

Figure 3.1: Free swelling index profiles [Speight, 2005]

3.2 Ultimate and Proximate Analysis

3.2.1 Ultimate Analysis

Ultimate analysis also known as elemental analysis is a method used to determine the composition of a coal sample without knowing the form in which these elements are present and without knowing the structure of the coal sample [Leonard III and Hardinge, 1991]. These elements in the coal which are determined by this method are: carbon, nitrogen, sulphur, hydrogen and oxygen (by difference). Some trace elements found in the coal samples are sometimes included in the analysis [Speight, 2005].

The carbon value determined for the coal accounts for all carbon present in the sample. Any carbon that occurs as part of minerals will also be added to the weight percentage. The hydrogen value is determined by the amount of water in the coal and the hydrogen bound in the structure of the coal and minerals. The nitrogen bound within the structure of the coal will determine the weight percentage for this element. Sulphur may be present as organic or inorganic species within the coal [Speight, 2005]. The ash content of the sample is determined as the weight percentage left after burning the sample. The conditions used to determine the ash percentage will influence the amount and properties of the ash formed. The oxygen content cannot be determined directly. Thus the sum of all the other elements subtracted from 100 will give the weight percentage value for the oxygen content [Leonard III and Hardinge, 1991].

3.2.2 Proximate Analysis

The term proximate analysis refers to a series of ASTM test methods used to determine the properties of the coal when it is heated under specific conditions. This analysis has also been used on higher ranking coals to determine the rank [Leonard III and Hardinge, 1991]. The product distribution of the coal sample can also be determined by using this method [Speight, 2005]. With this analysis the products of the coal are separated into the following groups:

i. Moisture content

Moisture determination can be done in three different ways.

- The total amount of moisture from the coal. This will include all the moisture present in the sample except for the moisture chemically bound to the coal structure [Leonard III and Hardinge, 1991].
- The inherent moisture in the coal. This is represented by the water present in the pores within the coal particles [Leonard III and Hardinge, 1991].

- And the free moisture that can be found on the surface of the coal. This value can be determined by difference between the total amount of moisture and the inherent moisture [Leonard III and Hardinge, 1991].

ii. Volatile matter

Volatile matter relates to the gases evolved during the heating of the coal under specific conditions. Moisture content is excluded from this value. Coal rank has an influence on the volatile content released during the heating procedure. Cleaning of coal may also affect the volatiles released [Leonard III and Hardinge, 1991].

iii. Fixed carbon

Fixed carbon is known as the combustible material in coal after the volatiles have been released. To determine the fixed carbon value for a sample the moisture, volatile matter and ash values are subtracted from 100 [Leonard III and Hardinge, 1991].

iv. Ash

The residue left by the coal after combustion of the sample is known as ash. The amount of ash formed may be less, equal or more than the mineral matter present in the coal. The combustion conditions and the composition of the mineral matter in the sample will have an influence on the properties and amount of ash produced during combustion [Leonard III and Hardinge, 1991; Speight, 2005].

3.3 Ash Fusion Temperature

The ash composition for different coals will vary according to the mineral matter that was present in the coal sample before burning. The ash fusion experiment was designed to study the behaviour of coal ash when it is heated in an oxidizing or reducing atmosphere. This experiment provides information on the temperatures at which the ash will start to get sticky and then start to melt [Speight, 2005; Leonard III and Hardinge, 1991]. By using the softening temperature value determined in this experiment, the slagging tendency and formation of clinkers can be estimated [Stutzer and Noè, 1940].

The ash of a coal sample is moulded into a standard cone shape. The cone is then placed in a furnace where it is heated according to the ASTM standard procedure [Speight, 2005]. Figure 3.2 shows the deformation of the ash cone along with the different temperature points at which these deformations takes place.

These four temperature points are;

- Initial deformation temperature (IT): The temperature where the cone starts to deform or fuse. Rounding of the tip of the cone can be seen [Speight, 2005].
- Softening temperature (ST): The temperature where the cone has fused into a spherical lump. The height of the cone and the width of the cone base are equal [Speight, 2005].
- Hemispherical temperature (HT): The temperature where the cone has fused to form a hemispherical lump. The height of the cone is half the width of the base [Speight, 2005].
- Fluid temperature (FT): The temperature where the cone has completely melted [Speight, 2005].

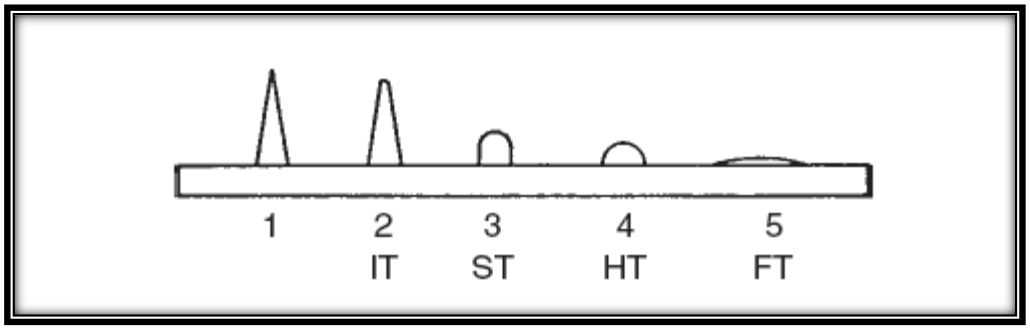

Figure 3.2: Temperature points [Speight, 2005]

3.4 X-Ray Diffraction and X-Ray Fluorescence

3.4.1 X-Ray Fluorescence (XRF)

XRF is a non-destructive analysis method that can be used on a variety of materials and different sample sizes [Bauer *et al*, 1978; Holler and Skoog, 1998]. Quantitative analysis of complex materials can be determined using this method [Holler and Skoog, 1998]. Known primary and secondary standards are used to determine the unknown intensities by comparing the test sample to these standards [Bauer, 1978].

The sample is bombarded with an X-ray beam. The resulting X-ray beams produced during this experiment are not only from the source beam but also generated from the atoms on the surface of the sample and also from atoms below the surface of the sample. The total intensity of the beam detected by the detector will depend on the concentration of the element producing the beam [Holler and Skoog, 1998; Bauer, 1978]. These beams are

analyzed by using a crystal that will reflect the different radiations produced into different angles [Leonard III and Hardinge, 1991]. In this study, XRF is used to determine the composition of ash attained from coal samples [Smith *et al*, 1994].

3.4.2 X-Ray Diffraction (XRD)

X-Ray diffraction is a non-destructive analytical method used to identify crystalline compounds present in a solid sample. Quantitative and qualitative data for the different crystalline phases can be obtained for these compounds [Holler and Skoog, 1998].

Samples are crushed to form a fine powder. The powder then contains a large number of small crystallites. When the X-ray beam passes through the sample, all the possible orientations and spacing of the crystallites will be reflected [Holler and Skoog, 1998]. Thus the crystalline compounds within the sample will refract the beams passing through the sample.

Using the refraction of the beams, two important values can be determined;

- The type of minerals present in the sample can be determined by the degree in which the X-ray beams are bent;
- And the amount of the minerals present can be determined from the amount of X-ray beams that are bent [Leonard III and Hardinge, 1991].

Identification of the crystalline minerals in the sample, the strongest peak or peaks on the graph is identified first according to a mineral that best relates to that peak position. Conformation of the mineral can then be made by finding the weaker peaks corresponding to the same mineral. When a set of peaks have been assigned to a mineral, the peaks are no longer considered in the identification of the other minerals present. The remaining peaks are solved by using the same technique until all the peaks have been assigned to a mineral [Moore and Reynolds, 1997].

3.5 CO_2 Surface area (BET)

Brunauer, Emmett and Teller developed a method to determine the surface area of a porous material. This method was based on the adsorption and desorption of nitrogen at low temperatures. Because coal consists of a variety of pore systems, the nitrogen used could not penetrate the micropores at these low temperatures as a result of its molecular volume and low activation energy at these low temperatures [van Krevelen and Schuyer, 1957].

Carbon dioxide adsorption and desorption has higher activation energy than nitrogen, and can therefore diffuse through the pore systems of the sample at low temperatures [van Niekerk *et al*, 2008].

By using the adsorption of carbon dioxide at low pressures and the Dubinin-Radushkevich model, this method has become the accepted way to determine the surface are of coal and char samples. Through determination of the surface areas of the coal or char, useful information may be obtained in understanding the reactivity of the sample [Sobolik et al, 1992].

3.6 Diffuse Reflectance Infrared Fourier Transform Spectrometry (DRIFT)

Using infrared spectroscopy on a sample, information on the structural and functional elements of the organic content present in the sample can be obtained. With coal samples, the presence of mineral matter in the sample may cause distortion of the peaks [Speight, 2005].

Diffuse Reflectance Infra-Red Fourier transform spectrometry is an easy way to obtain an IR spectrum for powdered samples. This method requires minimal sample preparation and the form in which the sample is used during these experiments are not altered much from their original form. During analysis of a sample, the powder is struck by a beam of radiation. The beam is directed to an ellipsoidal mirror which in turn reflects the beam to the sample. Because of a variety of elements present in the sample and the variety of orientations of these elements, the beam is reflected, scattered and absorbed before the beam is directed back to the detector. Because the sample is mixed with KBr as a dilutent, a reference sample is run. The ratio of the reference sample and the test sample is determined to give the reflectance of the test sample [Holler and Skoog, 1998]. Figure 3.3 represents the DRIFT attachment that can be placed inside the FTIR cell compartment.

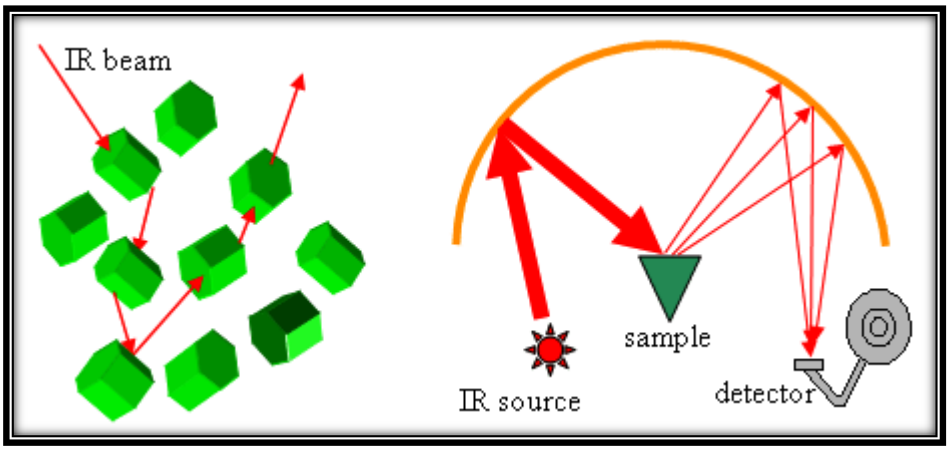

Figure 3.3: DRIFT attachment for an FTIR spectrometer [WEB 2]

3.7 Thermomechanical Analysis (TMA)

The use of thermomechanical analysis is to determine the dimensional changes undergone by a sample during heat treatment [Nel, 2009]. The samples are subjected to a specific heating program. The changes in the dimensions of the sample can be measured either as a function of temperature or as a function of time. The changes of the sample may occur as a result of chemical reactions, state changes of the sample, changes in the crystalline structure of the sample, etc.

The sample to be measured is placed on the support which is then moved into the furnace. Resting on the top surface of the sample is a probe, which will measure the dimensional changes of the sample as it is heated. A thermocouple is positioned near the sample within the furnace to indicate the temperature at a specific time during the heating program. During the heat treatment of the sample, a constant flow of gas is present within the instrument to prevent any oxidation occurring and also to promote heat transfer within the furnace [WEB 3]. A schematic representation of the thermomechanical analysis setup is presented in Figure 3.4.

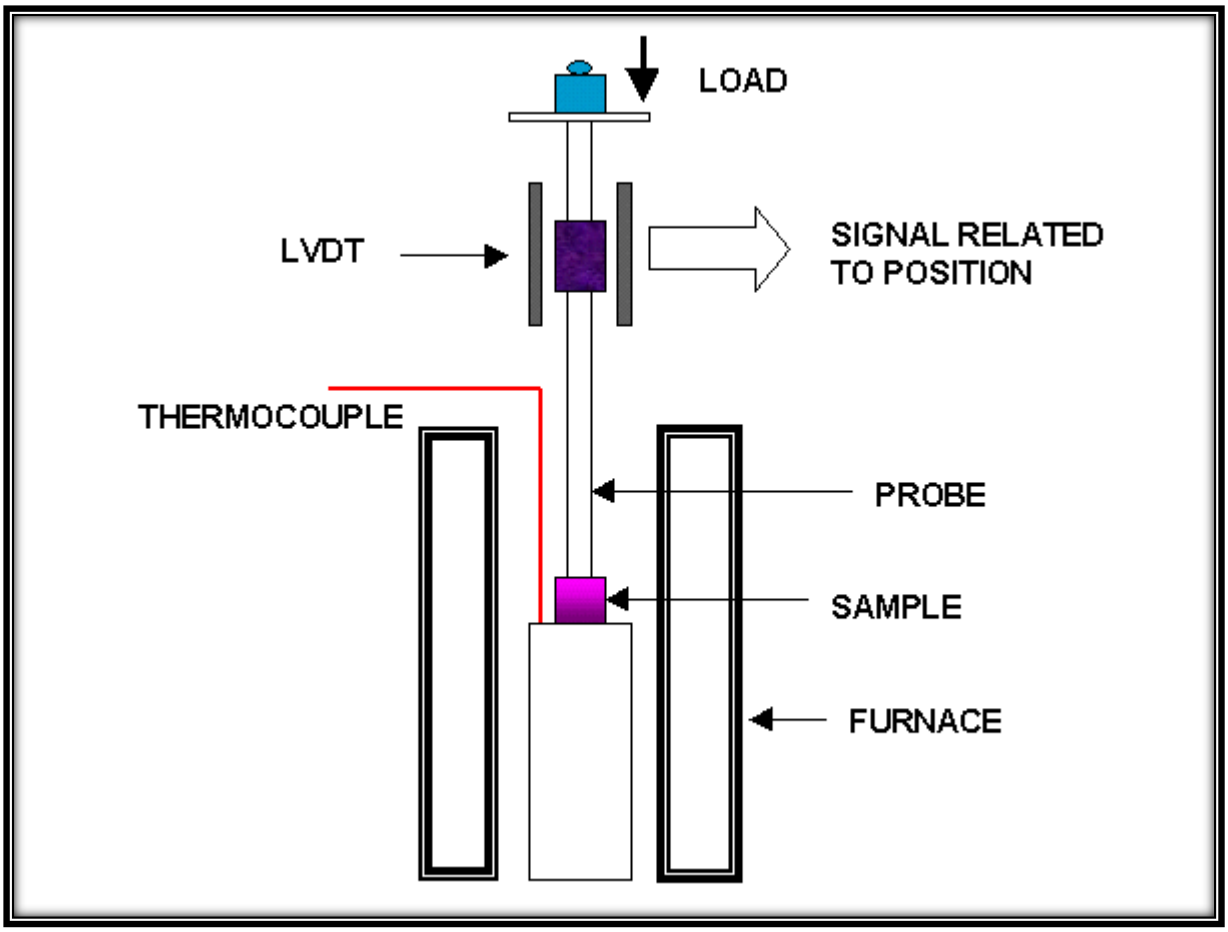

Figure 3.4: Thermomechanical analysis setup

3.8 Dilatometry

When determining the plastic behaviour of coal samples, dilatometry may be used as a measurement to determine these properties. One of the benefits of using dilatometry in determining the plastic behaviour of samples is that samples with the sample free swelling index will produce different dilatation results. The dilatometric behaviour of a sample is measured as a function of temperature where the sample is heated at a constant heating rate. During heat treatment, the sample goes through a plastic stage where volume changes occur [Schobert, 2013].

Dilatometry is characterized by three different parameters.

i. Contraction: when the sample shrinks during the first stages of heating
ii. Swelling: the change of sample volume measured from the lowest point during the contraction stage to the maximum volume reachable.
iii. Dilatation: the change in volume of the sample after the re-solidification stage compared to the volume of the sample before heat treatment [Schobert, 2013].

During the heat treatment of the samples, the coal particles will start to soften and deform and enter the metaplast state. Thus the contraction phase of the sample can be seen. Upon further heating of the sample, gas will be evolved from the sample. This will cause the metaplast to swell. When the swelling of the sample passes the initial contraction phase, an increase in the volume of the sample will be observed.

Four classes of plastic behaviour can be determined from this method;

i. Subplastic;
ii. Euplastic;
iii. Perplastic;
iv. Fluidoplastic.

When a sample is subjected to this analysis, one of these classes can then be assigned to the sample to explain its plastic behaviour. Figure 3.5 shows the graphs for the different classes for plastic behaviour [Schobert, 2013].

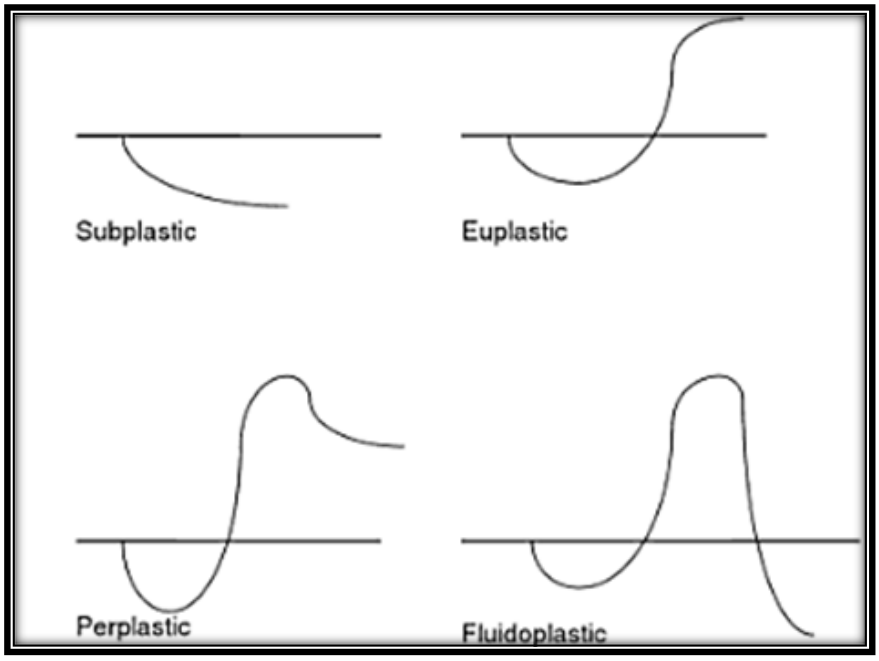

Figure 3.5: Classes of plastic behaviour [Schobert, 2013]

3.9 Thermogravimetric Analysis / DSC-Mass Spectroscopy (TG / DSC-MS)

3.9.1 TG

Small samples can be analyzed using this method to gain quantitative information on the mass loss behaviour of solid compounds as it undergoes heat treatment. Depending on the heating procedure and the equipment, a sample can be heated to high temperatures at a heating rate of 0.1°C/min to 100°C/min. It is therefore important that the furnace is insulated to prevent any heat transfer to the balance. The balance is used to determine the loss in mass of a sample [Holler and Skoog, 1998]. The rate at which this mass loss takes place is also measured during the heat treatment. Sample measurements take place in a controlled atmosphere and sometimes in an inert atmosphere. Any mass loss for a sample can be measured as a function of time or temperature.

3.9.2 DSC

While the sample temperature is changed, the heat flow into the sample and that of a reference pan is measured. The sample pan and that of the reference are heated in the same furnace with the same heating rate. Exothermic reactions will show an increase of the heat flow on a DSC graph and an endothermic reaction will show a decrease of the heat flow on the graph [Holler and Skoog, 1998].

3.9.3 MS

Mass spectrometry is used in many instances where gaseous species needs to be identified. During this method, a small amount of the gases that are to be analyzed are bombarded with a beam of electrons, which will collide with the gas species and remove an electron, thus forming a radical with a positive charge. When these charged particles move through the mass analyzers, the charged ions will separate according to their individual masses. The detector then registers these charged ion masses and converts the information received into an electrical signal. A spectrum of these signals is then generated [Silverstein et al, 2005]. A representation of the pathway followed by the sample in a mass spectrometer is presented in Figure 3.6.

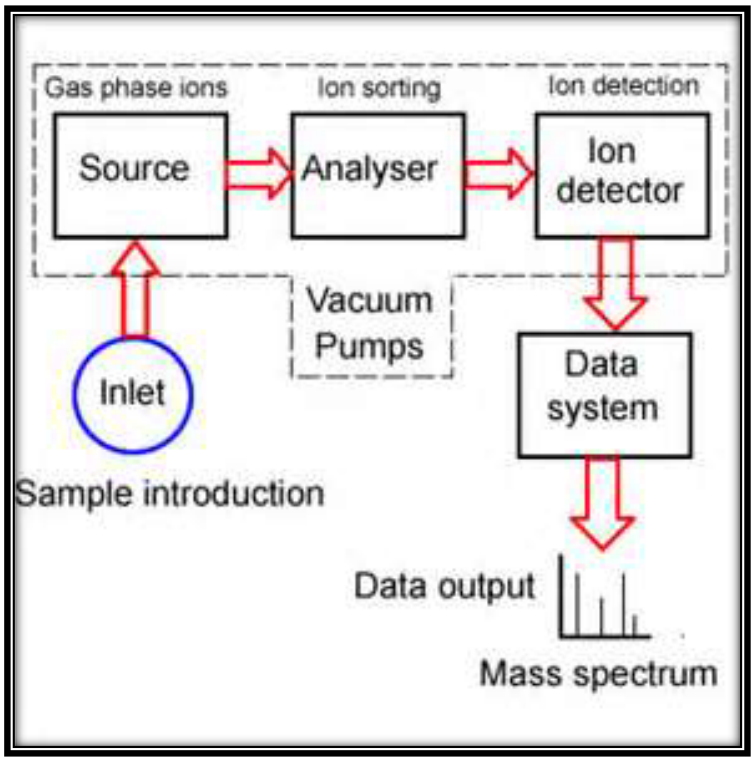

Figure 3.6: Pathway followed in as mass spectrometer

By joining a mass spectrometer with the TG, information about the volatile species evolved during the heat treatment can be gained. The amount of volatiles released and the chemical structure of these volatiles will depend on the heating conditions and on the original composition of the sample. Quantification of the information obtained is not possible because of the small size of the sample used during the experiment [Speigh, 2005].

Chapter 4

Experimental Procedures

In this chapter the different experimental procedures that were followed in this study will be described. The procedure used to demineralize the coal, also the selection and addition of the catalysts to the coal will be given. The different methods of analyses that were performed on the coal, demineralized coal and demineralized coal-alkali blends will be described.

4.1 Raw materials

4.1.1 Coal

The coal that was selected for this study comes from the Tshikondeni mine located in the Limpopo province. The selection of this coal was based on its high swelling properties that the coal exhibits during pyrolysis, which is the main focus of the study. The coal sample was crushed to -75 µm and then vacuum sealed to prevent oxidation. These sealed bags were stored at low temperatures until needed.

4.1.2 Materials

The chemicals and gases used throughout this study in the experimental procedures are listed in Table 4.1.

Table 4.1: Chemicals and gases used during experiments

Chemicals/Gases	Grade
32% Hydrochloric Acid	Analytical grade supplied by ACE Chem
40% Hydrofluoric Acid	Analytical grade supplied by ACE Chem
Nitrogen	Analytical grade supplied by Afrox
Carbon Dioxide	Analytical grade supplied by Afrox

4.1.3 Alkali compounds

Ten different alkali compounds (as listed in Table 4.2) were selected; five of which were calcium compounds and the other five were potassium compounds. Four of these compounds were selected for further study according to their influence on the coal swelling properties. Each of the compounds was ground to a powder using a mortar and pestle. Crushing of the alkali compounds prior the addition to the demineralized coal is to ensure thorough mixing to produce a homogeneous sample. The compounds were then dried in a vacuum oven for 12 hours at 60°C before use.

Table 4.2: Inorganic compounds used during this study

Alkali Salts	Grade
KOH	Analytical grade supplied by Merck
KCl	Analytical grade supplied by Rochelle Chemicals
K_2CO_3	Analytical grade supplied by Merck
KCH_3CO_2	Analytical grade supplied by Merck
KCO_2H	Analytical grade supplied by Industrial Analytical Ltd
$Ca(OH)_2$	Analytical grade supplied by Merck
$CaCl_2$	Analytical grade supplied by BDH Chemicals Ltd
$CaCO_3$	Analytical grade supplied by Merck
$Ca(CH_3CO_2)_2$	Analytical grade supplied by Merck
$Ca(CO_2H)_2$	Analytical grade supplied by Industrial Analytical Ltd

4.2 Demineralization of coal

Minerals can be removed from a coal sample using a number of different methods depending on the physical properties of the coal [Bolat *et al*, 1998]. Through use of sequential acid leaching of the coal, mineral matter can be removed from the coal, leaving less than 3% of the original content. It was found that during the HCl and HF leaching

processes, that the acids reacted with the minerals, thus rendering the insoluble minerals soluble [Steel and Patrick, 2001; Bolat *et a*l, 1998]. These soluble compounds can then be washed out of the coal [Oboirien *et al*, 2010].

500 g of the coal sample was weighed and the coal was washed in 2 L of a 5 M HCl solution for 24 hours. The coal was filtered and then washed in a 5 M HF solution for 24 hours. The coal was filtered again and then re-washed with 5 M HCl for 24 hours [van Niekerk *et al*, 2008]. The leaching procedures were done at room temperature. After this, the coal was washed with distilled water until a neutral pH was obtained. The filtering of the coal during washing was achieved by using a compressed air filtering system. The coal was dried under vacuum at 60°C. The dried coal was stored in a desiccator under nitrogen.

4.3 Free Swelling Index

In order to select four of the compounds from the 10 alkali compounds, the demineralized coal with 5 K/Ca-wt% (mass) alkali compound addition was subjected to free swelling index experiments (see paragraph 3.1). From these results, 3 alkali compounds, which showed an influence on the swelling of the coal, were selected and one alkali compound with no influence was chosen to act as a control for the compounds.

To prepare the samples, the demineralized coal and alkali compounds were weighed to prepare a 5 wt% alkali addition sample. The demineralized coal and alkali compounds were mixed using a Fritsch Analysette 3 Spartan Pulverisette 0 (Figure 4.1) ball mill. Using the 1ISO 501: 2003 method the experiment was conducted as follow: 1 g of the coal sample and the amount of alkali compound required to make up a 5 wt% addition thereof was placed in a clean crucible. The crucible was tapped on a bench to ensure a level surface on the coal. The crucible was covered with a lid. The covered crucible was placed on a triangle above the flame and heated to 820°C in 2.5 min. The gas was turned off and the crucible was left to cool down. The resulting coke button was then assigned a free swelling number according to the index (see paragraph 3.1, Figure 3.1). Each measurement was performed three times to ensure repeatability.

4.4 Tube Furnace Experiments

Tube furnace experiments for the raw coal, demineralized coal and demineralized coal-alkali blends with 10 wt% alkali addition to the coal was done to determine the effect pyrolysis had on the composition of these samples.

4.4.1 Sample Preparation

For the tube furnace experiments, 10 wt% of each of the chosen alkali compounds was separately added to demineralized coal. The samples were then placed into a ball mill container with a stainless steel ball. A Fritsch Analysette 3 Spartan Pulverisette 0 (Figure 4.1) was used to mix the samples thoroughly. The amplitude of the mill was set to 3 mm. Each sample was milled for 15 min to ensure good mixing, after which it was removed and placed into the tube furnace.

Figure 4.1: Mill used to obtain good mixtures the coal and alkali salt samples

4.4.2 Heating procedure

An Elite thermal system TSH 12/75/610-2416CG+2116 O/T furnace (Figure 4.2) was used for the heat treatment of the samples. 30 g of the prepared samples were weighted in each of the 2 heating boats. The boats were inserted into the furnace, in the centre of the tube where the temperature is approximately uniform. The nitrogen flow through the tube was 100 mL/min. The samples were left for 15 min to ensure that the sample was covered with nitrogen and the air purged to form an inert atmosphere. The program was set to a heating rate of 10°C/min from ambient temperature up to a maximum of 1200°C. Once 1200°C was

reached, the samples were to cool to room temperature under nitrogen. Photos of the sample products were taken from above. After the photos were taken, the sample products were crushed and stored under nitrogen for further analyses. For the raw coal, only 15 g could be used at a time due to the high swelling properties of the coal.

Figure 4.2: Elite thermal system tube furnace

The samples prepared in the tube furnace were analyzed using the techniques of ultimate and proximate analyses, DRIFT, CO_2 BET, XRF, XRD, and AFT (see paragraph 4.5 - 4.10).

4.5 Composition analyses of coal

Ultimate and proximate analyses were carried out according to the following ASTM standard methods listed in Table 4.3. The raw coal, demineralized coal and the demineralized coal-alkali blends that were pyrolyzed in the tube furnace (with the maximum alkali compound additions) were selected for further analyses. These analyses were not only done on the char samples but also done on the raw coal and demineralized coal.

Table 4.3: Methods used to characterize the samples

Ultimate analyses	ISO 29541 [SABS ISO; 2010]
Proximate analyses	
Moisture	SANS 5925 [SABS; 2007]
Ash Content	ISO 1171 [SABS ISO; 2010]
Volatile Matter	ISO 562 [SABS ISO; 2010]
Total sulphur	ISO 19579: 2006 [SABS ISO; 2006]
Fixed Carbon	Calculated

4.6 Ash Fusion Temperature

The ash fusion temperature measurements were done according to the ISO 540/SANS 43 method [SABS; 2008]. According to the method described in the standard, the coal sample is pressed into a standard shape. This shape has sharp edges to better observe the changes taking place.

4.6.1 Sample preparation

The ash used in this experiment was prepared according to the ISO 1171 method. The ash was ground and mixed with demineralized water and mixed into a paste. The paste is then moulded into the standard shape used during the experiment. The moulded sample was then allowed to dry before heating in a furnace to remove any water molecules still present in the sample.

4.6.2 Method

The sample was placed inside the furnace. The flow rate of the reducing atmosphere was set to the appropriate rate. The furnace was heated to a temperature below the temperature where deformation of the sample starts. After some time the heating rate was increased and the transformation of the samples observed and the results recorded.

4.7 X-Ray Fluorescence

The XRF sample analyses were done according to the ASTM D4326 standard method [ASTM; 2012]. The raw coal, demineralized coal and demineralized coal-alkali blends with the 10 wt% alkali additions were used.

4.8 X-Ray Diffraction

XRD analyses of the samples were done using a PANalytical X'Pert Pro powder diffractometer with an X'Celerator detector and variable divergence and fixed receiving slits with Fe filtered Co-Kα radiation. The phases were identified using X'Pert Highscore plus software. The relative phase amounts were estimated using the Rietveld method [Rietveld, 1969]. The raw coal, demineralized coal and demineralized coal-alkali blends with the 10 wt% alkali additions were used.

4.9 CO_2 Micropore surface area (BET)

4.9.1 Equipment

A Micromeritics ASAP2020 surface area analyzer was used to determine the CO_2 BET adsorption values of each sample, in order to calculate the micropore surface areas using the Dubinin-Radushkevich method [Sobolik *et al*, 1992]. The raw coal, demineralized coal and demineralized coal-alkali blends with the 10 wt% alkali additions were used.

4.9.2 Method

0.2 g of sample was weighed and then placed into a glass tube. The sample was degassed for 48 hours at 25°C. After degassing, the sample was analyzed by carbon dioxide adsorption and desorption at 0°C. The raw coal, demineralized coal and demineralized coal-alkali blends with the 10 wt% alkali additions were used.

4.10 Diffuse Reflectance Infrared Fourier Transform Spectroscopy

A Vertex 70 DRIFT spectrometer (Figure 4.3) was used to obtain the infrared spectroscopic spectra. 20-25 mg of the specific coal sample was mixed with ± 200 mg KBr. The sample mixing was done in a Wig-l-Bug to ensure thorough mixing. All the samples were prepared in the same way under the same conditions. The samples were placed in an oven at 60°C under vacuum for 24 hours. Before analysis, the samples were left for 30 minutes in a desiccator to cool to room temperature. The samples were scanned from wavelengths of 4000 cm^{-1} to 370 cm^{-1}. The raw coal, demineralized coal and demineralized coal-alkali blends with the 10 wt% alkali additions were used.

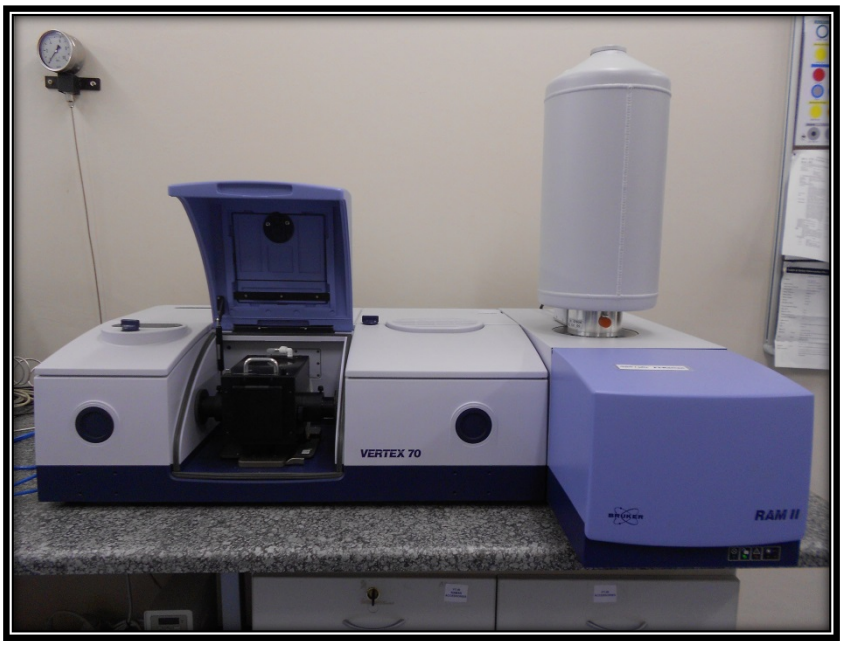

Figure 4.3: DRIFT spectrometer

4.11 Thermomechanical Analysis

4.11.1 Sample Preparation

1 g of coal and the mass needed to make up a specific wt% of the alkali compound were mixed in a wig-l-bug to obtain well mixed samples. This coal-alkali compound mixture was then mixed with water. The amount of water added was 10% of the weight of the sample it was added to. After mixing with the water, 0.3 g was weighed and a pellet was pressed using an Ametek Lloyd Intruments LRXplus. These pellets were then placed inside a vacuum oven for 12 hrs. to dry. The temperature used for the drying of the pellets was 60°C.

4.11.2 Heating Procedure

The dried pellet was placed into a stainless steel tube, the same width of the sample, between two stainless steel disks (1 mm each). The sample was then placed into the TMA (Figure 4.4). The sample was heated under nitrogen with a heating rate of 10°C/min and heated to 1000°C. Each sample measurement was repeated three times to ensure repeatability. Values reported are the average of the three measurements.

Figure 4.4: TMA (SII Technology TMA/SS6100 with EXSTAR6000)

4.12 Dilatometry

The dilatometry was done according to the ASTM method D5515. During these experiments, the coal is mixed with distilled water to form a pencil. The weight of the pencil is noted and the sample inserted into the furnace. The experiment is stopped when no further changes in volume can be detected. The raw coal, demineralized coal and demineralized coal-alkali blends with the 10 wt% alkali additions were used.

4.13 TG / DSC-MS

4.13.1 Sample Preparation

1 g of coal and the mass needed to make up the specific wt% of the alkali compound was mixed in a wig-l-bug to obtain well mixed samples. These were then used in the TG / DSC-MS.

4.13.2 Heating procedure

A SDT Q600 TGA coupled with a Cirrus mass spectrometer (Figure 4.5) was used to measure mass loss with increased temperature profiles, as well as obtain the mass spectra of the evolved gases (only low molecular mass gaseous compounds). 10 mg of sample was weighted in the crucible and placed in the thermogravimeter. The procedure was set with a

heating rate of 10°C/min and a nitrogen flow of 100 mL/min. The sample was heated to a temperature of 1200°C. Mass fragments for the evolved gases for the different samples were identified using the mass spectrometer. Each sample was repeated to assure repeatability. Mass loss spectra reported are the average of the repeated measurements.

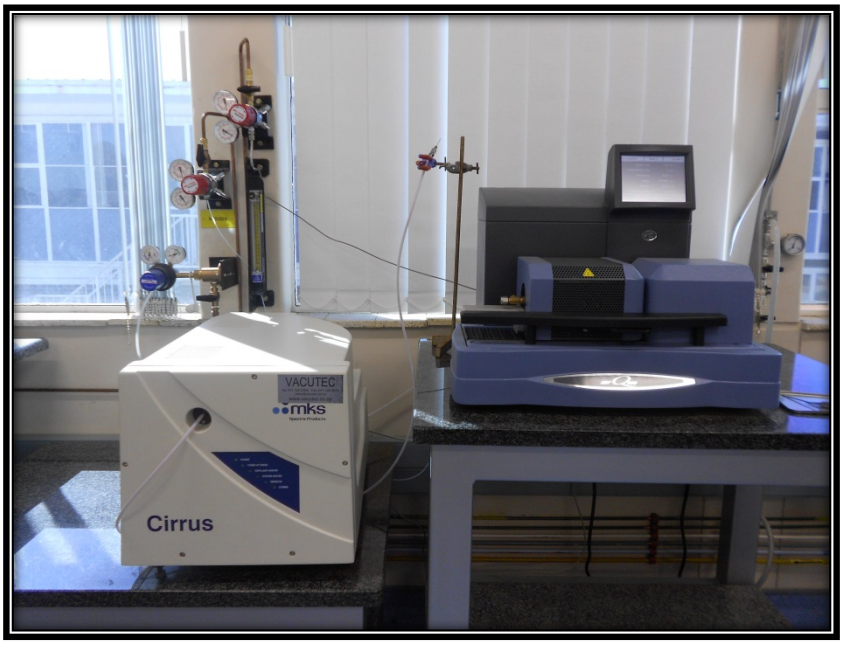

Figure 4.5: TG/DSC-MS instrument

Chapter 5

Results and Discussions

Coal Characterization

In this chapter the results of the different characterization techniques used on the raw coal, demineralized coal and four coal samples with alkali compound additions will be given and discussed. Eight samples were subjected to these characterization techniques; the raw coal, demineralized coal, and six char samples. The six char samples originated of raw coal, demineralized coal and the four demineralized coal-alkali blends. The four samples with the added alkali compound used, had a 10 wt % alkali compound addition. The influence of demineralization, the drying process, alkali compound addition and pyrolysis have on the samples will be discussed in this chapter.

The characterization techniques used and discussed in this chapter are the following:

- *Free swelling index (FSI);*
- *Ultimate analysis;*
- *Proximate analysis;*
- *Ash Fusion temperature (AFT);*
- *X-Ray Fluorescence (XRF);*
- *X-Ray Diffraction (XRD);*
- *CO_2 Surface Area (BET);*
- *Diffuse Reflectance Infrared Fourier Transform Spectrometry (DRIFT);*

5.1 Free Swelling Index

As described in Chapter 3 (see paragraph 3.1), the swelling indices for each of the samples, determined from the standard index profiles, will give an indication of the swelling propensity for the samples. Index numbers range from 1 to 9, with 9 being assigned to coal samples with the highest swelling propensity and 1 for coal samples which do not indicate any swelling propensity.

Samples used in the free swelling index experiments were the raw, demineralized coal and the demineralized coal-alkali blends with a 5 wt% alkali addition. By repeated measurements of the free swelling indices for the different samples, the averages could be determined for each of the samples. Presented in Table 5.1 are the average indices values determined for the different samples.

Table 5.1: Free swelling indices for the following samples; raw coal, demineralized coal, five potassium compound blends and five calcium compound blends to demineralized coal

Sample	**Index No**	**Sample**	**Index No**
Raw Coal	8	Demin Coal	8.5
Demin + KOH	6.5	Demin + $Ca(OH)_2$	5.5
Demin + KCl	8.5	Demin + $CaCl_2$	8
Demin + K_2CO_3	7.5	Demin + $CaCO_3$	8
Demin + KCH_3CO_2	4	Demin + $Ca(CH_3CO_2)_2$	7
Demin + $K(CO_2H)$	7	Demin + $Ca(CO_2H)_2$	8.5

*Demin = Demineralized coal

When coal samples are subjected to an acid leaching process, most of the minerals are removed from the coal [Steel and Patrick, 2001]. With low amounts of minerals present in the coal, as with the demineralized coal, the swelling of the coal increased in comparison to that of the untreated coal. Some minerals removed from the coal may play an important role in the reduction of the swelling of the coal [Bexley *et al*, 1986]. This may be the reason the demineralized coal has a higher swelling index number of 8.5 than the raw coal sample (swelling index = 8).

From Table 5.1 it can be seen that the potassium compounds had a more pronounced effect on decreasing the swelling of the coal compared to that of the calcium compounds. The different potassium compounds represent a variety of swelling numbers, indicating that the anion bound to the potassium has an influence on the catalytic activity during heat treatment [Bexley *et al*, 1986]. With the addition of the potassium compounds to the demineralized coal, a wider range of influence on the coal was observed when compared to the blends with the added calcium compounds. Since potassium compounds have a lower melting point than the calcium compounds, they will melt and therefore be more evenly distributed over the surface of the char. With the potassium compounds distributed over the surface of the coal, catalysed reactions occur on the whole surface of the sample. Calcium compounds do not exhibit this tendency to melt at low temperatures, thus distribution of the salt would not occur to the extent as for potassium salts. Thus the catalytic activity of calcium compounds during heat treatments would depend to a larger extent on the loading method [Liu and Zhu, 1986].

Due to the wider range of influence on the swelling index numbers with the addition of the potassium compounds, compared to the calcium compound addition, as can be seen in Figure 5.1, it was decided to proceed with the study by using the potassium compounds. The influence of the potassium compound additions to coal will thus be investigated with regard to the swelling and reactivity of the coal. The potassium compounds that were used in this study are: KOH, KCl, K_2CO_3 and KCH_3CO_2. It was decided to exclude $K(CO_2H)$ from further studies, since the swelling index number found for the sample with the added $K(CO_2H)$ was almost the same as that of the sample with the added K_2CO_3.

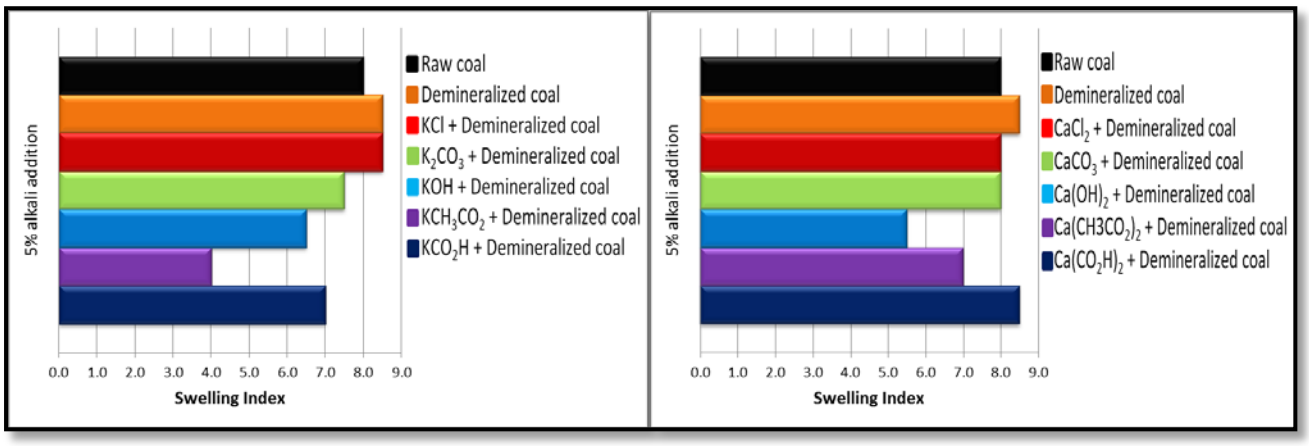

Figure 5.1: Schematic representation of the free swelling indices

5.2 Tube Furnace experiments

Presented in Figure 5.2 a-f are photographs of the coal samples used in this study after thermal treatment in the tube furnace (see paragraph 4.4). These photographs are for the raw coal, demineralized coal and the demineralized coal-alkali blend samples.

Figure 5.2a: When the raw coal sample is compared to the other samples, there is a visible difference in the appearance of the sample. The raw coal sample was lighter in colour and chambers inside the sample where gas was trapped during the heat treatment were visible. The sample broke during the resolidification stage.

Figure 5.2b and c: When comparing the demineralized coal and 10 K-wt% KCl + demineralized coal samples to those of the raw coal sample, these samples exhibited swelling behaviour during the heat treatment. Chambers formed during this heat treatment, are still present but to a much lesser extent compared to that of the parent coal. When comparing the swelling behaviour of the demineralized coal and the demineralized coal-KCl blend, the two samples show the same amount of swelling according to their swelling indices (see Table 5.1). From these result the assumption can be made that KCl does not affect the swelling behaviour of the coal during the pyrolysis stage.

Figure 5.2d, e and f: The last three samples, the 10 K-wt% KOH + demineralized coal, 10 K-wt% K_2CO_3 + demineralized coal and 10 K-wt% KCH_3CO_2 + demineralized coal did not show the swelling behaviour as the previous samples did.

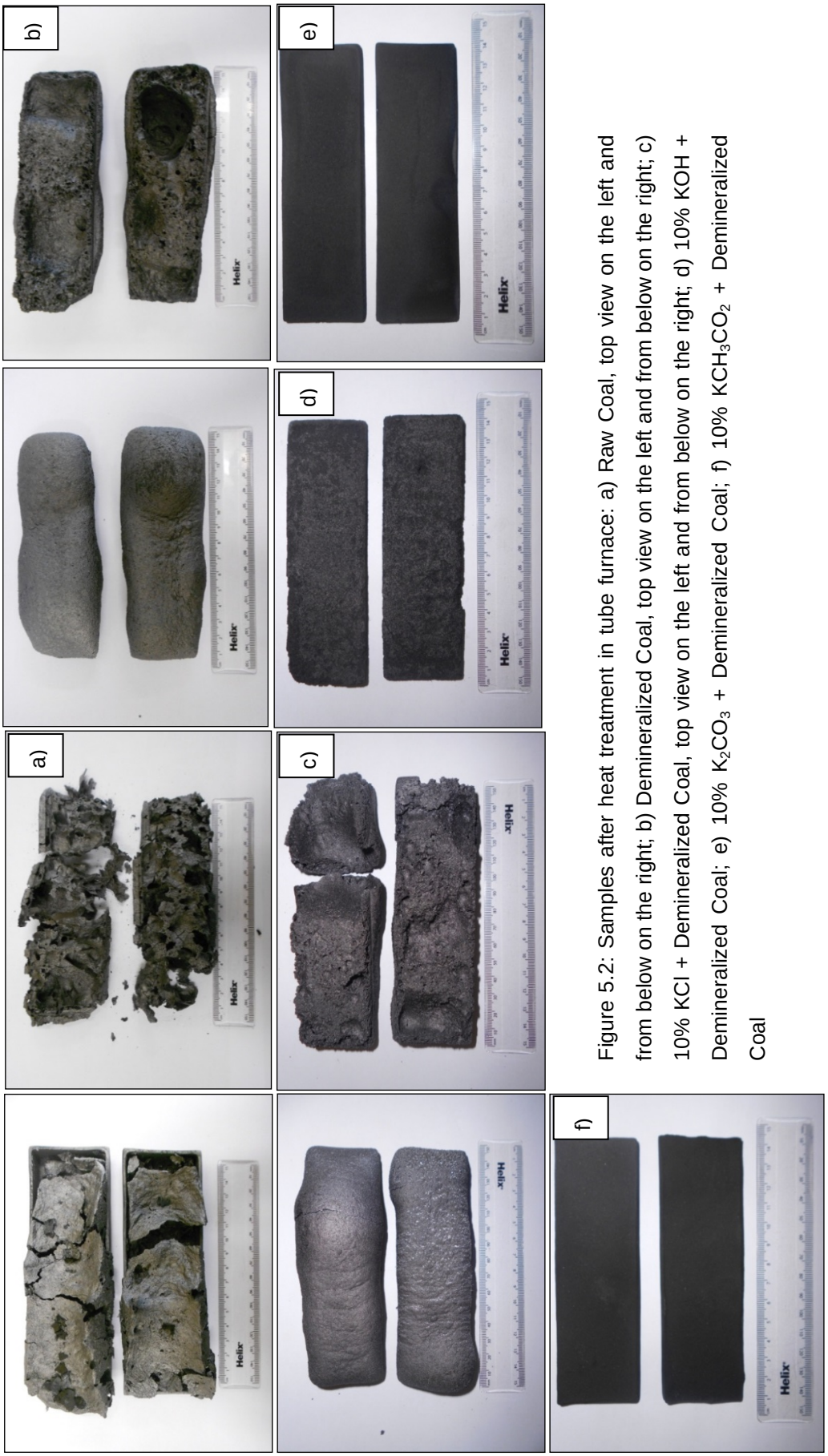

Figure 5.2: Samples after heat treatment in tube furnace: a) Raw Coal, top view on the left and from below on the right; b) Demineralized Coal, top view on the left and from below on the right; c) 10% KCl + Demineralized Coal, top view on the left and from below on the right; d) 10% KOH + Demineralized Coal; e) 10% K_2CO_3 + Demineralized Coal; f) 10% KCH_3CO_2 + Demineralized Coal

5.3 Ultimate and Proximate Analysis

5.3.1 Ultimate analysis

Table 5.2 presents the values for the ultimate analyses done on the raw coal and on the demineralized coal. These values were determined on an air-dried / dry-ash free basis. The ultimate analyses values presented in Table 5.3 are for the char samples prepared as described previously (see paragraph 4.5). The char samples are: raw coal char, the demineralized coal char and the four samples prepared from the demineralized coal with 10 K-wt% alkali compound addition. The values presented are dry and ash free.

From Table 5.2 it can be seen that the carbon content of the demineralized coal decreases compared to the content for the raw coal sample. This decrease was due to an increase in the oxygen content of the demineralized coal. This increase in the oxygen value may be caused by oxidation of the sample during storage or during the demineralization process.

Table 5.2: Ultimate analysis of the raw coal and demineralized coal samples

	Raw Coal (daf)	Demin Coal (daf)
%Carbon	90.1	87.3
%Hydrogen	4.9	4.8
%Nitrogen	2.1	2.0
%Sulphur	0.9	0.8
%Oxygen	1.2	5.0

*Demin = Demineralized coal

From the values in Table 5.3, it can be seen that there was a small increase in the oxygen content for the KCl and KCH_3CO_2 blended samples. For the KCl blend, it may be caused when the potassium reacts with water molecules to form K_2O which will increase the percentage oxygen in the sample [Veraa and Bell, 1978]. There was no significant increase or decrease observed when comparing the oxygen content of the other potassium compound blended samples.

Table 5.3: Ultimate analyses of the chars prepared from the raw coal, demineralized coal and the four demineralized coal-alkali blends with 10 K-wt% addition

	Raw Coal Char (daf)	Demin Coal Char (daf)	KOH + Demin Coal Char (daf)	KCl + Demin Coal Char (daf)	K_2CO_3 + Demin Coal Char (daf)	KCH_3CO_2 + Demin Coal Char (daf)
%Carbon	97.1	97.5	96.9	95.9	96.9	95.1
%Hydrogen	0.1	0.0	0.3	0.3	0.2	0.6
%Nitrogen	1.8	1.8	1.8	1.9	2.0	2.00
%Sulphur	0.9	0.8	0.9	0.6	0.8	0.8
%Oxygen	0.1	0.0	0.0	1.4	0.1	1.5

*Demin = Demineralized coal

When comparing the values of the raw and demineralized coal to the values of the chars for the raw and demineralized coal samples (Tables 5.2 and 5.3), it can be seen that there was an increase in the carbon content for both the raw coal char and demineralized coal char. When comparing the coal samples to the char samples, there is a decrease in all the values for the other elements determined. This decrease in values is caused by the release of volatile matter during the heat treatment of the samples. From the TG results presented in Chapter 7, it was seen that the evolution of volatiles was responsible for some of the weight loss observed for the blended samples. The percentage volatiles released for each of the samples will be shown in the proximate analysis.

5.3.2 Proximate analysis

The proximate analysis values determined for the raw and demineralized coal samples are presented in Table 5.4. The values determined for the char samples are presented in Table 5.5. The char samples are: raw coal char, the demineralized coal char and the four samples prepared from the demineralized coal with 10 K-wt% alkali compounds. The results are reported in Table 5.4 and 5.5 are on an air-dried basis.

When comparing the raw and demineralized coal samples, it can be seen from Table 5.4 that there was a significant decrease in the ash content. This decrease for the ash value is as a result from the leaching process where the minerals are removed from the coal, thus decreasing the overall ash content of the sample, confirming previously reported research on acid leaching procedures [van Niekerk *et al*, 2008]. There were no significant changes of the

other values determined for the raw and demineralized coal samples. An increase in the fixed carbon content can be seen as the ash content decreased.

Table 5.4: Proximate analysis of the raw coal and demineralized coal samples

	Raw coal	Demin coal
% Inherent Moisture	0.7	0.1
% Ash	17.7	0.6
% Volatile Matter	20.4	21.8
% Fixed Carbon	61.3	77.5

*Demin = Demineralized coal

From Table 5.5, it can be seen that the ash content of the demineralized coal char sample had decreased compared to that of the raw coal char sample. The percentage volatile matter for the raw coal char and that for the demineralized coal char are the same since most of the volatiles were released during the pyrolysis process.

When comparing the alkali compound blended samples to the demineralized coal char sample, it can be noted that there was a decrease in the fixed carbon content of the samples as the ash content increased for each sample. The percentage ash for each sample will be determined by the amount of the compound that was added to the coal sample. The samples with the alkali compound additions showed an increase in the volatiles released during this experiment when compared to the demineralized coal sample. One reason for the increase in the volatile matter values may be decomposition/sublimation of the alkali compounds, or reactions taking place between the alkali compounds and the coal.

(1) During heat treatment of KCl, the alkali compound may have decompose and to form K and Cl_2. But when H_2O is present in the sample, K_2O and HCl will form [Veraa and Bell, 1978]. From the XRD results (see Table 5.8), a small amount of the KCl added to the coal seems to have formed a sylvine crystalline structure within the coal.

(2)Decomposition of KOH will produce the following products; H_2O and K_2O. The K_2O reacts with the coal during the heat treatment and may form K and CO [McKee, 1983]. When following the reactions of KOH with C, the volatiles released by the samples with the added KOH will consist of H_2O, K and CO.

(3) The decomposition of K_2CO_3 will form K_2O and CO_2. The formed K_2O may react with the coal and produce the same products as explained for KOH, which is K and CO. The K_2CO_3 may also react with the coal without decomposing first when heated, and form potassium vapour and CO [McKee, 1983]. Following these reactions where the alkali compound decomposes and then reacts with the coal the following volatiles are released; K, CO_2 and CO. If the K_2CO_3 reacts with the coal without decomposing, K and CO are released.

(4)The decomposition of KCH_3CO_2 follows a series of reactions. During these reactions, K_2CO_3 is formed in the first step. Volatiles formed during this step include CO and C_2H_6/CH_4+ $CH_2/2CH_3$. The K_2CO_3 decomposes further to form K_2O and CO_2. The K_2O will then react with the coal and form K and CO [Afzal, 1991].

Thus the amount of volatiles released during the heat treatment will depend on the ions bound to the potassium, the amount of the compound added to the coal and the presence of moisture and minerals (see Chapter 7.1.1.1 for decomposition equations).

Table 5.5: Proximate analysis of the chars prepared from the raw coal, demineralized coal and the four demineralized-alkali blends with the 10 K-wt% additions

	Raw Coal Char	Demin Coal Char	KOH + Demin Coal char	KCl + Demin Coal char	K_2CO_3 + Demin Coal char	KCH_3CO_2 + Demin Coal char
% Inherent Moisture	0.0	0.1	1.8	0.2	1.5	0.0
% Ash	17.7	2.2	14.4	15.3	17.0	16.1
% Volatile Matter	0.7	0.7	2.9	1.1	5.3	6.1
% Fixed Carbon	81.6	97.0	80.9	83.4	76.6	77.8

*Demin = Demineralized coal

When comparing the raw and demineralized coal samples with the char for the raw and demineralized samples, it was clear that volatiles are released during the heat treatment of the samples. The ash content for the raw coal sample and the raw coal char sample did not change. There was an increase in the ash content for the demineralized coal char sample. This increase may be due to a decrease in the volatiles and thus a decrease in the total mass of the sample from which these values have been normalized.

5.4 Ash Fusion Temperature

Ash fusion temperatures for the raw coal and demineralized coal samples are presented in Table 5.6. When comparing the initial deformation temperature for these two samples, it can be seen that they do not differ much from one another. But from Table 5.6, it can be seen that there was a decrease of approximately 100°C in the softening temperature of the ash samples when comparing the demineralized coal to that of the raw coal sample. This reduction in the temperature might be due to the removal of minerals and clay from the coal during the demineralization process. As the raw and demineralized coal samples passed through the other stages until the fluidity temperature was reached, a temperature difference of about 150°C could be seen when comparing the samples to one another. By removing the minerals from the parent coal, the possibility of interaction and possible catalytic influence between the minerals and the coal are removed and thus a lowering of the softening temperature is observed for the sample.

Table 5.6: Ash fusion temperatures of the chars prepared form raw coal and demineralized coal

	Raw Coal (°C)	Demin Coal (°C)
Initial deformation temperature	1261	1242
Softening temperature	1383	1266
Hemispherical temperature	1448	1302
Fluid temperature	1494	1358

*Demin = Demineralized coal

5.5 X-Ray Diffraction and X-Ray Fluorescence Analyses

5.5.1 X-Ray fluorescence (XRF)

XRF analysis was done on two coal and six char samples. The raw and demineralized coal represents the two coal samples. The six char samples consist of the following: raw coal char, demineralized coal char and the four demineralized coal-alkali blends. The normalized results obtained for these samples are presented in Table 5.7. These normalized values in Table 5.7 are determined on a dry and LOI free basis.

According to the XRF analysis, the raw coal was made up primarily of silica oxide (SiO_2) and aluminium oxide (Al_2O_3). When comparing the XRF results for the raw coal and the

demineralized coal samples, it is clear that there is a decrease in these compounds within the demineralized coal sample. During the leaching process (see Chapter 4, paragraph 4.7), the hydrofluoric acid will react with the silica oxide and aluminium oxide to form more soluble compounds that can then be washed from the coal. There was also a decrease in the other minerals present in the coal, indicating that the leaching process removed most of the clay minerals from the coal.

After the addition of the potassium compounds to the demineralized coal and mechanical mixing, the samples were charred and the composition of the ash determined. From the values presented in the Table 5.7, it is clear that there was an increase in the potassium oxide (K_2O) for the samples with the added compounds. This may be due to transition of the potassium compounds from the form in which they were added to the demineralized coal, to other potassium containing compounds during the pyrolysis process with the evolution of volatiles. The amount of K_2O formation will depend on the potassium compound used in the specific sample. The other oxides found in the coal samples do not increase or decrease significantly with the addition of the potassium compounds.

Table 5.7: XRF results of raw and demineralized coal and chars prepared from the raw coal, demineralized coal and the four demineralized coal-alkali blends with the 10 K-wt% addition

Sample name	Fe_2O_3	MnO	Cr_2O_3	V_2O_5	TiO_2	CaO	K_2O	P_2O_5	SiO_2	Al_2O_3	MgO	Na_2O
Raw coal	3.39	0.03	0.01	0.02	1.13	3.10	1.55	0.42	60.71	27.95	1.02	0.67
Demin coal	27.23	2.35	1.41	0.94	10.80	1.88	20.19	0.47	20.66	4.69	4.69	4.69
Raw coal char	5.68	0.07	0.21	0.06	1.48	3.43	2.05	0.60	58.06	26.30	1.18	0.87
Demin coal char	17.98	0.09	1.49	0.35	13.47	1.02	9.33	0.97	37.87	16.07	0.65	0.72
KOH+demin coal	0.27	0.18	0.27	0.09	0.09	0.09	93.73	0.18	0.91	1.73	0.91	1.55
KCl+demin coal	9.31	0.98	0.49	0.25	6.13	0.98	58.82	0.49	12.75	4.90	2.45	2.45
K_2CO_3+demin coal	0.08	0.32	0.63	0.32	0.08	0.08	95.27	0.08	0.79	0.79	0.79	0.79
KCH_3CO_2+demin coal	0.08	0.16	0.39	0.08	0.08	0.08	95.86	0.16	0.78	0.78	0.78	0.78

*Demin = demineralized

5.5.2 X-Ray diffraction (XRD)

The XRD results presented in the Table 5.8 were obtained from the char samples (see paragraph 4.8). The percentages determined and presented in the table below are from the crystalline matter of minerals found within the samples after charring has occurred. Since quartz can be found in all coal samples, it can be used as an internal standard for the determination of the other crystalline values [Moore and Reynolds, 1997].

From Table 5.8 it can be seen that some clay mineral crystalline structures were present in the raw coal sample. When comparing the demineralized coal sample to that of the raw coal sample, it can be noted that an increase in the graphite value was observed. A decrease in the quartz value was also observed comparing the raw and demineralized coal samples. This increase in the graphite and decrease in the quartz values might be due to the removal of the minerals through the acid leaching processes [Steel and Patrick, 2001].

When comparing the demineralized coal sample values to that of the demineralized coal-alkali blends, the values obtained for the quartz does not change to a notable extent. The observed increase is thus only relative. From Table 5.8 it can also be seen that the charred samples with the added potassium compounds had formed crystalline structures in the sample. These crystalline structures formed as a result of char formation under high temperatures. In the samples where KOH and K_2CO_3 were added to the demineralized coal, kalicinite (C1 H1 K1 O3) crystalline structures formed. For the sample with the added KCl, sylvine (Cl1 K1) formed. From table 5.8 it can be seen that no crystalline values could be determined for the sample with the addition of KCH_3CO_2. No structural data was available as these crystalline structures may have been destroyed by moisture present in the sample.

Presented in Figure 5.3 are the XRD diffractograms for the char samples derived from raw coal, demineralized coal and the four demineralized coal-alkali blends with 10 K-wt% addition.

Table 5.8: XRD results of chars prepared from the raw coal, demineralized coal and the four demineralized coal-alkali blends with 10 K-wt% addition. (Percentages reported as total of crystalline matter)

Raw Coal	Weight %	Demineralized Coal	Weight %
Graphite	95.7	Graphite	99.8
Quartz	2.5	Quartz	0.2
Mullite	1.7		
Gehlenite	0.2		
10% KOH + Demineralized Coal	**Weight %**	**10% KCl + Demineralized Coal**	**Weight %**
Graphite	98.1	Graphite	94.7
Quartz	0.2	Quartz	0.2
Kalicinite K(HCO_3)	1.7	Sylvine (Cl1 K1)	5.1
10% K_2CO_3 + Demineralized Coal	**Weight %**	**10% KCH_3CO_2 + Demineralized Coal**	**Weight %**
Graphite	95.5	The quantification for KCH_3CO_2 was not possible.	
Kalicinite (C1 H1 K1 O3)	4.5		

a)

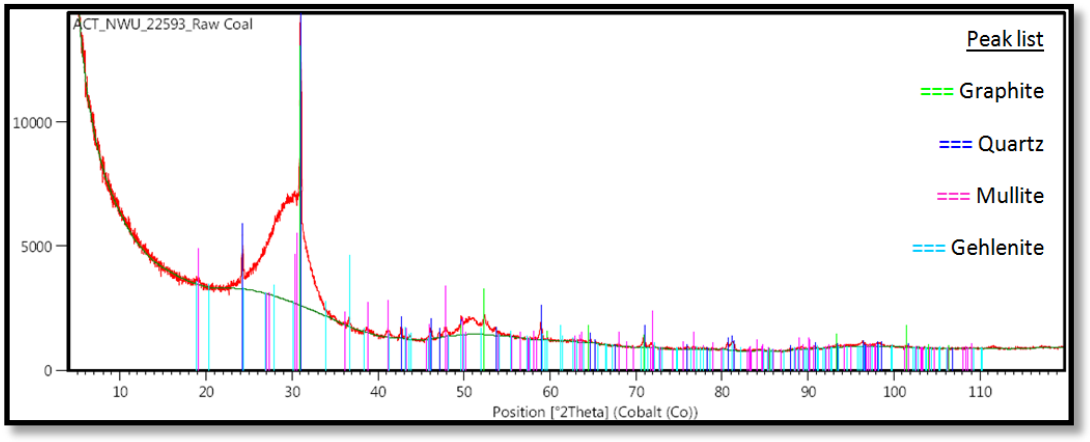

b)

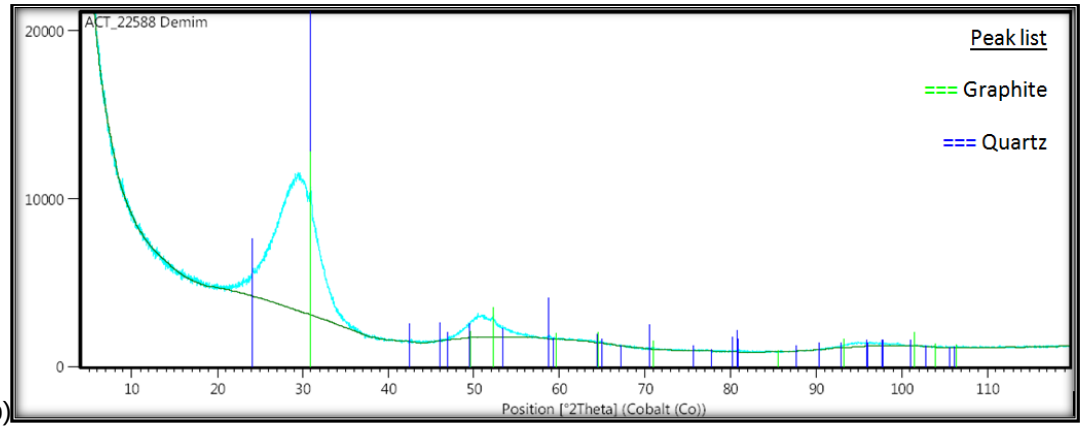
ACT_22588 Demim
Peak list
=== Graphite
=== Quartz
20000
10000
0
10
20
30
40
50
60
70
80
90
100
110
Position [°2Theta] (Cobalt (Co))

c)

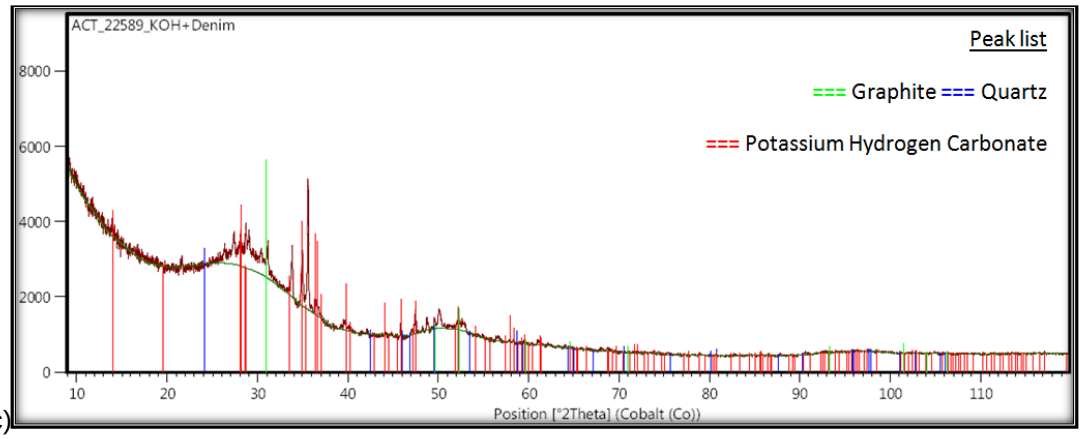
ACT_22589_KOH+Denim
Peak list
=== Graphite === Quartz
=== Potassium Hydrogen Carbonate
8000
6000
4000
2000
0
10
20
30
40
50
60
70
80
90
100
110
Position [°2Theta] (Cobalt (Co))

d)

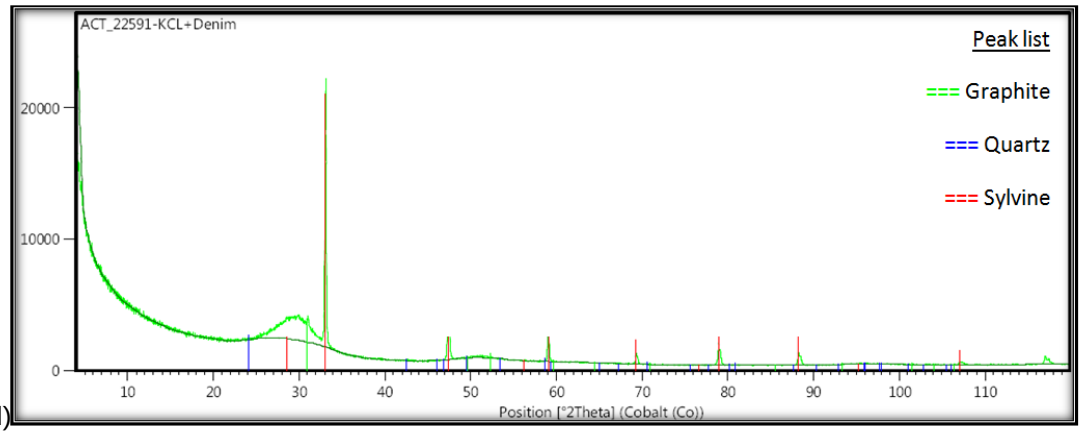
ACT_22591-KCL+Denim
Peak list
=== Graphite
=== Quartz
=== Sylvine
20000
10000
0
10
20
30
40
50
60
70
80
90
100
110
Position [°2Theta] (Cobalt (Co))

e)

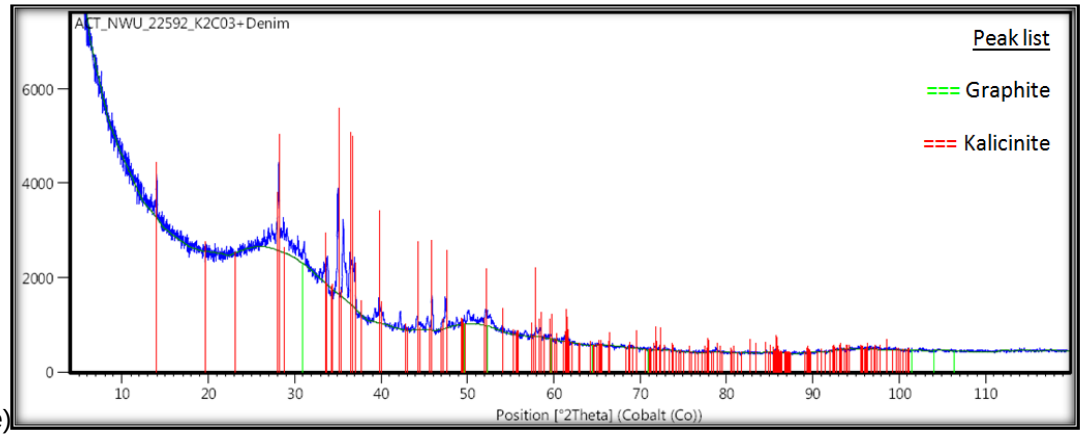
ACT_NWU_22592_K2C03+Denim
Peak list
=== Graphite
=== Kalicinite
6000
4000
2000
0
10
20
30
40
50
60
70
80
90
100
110
Position [°2Theta] (Cobalt (Co))

f)

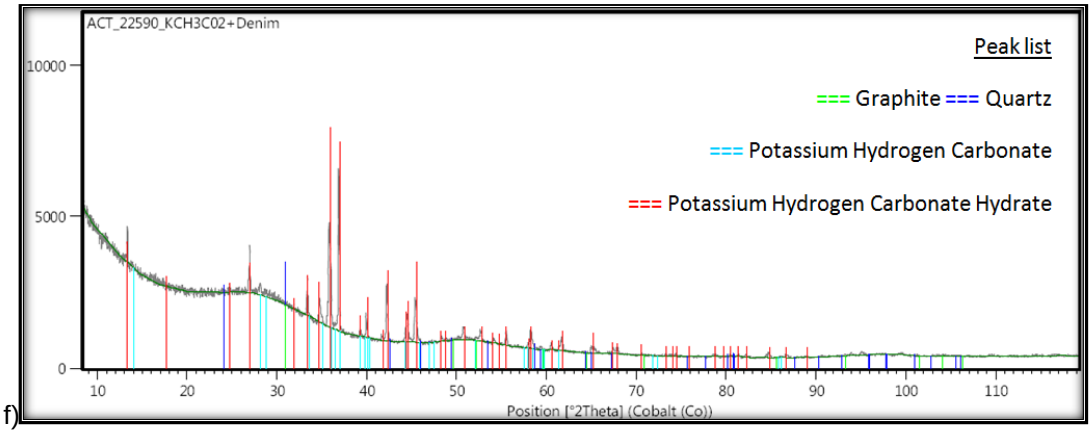

Figure 5.3: XRD diffractograms for the demineralized coal-alkali blend char: a) Raw coal char; b) Demineralized coal char; c) 10% KCl + Demineralized Coal; d) 10% KOH + Demineralized Coal; e) 10% K_2CO_3 + Demineralized Coal; f) 10% KCH_3CO_2 + Demineralized Coal

5.6 Micropore Surface Area (BET)

The surface area values, determined by using CO_2 desorption, for the raw coal and demineralized coal samples are presented in Table 5.9. Table 5.10 represents the CO_2 surface area values for the char samples prepared from the raw coal, demineralized coal and the four demineralized coal-alkali blends with 10 K-wt% addition of KOH, KCl, K_2CO_3 and KCH_3CO_2. These values were determined using the Dubinin-Radushkevich model using the adsorption and desorption of CO_2 [Sobolik *et al*, 1992]

Form Table 5.9 it can be seen that there was an increase in the surface area of demineralized coal in comparison with that of the parent coal. This increase in the surface area for the sample may be due to the removal of the minerals from the parent coal sample.

Table 5.9: Micropore surface area for the raw coal and the demineralized coal

Sample Name	Micropore Surface Area (m^2/g)
Raw Coal	104.50
Demineralized Coal	124.18

From the values in Table 5.10, it is clear that all the samples that have been subjected to the heat treatment has a low micropore surface area compared to the raw and demineralized samples that have not been subjected to heat treatments. According to Audley [1987], caking coals will form a char with low surface areas after the coal has been subjected to heat treatment. This low micropore surface area of the char suggests that the coal was fluid

during the pyrolysis process [Audley, 1987]. When comparing the surface areas of the char for the raw and demineralized coal samples, there was a decrease in the surface area for the demineralized char sample. Drying of the coal may play a role in the collapsing of some micropores [Amarasekera *et al*, 1995].

Comparing the chars samples with the addition of potassium compounds to the demineralized coal, a small increase in the surface area was observed. This difference in the surface area may be caused by the added potassium compound. When heating the coal with the potassium compound, the potassium compound will become mobile. While the potassium compound is mobile it will distribute itself over the surface of the coal and may cover the surface area of the pores and prevent some of them from collapsing during the resolidification stage [Nishiyama, 1991; Wood et al, 1984].

Table 5.10: Micropore surface areas for the chars prepared from the raw coal, demineralized coal and the four demineralized coal-alkali blends with 10 K-wt% addition

Sample Name	Micropore Surface Area (m^2/g)
Raw Coal char	17.49
Demineralized Coal char	5.87
10 % KOH + Demineralized Coal char	14.48
10 % KCl + Demineralized Coal char	9.84
10 % K_2CO_3 + Demineralized Coal char	11.26
10 % KCH_3CO_2 + Demineralized Coal char	12.14

Comparing the surface areas of the raw and demineralized coal to the surface areas of the chars prepared from the raw and demineralized coal samples, it is clear that there was a significant decrease in the surface areas for the char samples. It is possible that during the heat treatment, micropores may be destroyed when the coal sample passes through the plastic range, thus decreasing the surface area of the sample [Hang *et al*, 1987].

5.7 Diffuse Reflectance Infrared Fourier Transform Spectroscopy (DRIFT)

DRIFT analysis was done on the coal samples to determine what happened to the functional groups bound to the sample, when the sample is heated during the pyrolysis process. DRIFT spectra for the charred and untreated raw coal, demineralized coal and demineralized coal-alkali blended samples are presented in Figures 5.4-5.9. Also in these

figures are the spectra for samples that were heated to 300°C. These samples were heated to 300°C under nitrogen and held at that temperature for 60 min. The samples were cooled under nitrogen until room temperature. DRIFT was done on the samples with a 10 K-wt% alkali compound addition. The spectra representing the different samples are as follow: untreated samples (blue line), the samples heated to 300°C (red line) and the charred samples (black line).

From spectrums shown in Figures 5.4-5.9 it can be seen that there was a general decrease in some of the functional groups when comparing the untreated coal samples to that of the heat treated samples. This decrease indicated evolution of functional groups at low temperatures. When comparing the charred sample spectra to that of the untreated and heat treated samples, it is clear that no functional groups (as expected) were detected for the char samples. Aromatic C-H bonds (900-675 cm^{-1}) and out of plane aromatic C-H bonds (600-420 cm^{-1}) was observed for the char samples. When coal is charred at high temperatures (1200°C) most, if not all the functional groups have been transformed into aromatic structures, or were evolved.

Considering the untreated- and heat treated coal samples, the following was observed; O-H stretch vibrations can be seen at wavenumbers 3700-3200 cm^{-1} for the raw coal and for the demineralized coal-alkali blends (KOH, KCl, K_2CO_3, KCH_3CO_2). Sharp peaks appearing between 3700-3560 cm^{-1} indicates non-hydrogen bonded O-H groups such as phenols and alcohols. When intermolecular hydrogen bonding takes place and O-H groups take part in these reactions, additional bands starts to form at 3350-3200 cm^{-1} [van Niekerk *et al*, 2008]. Thus, from the spectra the following can be summarized;

- Phenol/alcohol groups are present in the untreated and heat treated (sample that was heated to 300°C) raw coal samples with additional hydrogen bonded O-H groups.
- The demineralized coal does not contain any peaks between 3700-3200 cm^{-1}, which would suggest that no O-H groups are present in untreated and heat treated samples.
- The demineralized coal-alkali blends exhibits a band between the wavenumbers of 3700-3200 cm^{-1} for the heat treated samples. This may be due to cross-linking reactions taking place between the alkali compounds and the coal to form hydrogen bonds to O-H groups at low temperatures.
- The untreated KCH_3CO_2 blend also presents a band at wavenumbers 3700-3200 cm^{-1}, which may suggest that reactions take place between this alkali compound and the coal before heat treatment.

For the heat treated samples – raw coal, demineralized coal and KOH blend - a decrease in peak intensity was observed at 2940 and 1445 cm^{-1}. The KCl blend did not display any change in these peaks but the K_2CO_3 and KCH_3CO_2 blends did display an increase in these peaks. These peaks commonly indicate the aliphatic C-H groups. This increase and decrease of the peaks may indicate a change in the structure of the coal due to reactions taking place between the alkali compounds and the coal.

Ketones, aldehydes, esters and carboxylic acids produce a peak in the 1870-1550 cm^{-1} region. From the spectra it can be seen that there is a decrease in the peaks for the heat treated samples. According to Bexley *et al* [1986] reactions occur between the compounds and these groups. The KCH_3CO_2 blend shows an increase in this peak, which may suggest that the formation of some of these groups take place as a result from the ion bound to the potassium.

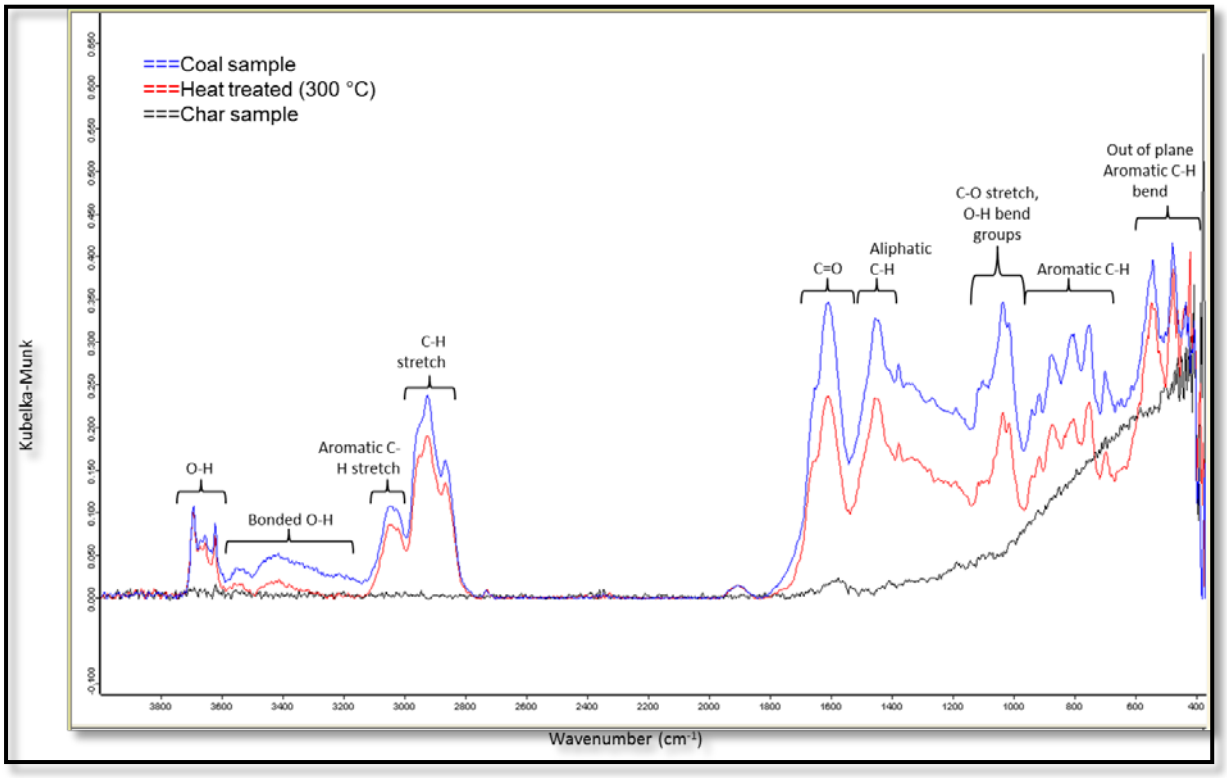

Figure 5.4: DRIFT spectra for Raw coal (untreated, heat treated and char samples)

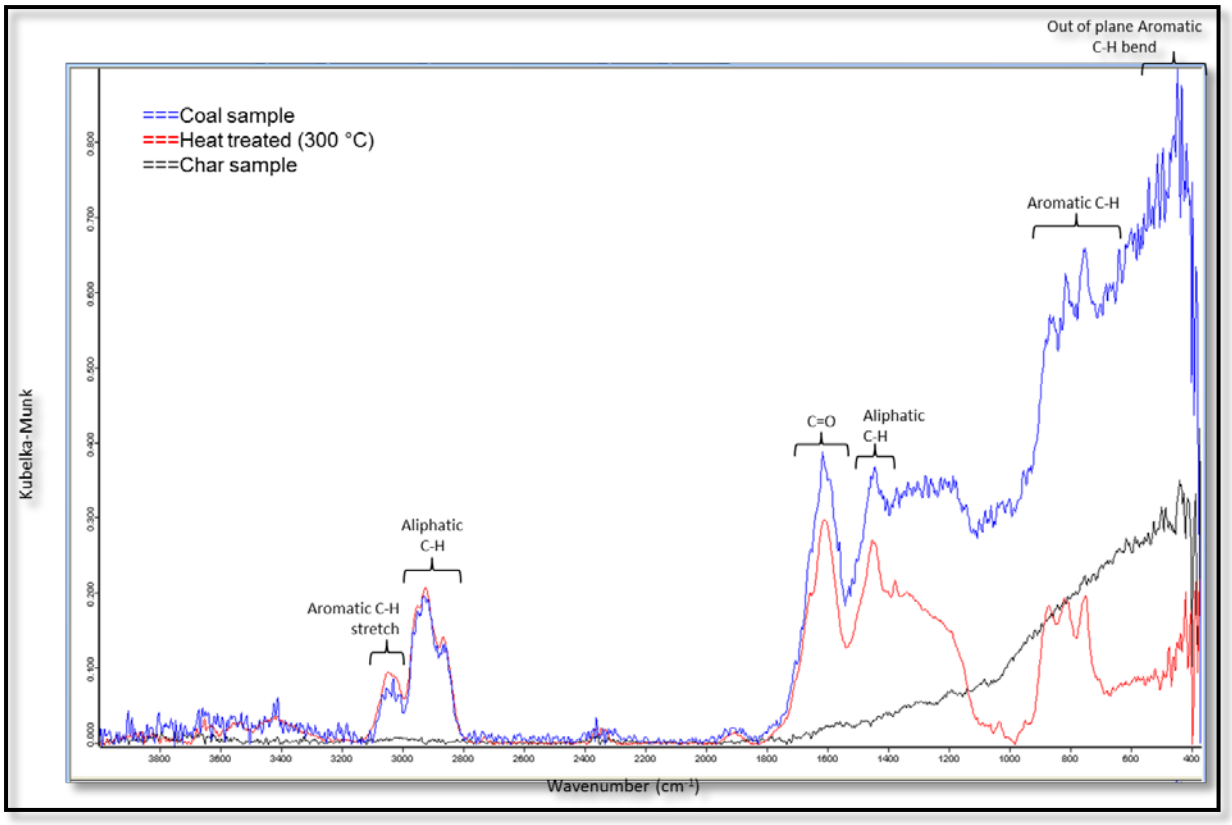

Figure 5.5: DRIFT spectra for Demineralized coal (untreated, heat treated and char samples)

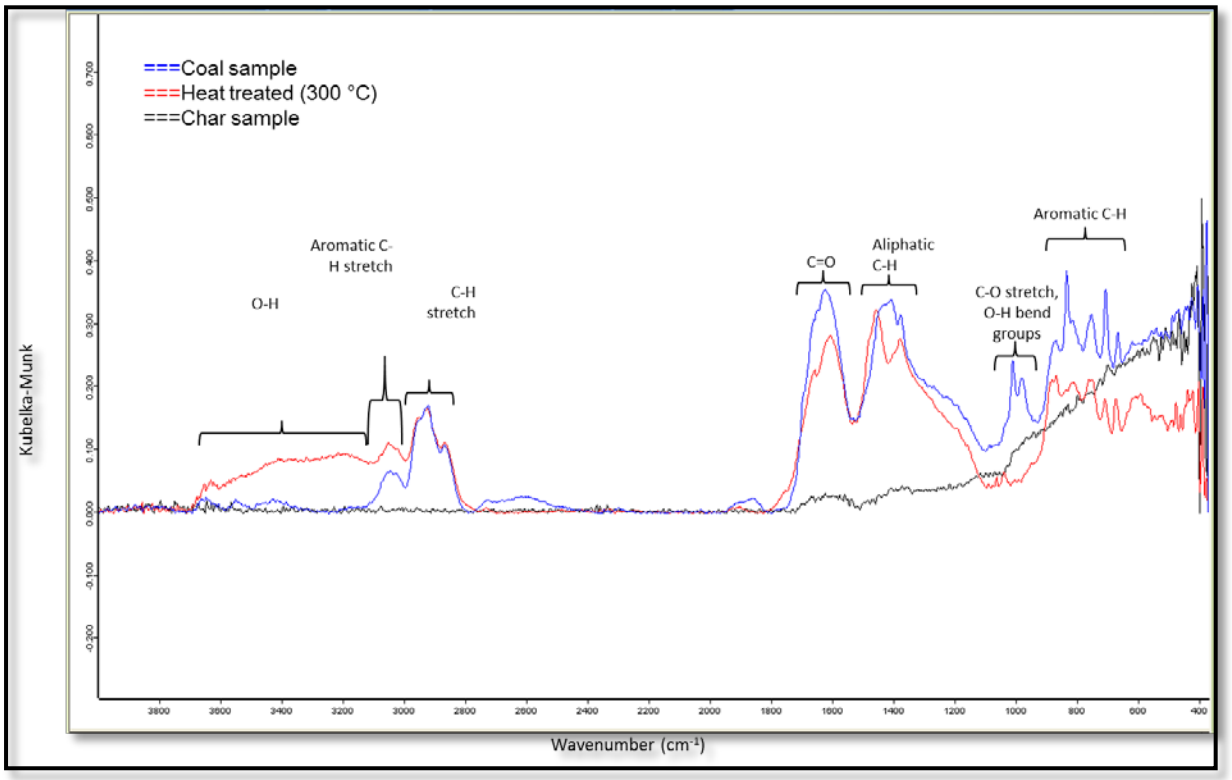

Figure 5.6: DRIFT spectra for 10 K-wt% KOH blend (untreated, heat treated and char samples)

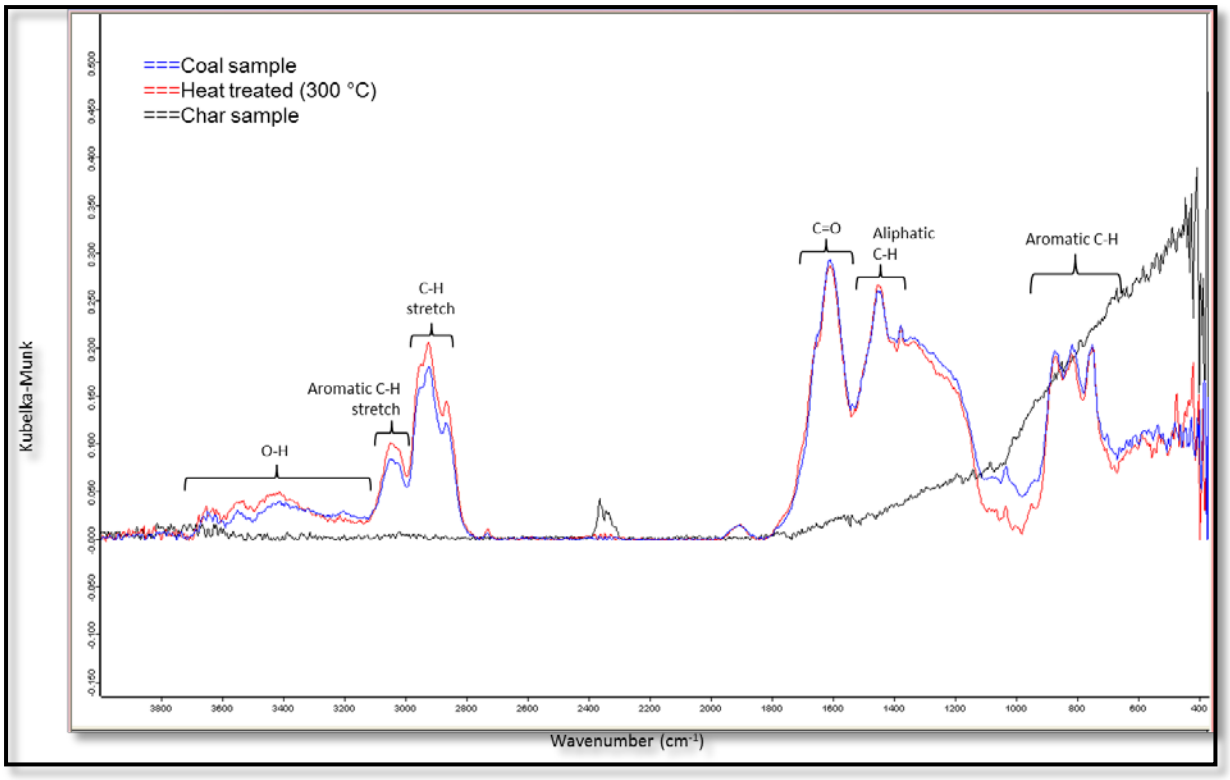

Figure 5.7: DRIFT spectra for 10 K-wt% KCl blend (untreated, heat treated and char samples)

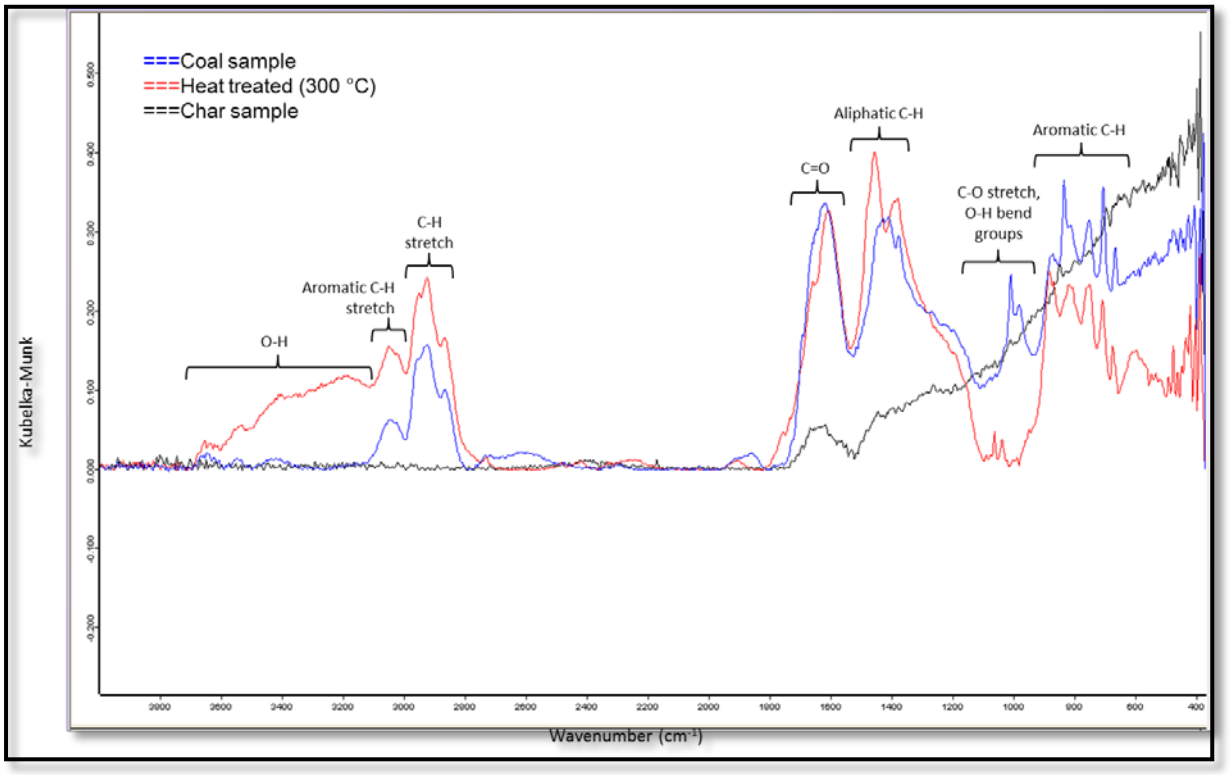

Figure 5.8: DRIFT spectra for 10 K-wt% K_2CO_3 blend (untreated, heat treated and char samples)

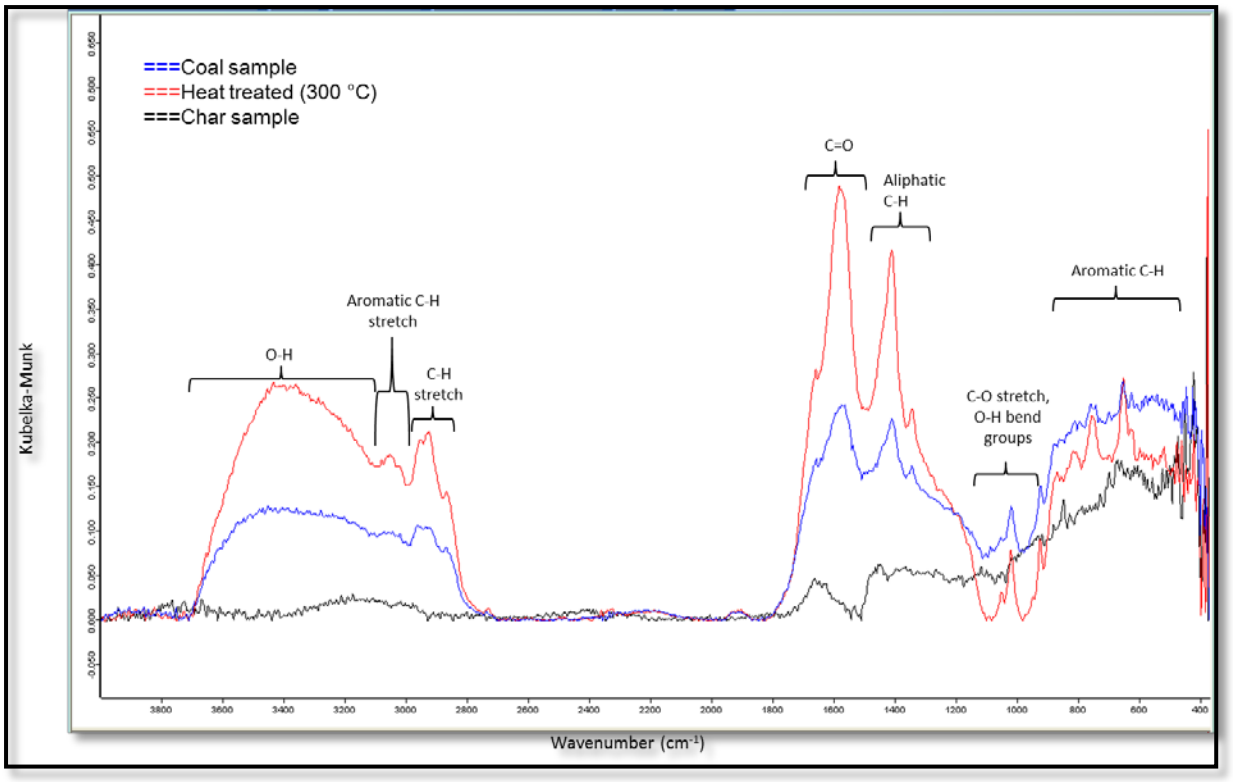

Figure 5.9: DRIFT spectra for 10 K-wt% KCH_3CO_2 blend (untreated, heat treated and char samples)

Chapter 6

Results and Discussions

TMA and Dilatometry

In this chapter the results for thermomechanical analysis (TMA) and dilatometry analysis done on the samples will be discussed. The four samples subjected to TMA were the demineralized coal-alkali blends. The samples subjected to dilatometry analysis were the raw coal, demineralized coal and the demineralized coal-alkali blends. The samples with 10 K-wt% addition were used in these analyses.

6.1 Thermomechanical Analysis

During heat treatment of the coal sample, physical and chemical changes occur within the sample. When these changes take place within a swelling coal, the coal forms a metaplast and volatiles are released. When trapped, these volatiles will cause the coal to swell, and thus a change in the volume of the sample. Thermomechanical analyses were done on the samples to determine the volume change that these samples undergo during heat treatment. The samples were heated to 1000°C in a cylindrical tube, thus limiting the direction in which volume change can take place. The heating procedure is discussed in Chapter 4 (see paragraph 4.11). Samples subjected to this analysis were the samples with the added potassium compounds. The analysis was repeated five times to ensure reproducibility. The averages of these runs were used to draw the curves for the samples.

Analysis done on the raw and demineralized coal samples could not be used. As described in paragraph 4.11 two thin (1 mm) disks were used to close the openings of the cylindrical tube. As a result of the high swelling propensity for this coal, when heated the samples did not only swell, but displaced the disk at the bottom. This caused irregular swelling and corruption of the data. None of the runs done on the raw and demineralized coal samples produced any usable data. Presented in Figure 6.1 are the TMA curves for the demineralized coal-alkali blends. The curves for the samples are drawn from ambient temperature up to 1000°C. It can be seen that the sample with the added KCl did not show a significant influence on decreasing the swelling behaviour of the demineralized coal as can be seen for the samples with the other potassium compounds (KOH, K_2CO_3 and KCH_3CO_2) added to the demineralized coal. The change in volume for the demineralized coal-KCl blend in the figure started at around 450°C, where it rapidly increased until the maximum volume change for the samples has been reached. The maximum volume change was reached at a temperature of 550°C. This may suggest that the volume change for the samples with the added KCl compound took place at a rapid pace. A volume change of about 65% was observed for the KCl-coal blend. After this maximum has been reached, a decrease in the sample volume was seen. After the release of volatiles, resolidification of the sample started to take place, and this may account for the slight decrease in the sample volume. For the KOH, K_2CO_3 and KCH_3CO_2 blends, little information on their effect on the volume change could be obtained from this graph and results are discussed using Figure 6.2.

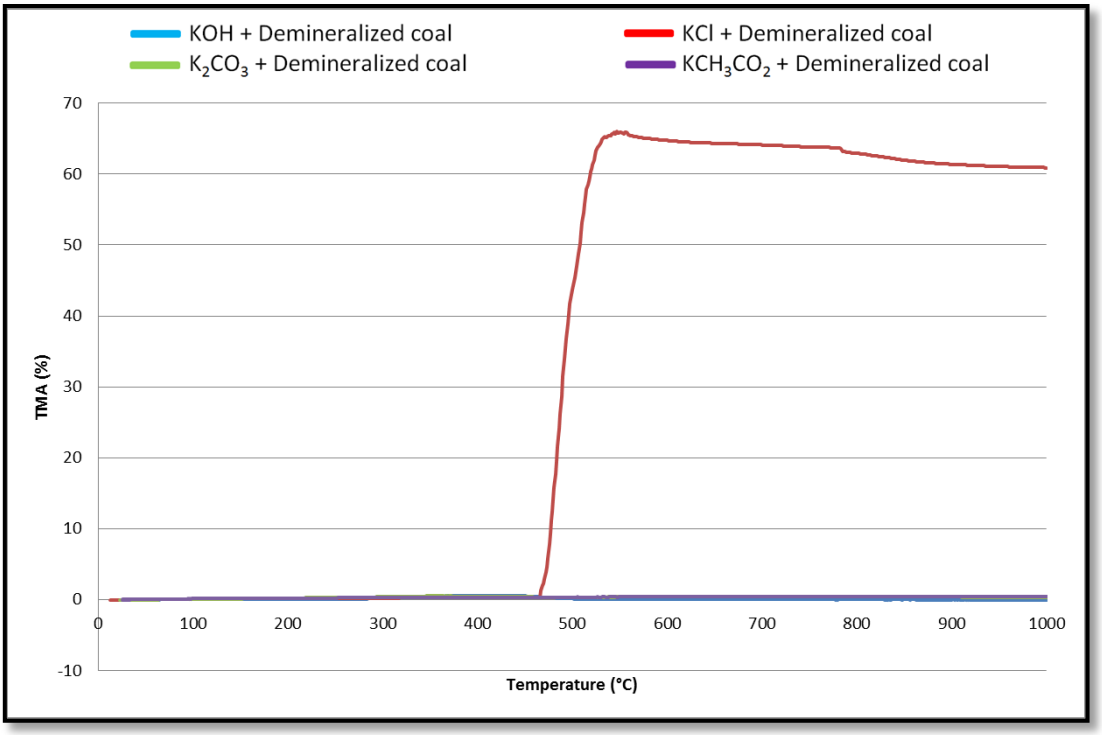

Figure 6.1: Thermomechanical analysis curves for the potassium-coal blends up to 1000 °C

From Figure 6.1 it was unclear as to how the other potassium compounds (KOH, K_2CO_3 and KCH_3CO_2) influenced the swelling behavior of the coal during this heat treatment. Figure 6.2 represents the thermomechanical analysis for the compounds up to a temperature of 450°C, to better understand the influence of these compounds on the softening temperature of the samples and thus the swelling behavior.

Considering Figure 6.2, it can be seen that the change in volume for the KCl-coal blend (red line) started to occur at around 450°C as suggested above. According to Figure 6.2 the onset of volume change for the other potassium containing samples was as follow: KOH-coal blend (blue line) started at a temperature of 260°C, the K_2CO_3-coal blend (green line) at a temperature of 100°C. These volume change values for the demineralized coal-alkali blends (KOH, K_2CO_3 and KCH_3CO_2) was less than 1% and thus can not be quantitatively reported. It can still be noted that these compounds decrease the volume change (swelling) of the demineralized coal when compared to the results obtained by adding KCl to the demineralized coal. Furthermore, without considering the volume change for the samples presented in Figure 6.2, it can be seen that the potassium compounds affect the temperature at which softening of the coal takes place. This decrease in softening temperature may be caused by reactions taking place between the coal and potassium compounds. From these curves it can also be seen that the ion (-OH, -Cl, $-CO_3$ and $-CH_3CO_2$) bound to the potassium influenced the reactions taking place duringheat treatment.

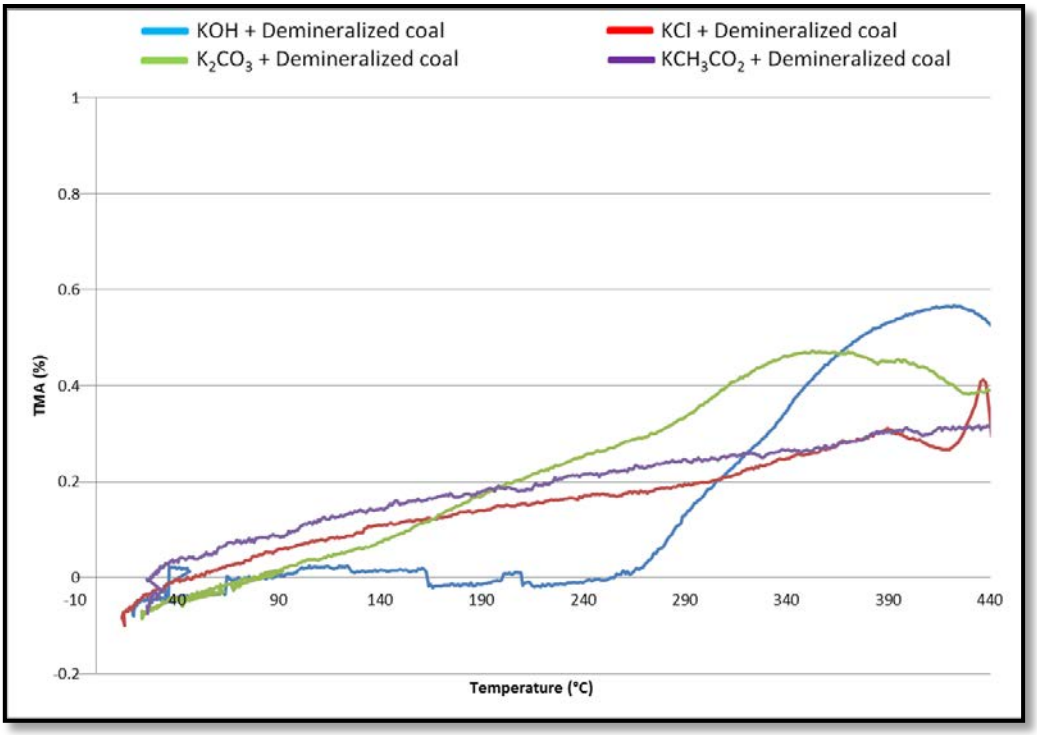

Figure 6.2: Thermomechanical analysis curves for the potassium-coal blends up to 450°C

6.2 Dilatometry

When coal is subjected to heat treatments, physical and chemical changes take place within the structure. These changes of the coal take place within a certain temperature range depending on the coal rank and composition. Coal swelling is one of the physical changes that some coal undergoes during heat treatment. The swelling behaviour of coal may be determined via different analytical techniques. When using dilatometry, information on the behaviour of the sample during the heat treatment can be obtained from the graphs generated from the data produced during the dilatation experiments.

Presented in Figure 6.3 is a typical dilatation curve for a coal sample heated at ambient pressure. By using the curve generated with this analysis technique, information on the effect that temperature has on physical properties of the sample may be determined. From the curve the following information can be obtained: softening, contraction, dilatation temperatures and percentage swelling, contraction and dilatation.

The softening temperature (T_s) which indicates the temperature at which the coal starts to soften can be observed where contraction/expansion of the sample starts. The maximum contraction temperature (T_c) is the temperature where the highest contraction percentage is observed for the sample. The maximum swelling temperature (T_e) is found where maximum swelling for the sample has occurred. And the resolidification temperature (T_r) is the temperature where no further change in the physical structure of the coal takes place.

Information on the percentage change in volume for the sample can also be determined from this curve. The contraction volume (V_c) is the value found at the maximum contraction temperature. The swelling volume (V_s) is the value at which maximum swelling took place. After resolidification, the volume of the sample may also be determined (V_r). The dilatation value (V_e) is the maximum volume reached for the sample to the lowest volume reached during contraction of the sample [Hang *et al*, 1987; Yu *et al*, 2007].

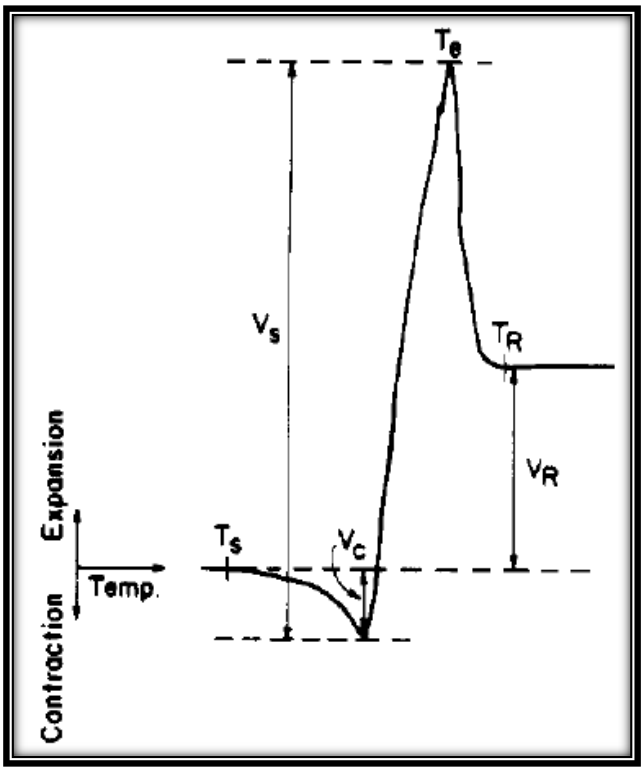

Figure 6.3: Typical dilatation curve for a swelling coal [Hang *et al*, 1987]

Six samples were subjected to dilatometry analyses to determine their behaviour during this heating process and to gather information on physical changes and the temperatures at which these take place. The samples subjected were as follows: raw coal, demineralized coal and four demineralized coal-alkali blends. For the samples with the added potassium compounds, 10 K-wt% of the compound was added to the demineralized coal to create the blended samples. Two runs were done for each of the samples to determine the reproducibility.

The dilatation curves for the raw coal, demineralized coal and demineralized coal-alkali blends are presented in Figure 6.4. From these curves, it can be seen that not only do the two runs for each of the different samples follow the same trend, but are reproducible with only some minor deviation in some of the values.

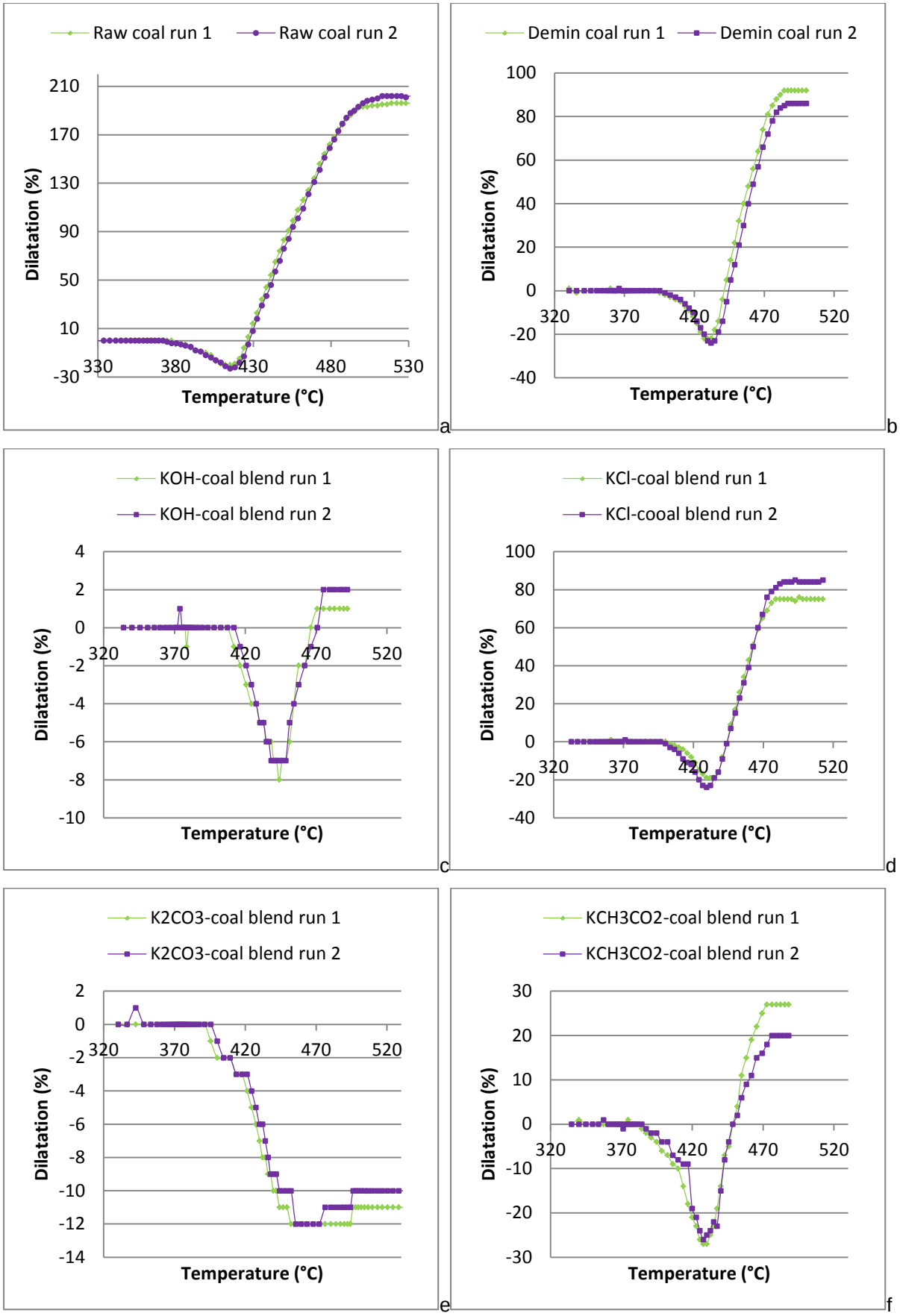

Figure 6.4: Dilatation curves for the coal and potassium-coal blends; a) Raw coal, b) Demineralized coal, c) KOH-coal blend, d) KCl-coal blend, e) K_2CO_3-coal blend and f), KCH_3CO_2-coal blend

The average values for the repeat runs were determined for each of the blended samples. These values were plotted and the curves for each of the samples are presented in Figure 6.5. The difference in behaviour for the samples with the different potassium compounds can be seen in Figure 6.5.

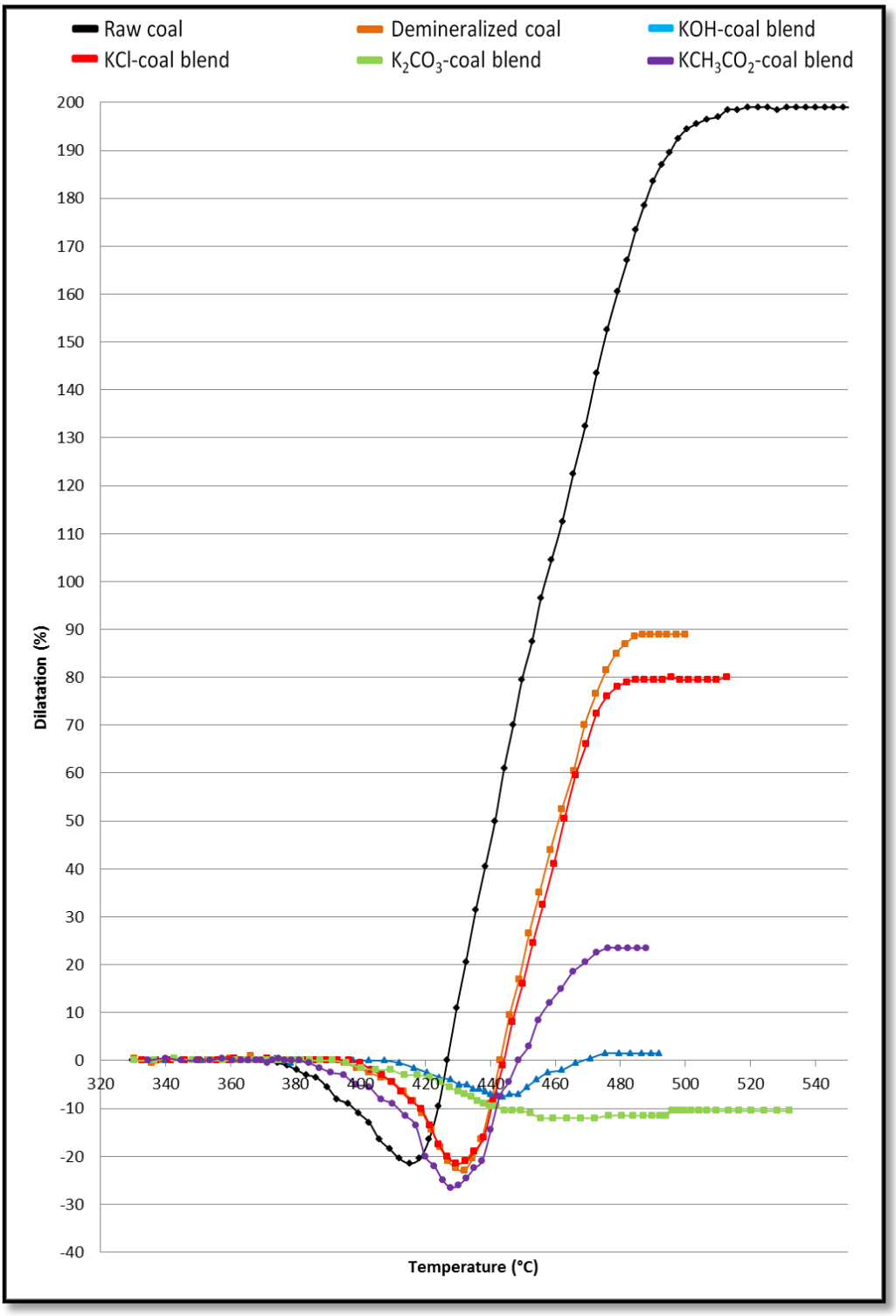

Figure 6.5: Dilatation curves for the coal-alkali blends

The softening temperature, temperature of maximum contraction and maximum dilatation temperature for the six blended samples were determined by using the dilatation curves in

Figure 6.5. Also determined from the curves were the maximum contraction and dilatation observed. These values are presented in Table 6.1.

From Table 6.1 it can be seen that the softening temperature for the raw coal sample (370°C) was lower than that of the demineralized coal sample (397°C). After removal of the minerals through demineralization, cross-linking reactions between the coal particles may take place at higher temperatures and thus the observed increase in the softening temperature. With the addition of the potassium compounds to the demineralized coal, an increase in the softening temperature can be seen for compounds KOH (414°C) and KCl (402°C). This increase may be caused by reactions taking place between the coal and the potassium compound. No change in the softening temperature was observed for the K_2CO_3 blend. For KCH_3CO_2 a decrease in the softening temperature was observed (386°C) when compared to the demineralized coal sample.

The maximum contraction temperature increases when comparing the raw and demineralized coal samples to one another. Comparing the contraction temperatures observed for the demineralized coal-alkali blends, an increase in the temperature was observed for the samples with the KOH and K_2CO_3 additions.

A decrease in the maximum swelling temperature was observed when comparing the raw coal (516°C) to the demineralized coal (486°C). This may indicate that swelling of the demineralized coal took place at a faster rate than that of the raw coal sample. When comparing the coal – alkali blends with the raw coal sample, a decrease in the swelling temperature was observed.

The contraction volume of the raw and demineralized coal remains unchanged during heat treatment. Contraction values for the blends with the addition of KOH and K_2CO_3 showed a decrease in the value compared to that of the demineralized coal, thus less contraction took place for these two samples. Bexley *et al* [1986] found that with the addition of alkali metal carbonates to the coal, the dilatation for the sample was reduced until only contraction was observed. From Figure 6.5, the same results were observed for the sample with the added K_2CO_3. A small increase in the contraction value was observed for the KCH_3CO_2 blends.

Comparing the dilatation values of the raw coal to that of the demineralized coal sample, a decrease in the value was observed. This decrease may result from the removal of the mineral content of the parent coal. From Table 6.1 it can be seen that the addition of potassium compounds decreases the dilatation volume of the demineralized coal after the addition. Also form table 6.1, it can be seen that the K_2CO_3-blend had the smallest dilatation

values, when compared to the other potassium blends. This suggests that a big decrease in the swelling behaviour occurred with the addition of K_2CO_3. The blend with the addition of KCl to the demineralized coal did not show a change in the dilatation volume for the sample. This supports the assumption that the KCl does not affect the swelling behaviour of the coal, as was seen from the results obtained from the free swelling experiments and the thermomechanical analysis. From the Table 6.1, it can be seen that potassium compounds affected the dilatation volume of the coal in the following order; K_2CO_3 > KOH > KCH_3CO_2 > KCl with KCl showing no decrease in the dilatation volume for the sample.

Table 6.1: Values determined from dilatation curves

		Raw coal	Demin coal	KOH-coal blend	KCl-coal blend	K_2CO_3-coal blend	KCH_3CO_2-coal blend
Softening temperature (°C)	T_s	377	397	414	402	398	386
Max contraction temperature (°C)	T_c	415	431	444	429	464	428
Max dilatation temperature (°C)	T_e	516	486	473	482	496	475
Max contraction (%)	V_c	22	23	8	22	12	27
Max dilatation (%)	V_e	199	89	2	80	-11	24

From the thermo mechanical analyses and dilatation results of the samples with the added potassium compounds, it was found that the KCH_3CO_2 had the biggest influence on the temperature at which the coal starts to soften and the temperature of maximum dilatation. The KCl had the least influence on the softening and maximum dilatation temperatures. For the blend with the added KOH, the influence on the demineralized coal was greater than that of the K_2CO_3 according to the dilatation results. The thermomechanical analysis showed that the influence of the K_2CO_3 was greater than that of the KOH. The different outcome between these analysis techniques might be due to the sample size, heating procedure or the analysis technique.

Chapter 7

Results and Discussions

TGA - MS

In this chapter, the thermogravimetric analyses and mass spectroscopy results of the different samples will be discussed. The samples with which these experiments were performed on were the raw coal, the demineralized coal and the demineralized coal-alkali blends.

Thermogravimetric analyses were done on the coal and demineralized coal-alkali blends to determine the influence these potassium compounds have on the mass loss of the coal and the relative reactivity of the samples during the pyrolysis stage.

Four potassium compounds were used in this study to determine their influence. The potassium compounds (KOH, KCl, K_2CO_3 and KCH_3CO_2) were added to the demineralized coal in weight percentages of 1, 4, 5 and 10 K-wt%. These samples were all subjected to the heat treatment procedure discussed in Chapter 4 (see paragraph 4.13). Using the TG graphs of each of the samples, these values (mass loss and relative reactivity) were determined. The MS graphs were used to determine the effect of the potassium compounds on the gas evolution.

7.1 Thermogravimetric Analysis

7.1.1 *TG Curves of the different samples*

7.1.1.1 Thermal analysis of the potassium compounds

Since compounds behave differently under heat treatment, the four potassium compounds used in this study were subjected to thermogravimetric analysis to determine the behaviour of the compounds under pyrolyzing conditions and also to determine the amount of potassium compound that may have decomposed or evaporated during the treatment. By using the curves generated during this heat treatment, the mass losses for the individual compounds were determined. This mass loss for each of the potassium compounds will be used to determine the coal mass loss as described in paragraph 7.1.1.2. Presented in Figures 7.1.1 – 7.1.4 are the TG curves for the potassium compounds which were heated to 1200°C in a nitrogen atmosphere.

Figure 7.1.1 presents the curve for the KOH sample subjected to the heat treatment. Decomposition of this compound mainly yielded two products; namely potassium oxide (K_2O) and water (H_2O). The first mass loss observed on the TG curve may be due to absorbed water being released during the heat treatment, since KOH is hygroscopic and will absorb water from the atmosphere. According to Seward and Martin [1949], the melting point for KOH starts at around 380°C. The second mass loss observed on the TG curve may be due to reactions taking place between the KOH molecules. These reactions will form K_2O (solid) and water. Because of the low melting temperature of the compound, reactions taking place would occur in the liquid phase. During the decomposition reaction, water molecules are formed and evolved from the sample, decreasing the mass of the sample.

To determine the extent to which the decomposition reaction of the KOH sample has taken place, the percentage of theoretical mass loss for KOH was determined. The reaction path for the decomposition of KOH is as follows: $2KOH \rightarrow K_2O + H_2O$ [Khan and Jenkins, 1986] and was used in the calculations of the theoretical mass loss percentage. The experimental mass loss of the KOH sample as determined from the TG curve was about 75%. The theoretical mass loss determined via the decomposition equation was 16%. By comparing the theoretical and experimental values, it can be seen that the experimental value was greater than that of the theoretical value, indicating that KOH was lost during the heating process.

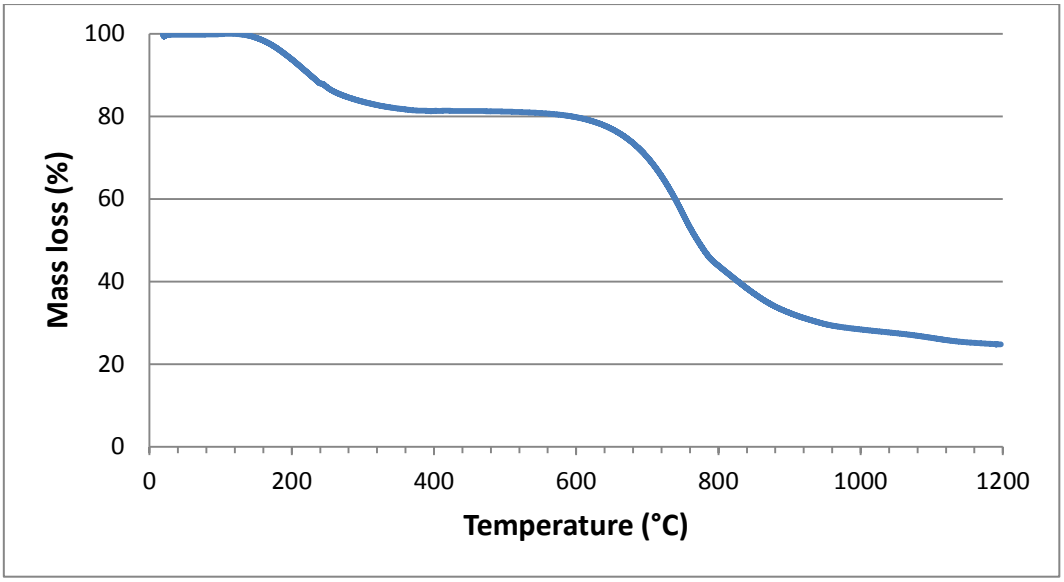

Figure 7.1.1: TG curves for the potassium hydroxide during heat treatment in N_2

Presented in Figure 7.1.2 is the TG curve for the KCl sample when subjected to the heat treatment. From this curve it can be seen that no mass loss occurs at temperatures below 760°C. According to Basin *et al* [2008], the melting temperature for KCl was found to be around 770-774°C, which corresponds with the onset of mass loss for this sample. From this curve it can be noted that after heat treatment of the sample, only a small amount of compound was left. From the TG curve, the weight loss for the KCl was more than 95%. Due to the lack in literature on reactions of KCl during heat treatment, reactions during heat treatment of other metal chlorides was investigated. According to Tomeczek and Palugniok, [2002] sodium chloride (NaCl) evaporates almost completely when heated in an inert atmosphere. Speculating that KCl would react in the same way as NaCl during heat treatment (since they are in the same group in the periodic table), the assumption can be made that the KCl does not decompose but evaporates during heat treatment.

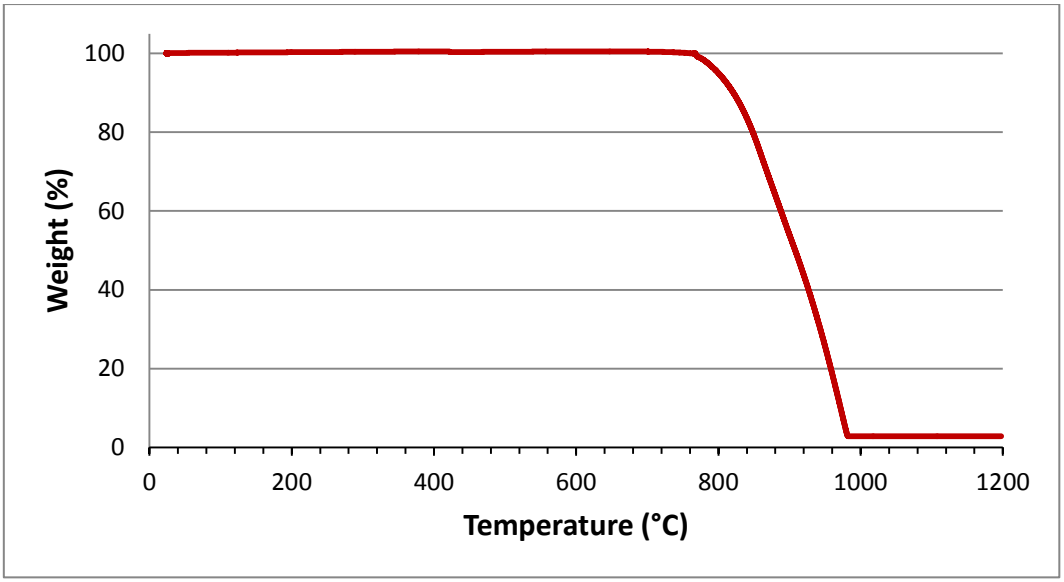

Figure 7.1.2: TG curves for the potassium chloride during heat treatment in N_2

When heating K_2CO_3 under the specified pyrolysis conditions, the TG curve presented in Figure 7.1.3 was observed. From this curve, the mass loss for the K_2CO_3 sample was observed around 900°C. As found by Lehman *et al* [1998], the melting temperature for K_2CO_3 in a nitrogen rich atmosphere, corresponds to the temperature at which mass loss starts to occur in this figure. It can be assumed that reactions between potassium molecules occured in the liquid phase, since no significant mass loss was observed before the melting temperature was reached. Lehman *et al* [1998] also found that the mass loss observed of the potassium carbonate was due to decomposition of the compound and not evaporation thereof. Decomposition of K_2CO_3 during heat treatment yields two products: potassium oxide (K_2O) and carbon dioxide (CO_2). The mass loss observed for the K_2CO_3 sample was due to the evolution of CO_2. From this curve it can be seen that complete decomposition of the potassium compound does not take place during the heat treatment conditions used in this study.

The extent to which the reaction has taken place during the heat treatment was determined by calculating the percentage theoretical mass loss for the sample and comparing this value with the experimental value. The decomposition reaction for potassium carbonate: $K_2CO_3 \rightarrow K_2O + CO_2$ [McKee, 1983]. The experimental mass loss for the sample determined from the TG curve was 63%. The theoretical mass loss determined from the decomposition reaction for K_2CO_3 was 31.8%. When comparing the values for the theoretical and experimental, it van be seen that some of the K_2CO_3 sample evaporated above the decomposition temperature.

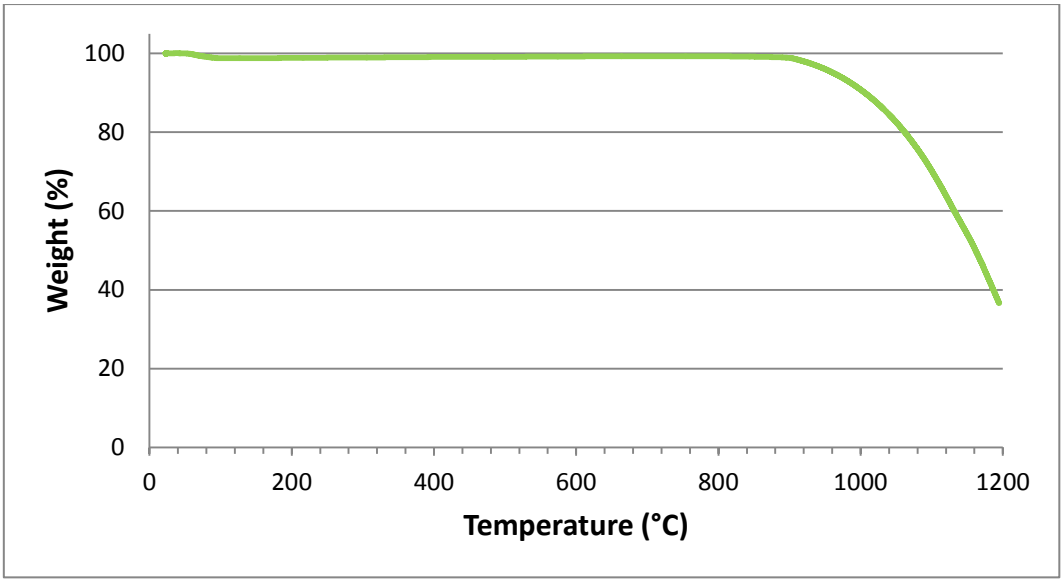

Figure 7.1.3: TG curves for the potassium carbonate during heat treatment in N_2

Presented in Figure 7.1.4 is the TG curve obtained for the thermal behavior of KCH_3CO_2. Decomposition of the potassium compound takes place in two steps. The first step is where potassium acetate decomposes to form potassium carbonate (K_2CO_3) and the second step is where decomposition of the potassium carbonate takes place. The latter decomposition step has been described earlier in the chapter. Water molecules present in the compound, or that may have been absorbed from the atmosphere are removed from the sample upon heating. Removal of water takes place at low temperatrues [Afzal *et al*, 1991]. The onset of the first decomposition step is between 400-460°C as found by Afzal et al [1991]. During this decompostion step the products formed are potassium carbonate (K_2CO_3) and acetone $(CH_3)_2CO$. The second step is the decomposition of K_2CO_3, where potassium oxide (K_2O) and carbon dioxide (CO_2) froms. From the curve it can be seen that the compound decomposes almost completely during heat treatment.

To determine the extent of decomposition for the compound, the percentage of theoretical mass loss must be determined and compared with the experimental mass loss percentage determined from the curves. Since decompostion takes place in two stages, the theoretical mass loss for each stage must be determined. By using the decomposition equations $2KCH_3CO_2 \leftrightarrow K_2CO_3 + (CH_3)_2CO$ (first) and $K_2CO_3 \leftrightarrow K_2O + CO_2$ (second) [Afzal *et al*, 1991], the theoretical mass lossed where determined. The experimental mass loss determined from the TG curve for the sample during the first step of decomposition was 28%. The theoretical mass loss calculated from the decomposition equation was about 29.6%. This mass loss was due to the formation of $(CH_3)_2CO$. This indicates that 95% of the expected mass loss during the first decomposition step was observed. During the

second step of decomposition, the experimental mass loss determined from the TG curve was about 63%. The theoretical percentage mass loss calculated was 31.8%. This would suggest that decomposition and evaporation of the formed K_2CO_3 takes place during this step.

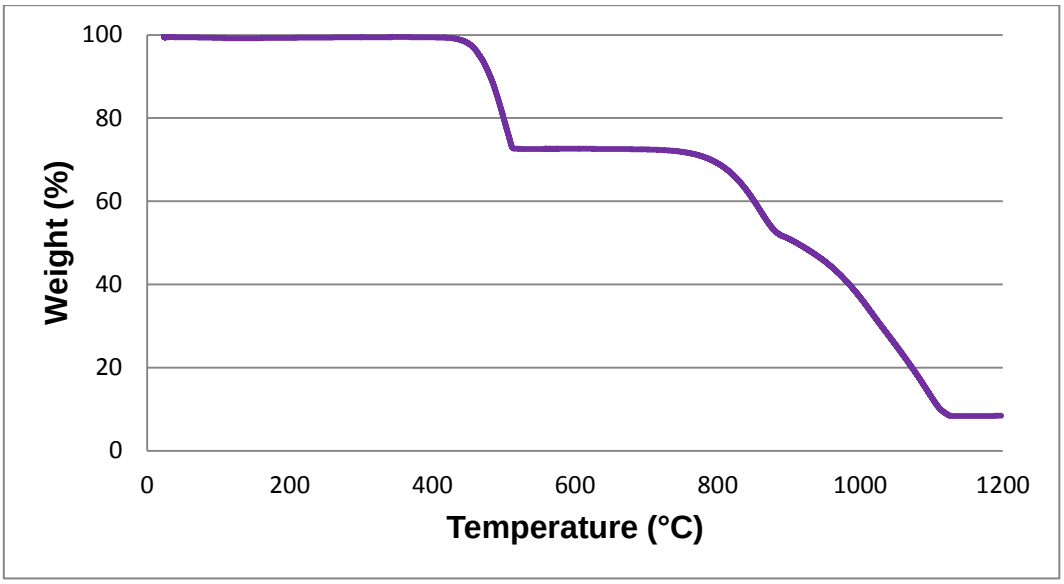

Figure 7.1.4: TG curves for the potassium acetate during heat treatment in N_2

7.1.1.2 Thermal analysis of the coal – alkali blends

As seen in section 7.1.1.1, alkali compounds behave differently during the heat treatment. To determine the effect of the alkali compounds on the coal mass loss and reactivity, the alkali compounds was added to the coal in mass percentages of 1, 4, 5 and 10 K-wt%. The mass loss determined for all the samples was determined on an alkali free basis; meaning the observed mass loss was due to the coal only. The loss of alkali compound during the heat treatment was determined using the TG curves for each of the compounds and subtracted from the coal-alkali blends results to obtain the mass loss for the coal.

To determine the mass loss of the alkali compounds during heat treatment, each of the alkali compounds were subjected to the heating conditions individually (see Figures 7.1.1-7.1.4). From these curves, the mass loss for the potassium compounds was determined up to a certain temperature (1200°C). This was done for all four of the potassium compounds. Since the alkali compounds were added to the coal in different weight percentages, the mass losses for the alkali compound must be determined accordingly to the percentage of alkali compound added to the demineralized coal.

The TG curves for the different blended samples (see Figure 7.1.5) were used to determine the total mass loss for each of the samples. By subtracting the mass loss of the alkali compound (depending on the weight percentage added to the coal) from the total mass loss for the blended samples, the coal mass loss was determined. Presented in Figure 7.1.5 are TG curves for the demineralized coal-alkali blends.

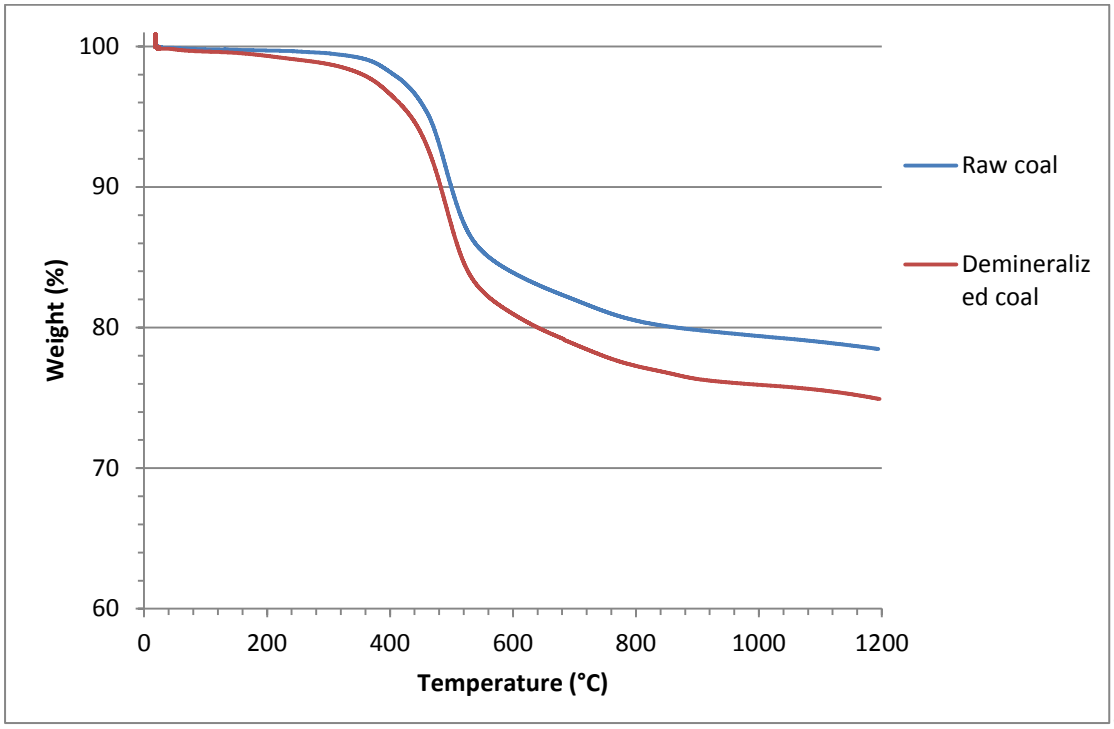

a)

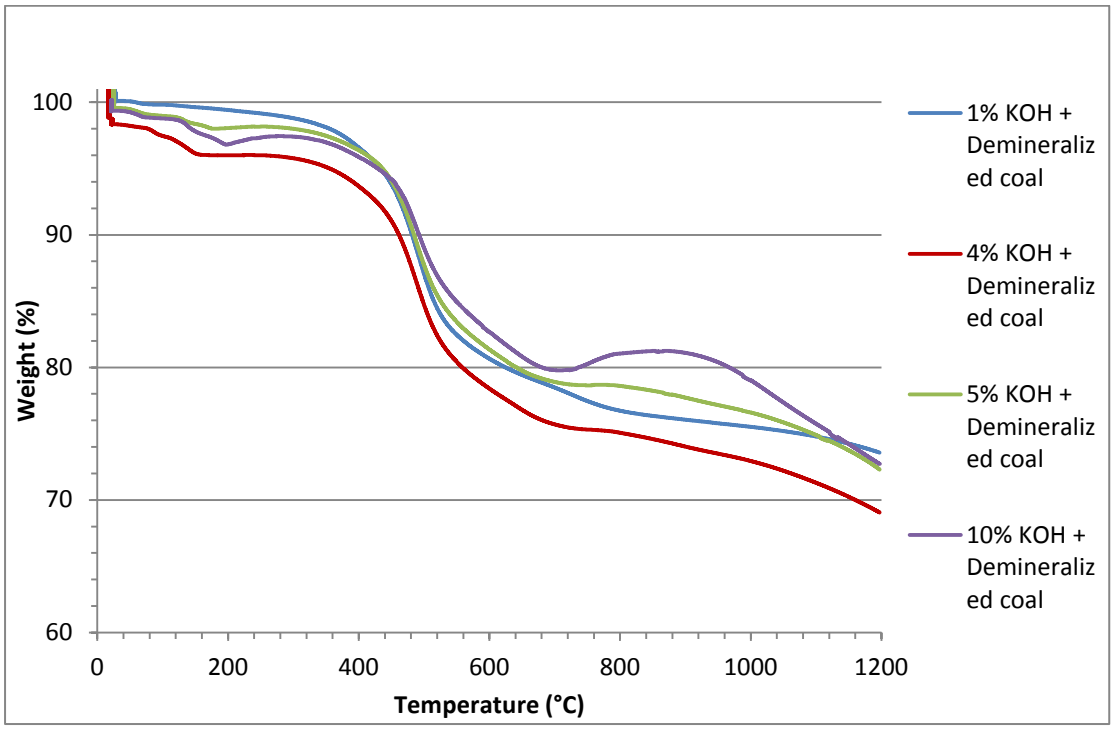

b)

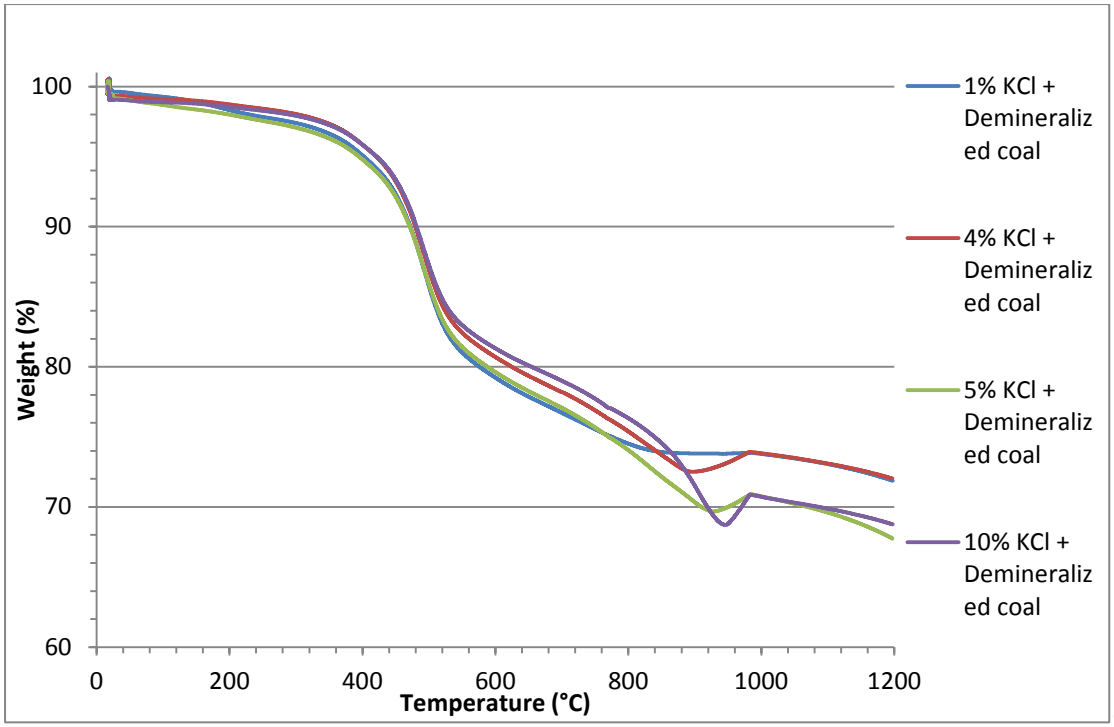
100
90
80
70
60
Weight (%)
0
200
400
600
800
1000
1200
Temperature (°C)
1% KCl + Demineralized coal
4% KCl + Demineralized coal
5% KCl + Demineralized coal
10% KCl + Demineralized coal

c)

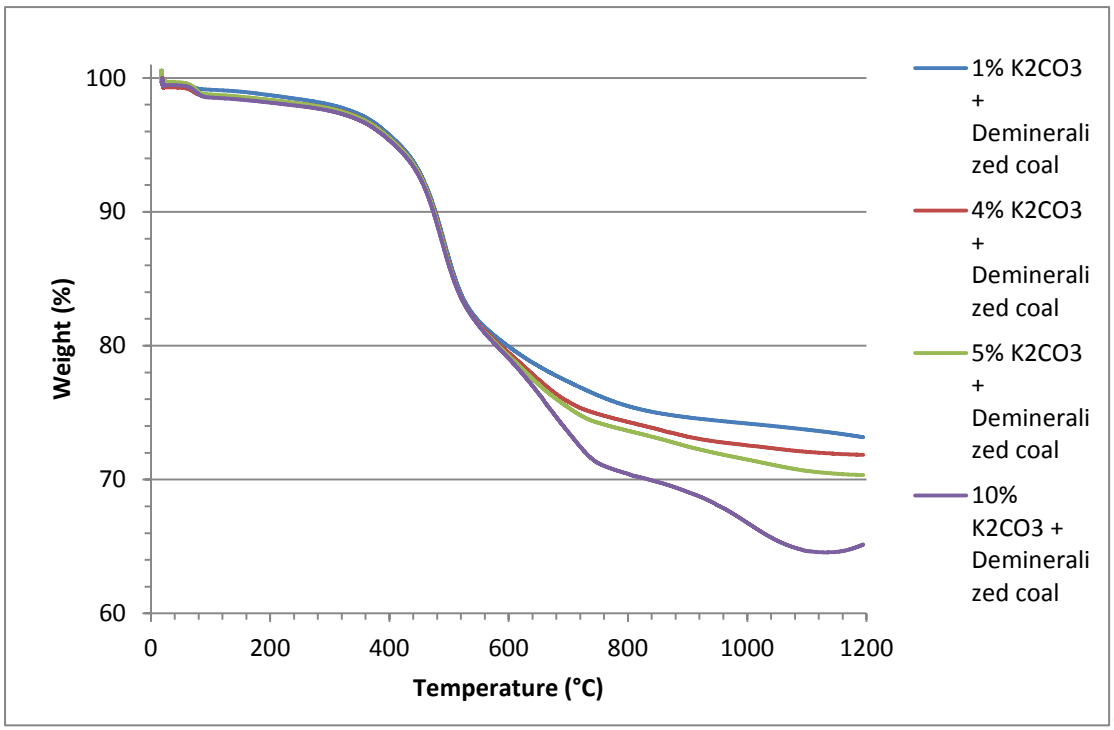
100
90
80
70
60
Weight (%)
0
200
400
600
800
1000
1200
Temperature (°C)
1% K2CO3 + Demineralized coal
4% K2CO3 + Demineralized coal
5% K2CO3 + Demineralized coal
10% K2CO3 + Demineralized coal

d)

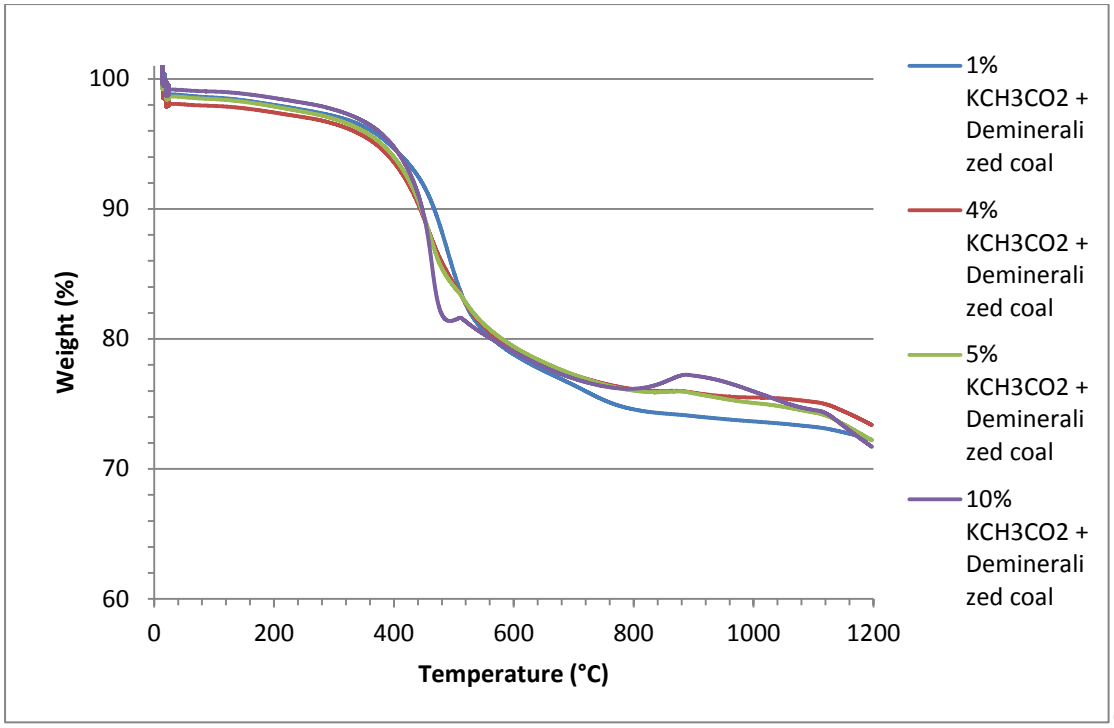

e)

Figure 7.1.5: TG graphs for the a) raw and demineralized coal and the demineralized coal-alkali blends: b) KOH, c) KCl, d) K_2CO_3 and e) KCH_3CO_2

From Figure 7.1.5 it can be seen that the coal mass loss during pyrolysis for the demineralized coal and the coal-alkali blends (at different weight percentages of alkali compounds loaded, for each compound) do not differ greatly when compared to one another. The coal mass loss was found to be within the 25-35% range. This mass loss observed may be due to the loss of volatiles during pyrolysis. Volatiles may be produced as a result of decomposing functional groups bound to the coal structure. Presented in Table 7.1.1 are the coal mass loss values determined from the TG graphs for all of the samples.

Table 7.1.1: Total coal mass loss up to 1200°C for the demineralized coal and potassium – coal blended samples

Mass loss of coal up to 1200°C (alkaline free basis)					
Sample Name	wt % compound addition	% Coal mass loss	Sample Name	wt % compound addition	% Coal mass loss
Demineralized coal		25			
KOH + Demineralized coal	1%	26	K_2CO_3 + Demineralized coal	1%	27
	4%	27		4%	27
	5%	28		5%	30
	10%	31		10%	35
KCl + Demineralized coal	1%	28	KCH_3CO_2 + Demineralized coal	1%	28
	4%	28		4%	27
	5%	32		5%	28
	10%	31		10%	29

7.1.1.3 Relative reactivity

The relative reactivities for each of the blends with the different weight percentages of potassium compound added were determined. To determine the relative reactivity for a sample, the temperature ($T_{50\%}$) at which 50% mass loss for the coal occurs was determined. By obtaining the inverse of this temperature ($T_{50\%}$), the relative reactivity may be determined (1/T). Figure 7.1.5 was used to determine the $T_{50\%}$ for all the samples, where these temperatures were used to determine the relative reactivity.

Presented in Figure 7.1.6 are the relative reactivities determined for the samples with the different alkali compounds and K-wt%. When the samples are heated in an inert atmosphere (N_2) to a high temperature (1200°C), a mass loss of 25-35% was observed. This mass loss suggests that partial conversion of the samples took place during pyrolysis. Conversion taking place within the sample may be due to decomposition reactions and also reactions between the potassium compounds and the demineralized coal particles.

With the addition of 1 K-wt% alkali compound to the demineralized coal, little to no change in the relative reactivity was observed for the different compounds. As the K-wt% loading for the samples increased, a decrease was observed for the samples with the KOH, KCl and K_2CO_3 loadings. This decrease in the relative reactivity may be caused by the gaseous

species, which may inhibit some reactions from taking place. An increase in the relative reactivity was observed for the samples with the added KCH_3CO_2. This increase in the relative reactivity may be caused by secondary gasification taking place with the coal, since carbon dioxide (CO_2) forms during the decomposition of the potassium compound. When comparing the different potassium compounds with one another, the order of relative reactivity for the different samples will be as follows: KCH_3CO_2 showed an increase in value whereas the other potassium compounds showed a decrease: in decreasing order KOH > K_2CO_3 > KCl. The last three compounds thus seem to have an inhibiting effect.

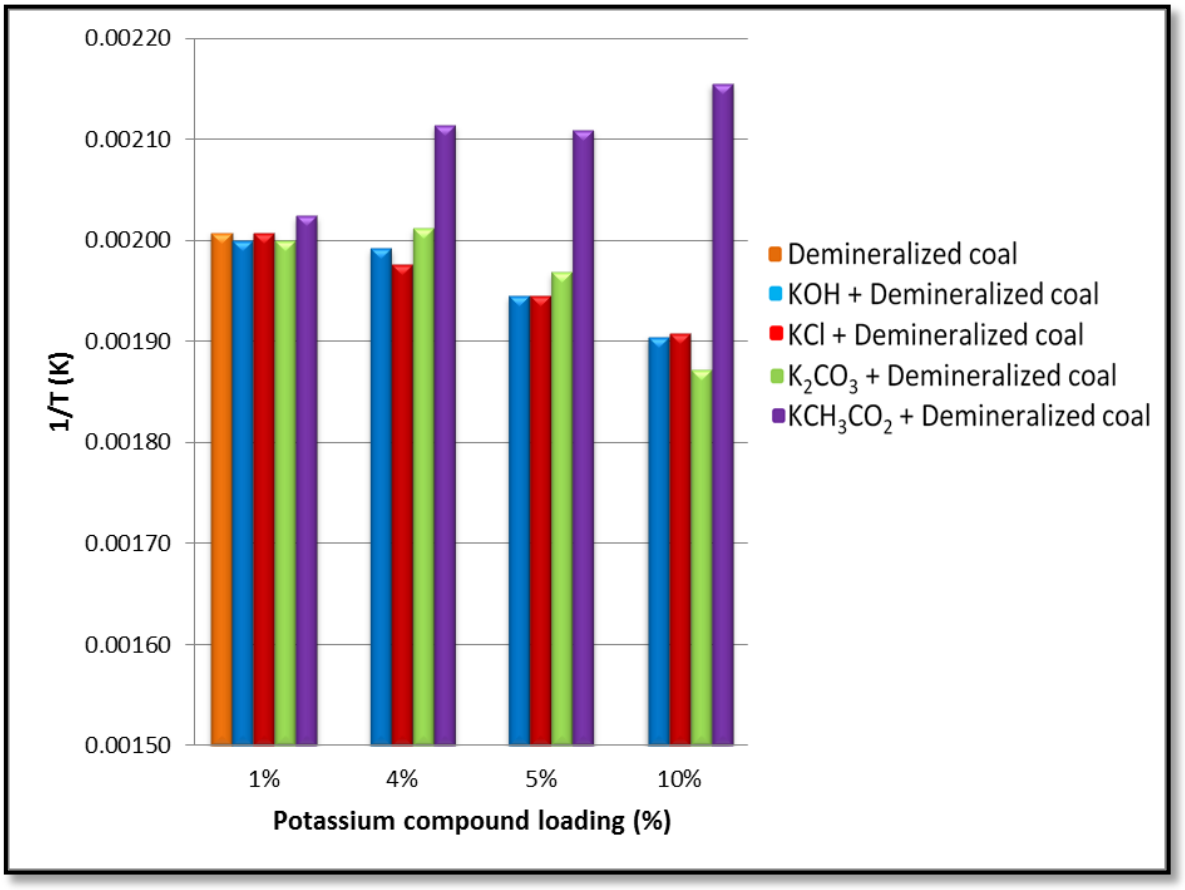

Figure 7.1.6: The coal mass loss for the demineralized coal and alkali-coal blends for temperatures up to 1200°C

7.1.2 Synergetic effect

A subject long researched and discussed is whether interaction between the coal and additives takes place during heat treatment. An equation was compiled to generate a theoretical thermogravimetric curve. The theoretical curve would then be compared to the experimental curve to see if any discrepancies occurred between the two curves. A change would indicate interaction between the coal and the additive. This interaction might influence the mass loss observed for the sample.

The theoretical curves were drawn using the following equation:

$$W_{blend} = (x_1 \times w_{coal}) + (x_2 \times w_{compound})$$

Where w_{blend} presents the sum of the components in the sample, the components being the demineralized coal and potassium compounds, x_1 represents the mass fraction of the coal and x_2 represent the mass fraction of the potassium compound in the sample. The mass losses during the heat treatment for the components (coal and potassium compounds) are represented by w_{coal} and $w_{compound}$ [Niu *et al*, 2010]. The components of each sample must be subjected to the same heat treatment conditions. To determine the theoretical mass loss for each of the blended samples, the demineralized coal blends and the potassium compounds had to be subjected to the heat treatment. By using the data gained from these experiments, the abovementioned equation can be used to determine the theoretical values.

Figure 7.1.7 presents the theoretical and experimental TG curves for the demineralized coal-alkali blended samples with the addition of 10 K-wt % alkali compound. From these curves, it can be seen that deviation occurs when comparing the experimental and theoretical curves.

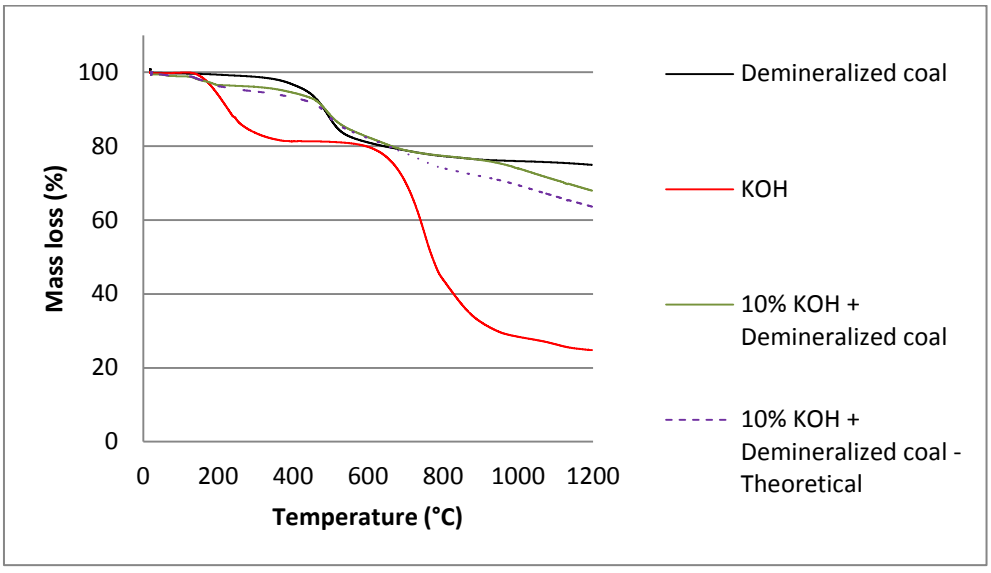

a)

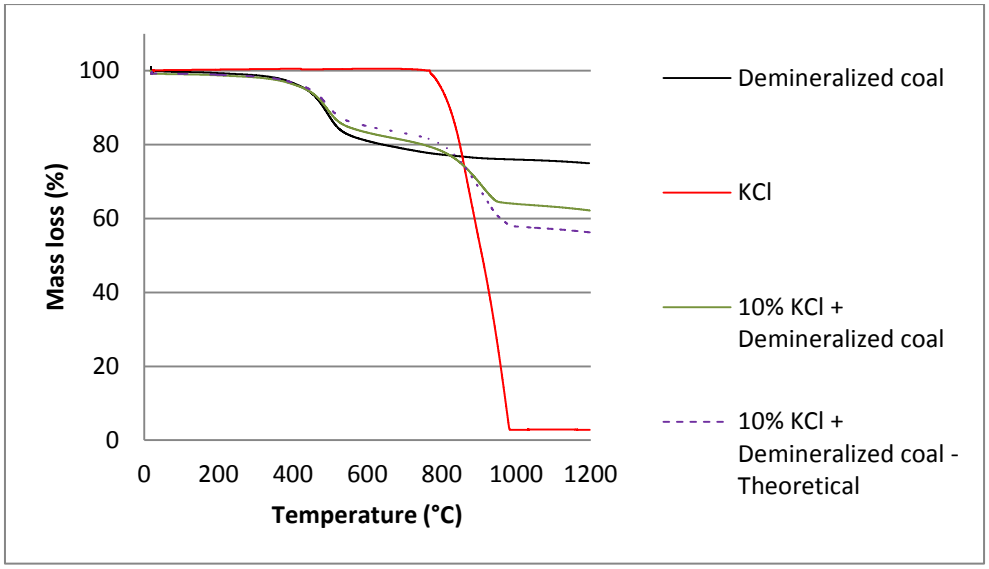

b)

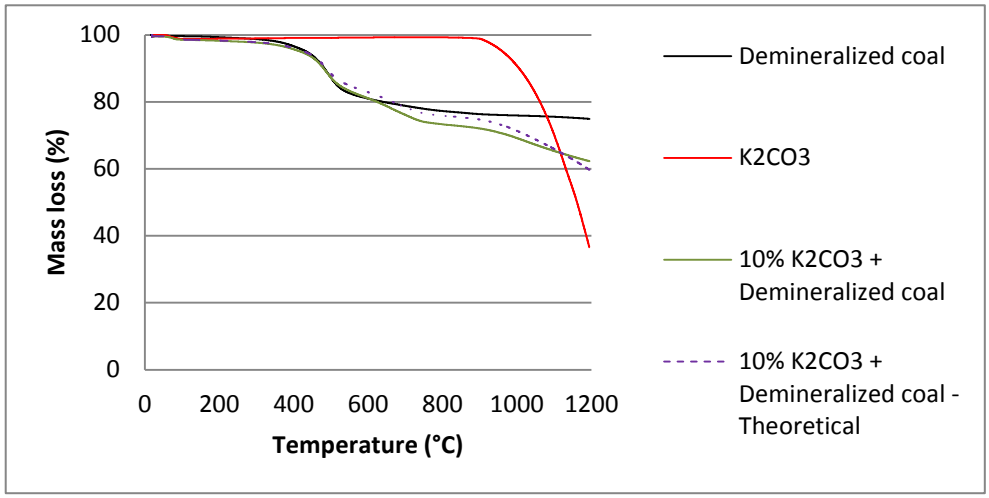

c)

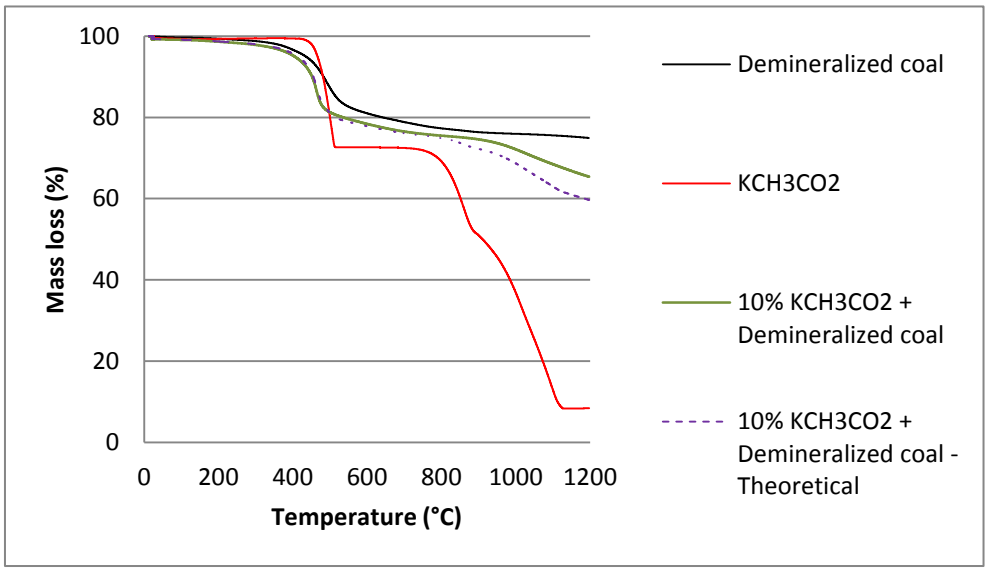

d)

Figure 7.1.7: Theoretical TG curves for the demineralized coal-alkali blends: a) coal-KOH blend, b) coal-KCl blend, c) coal-K_2CO_3 blend, d) coal-KCH_3CO_2 blend

These results obtained and the TG curves shown in Figure 7.1.7 were used to determine the average percentage of deviation between the experimental and theoretical curves. Also determined for these blended samples were the maximum deviation percentage and the temperature ranges where maximum deviation occurred. Presented in Table 7.1.2 are the deviation percentages determined for the alkali blends. From these values in Table 7.1.2, it can be seen that the average deviation between the experimental and theoretical curves does not exceed 2.5% for the demineralized coal-alkali blends. Also from the table, it can be seen that maximum deviation of the curves occurred in the high temperature region (>1000°C). The maximum deviation found for the alkali blends were KCl > KCH_3CO_2 > KOH > K_2CO_3. Deviation of the theoretical curve may be influenced by the anion bound to the potassium, since the anion will react differently during heat treatment of the sample. Some anions will undergo decomposition to create gaseous species which might promote reactions within the sample. Jones *et al* [2005] also suggested that the degree to which synergy for the sample is observed may be influenced by the demineralization of the coal.

Table 7.1.2: Deviation percentages determined for the alkali blend samples

Sample Name	**Alkali compound loading wt %**	**Average Deviation (%)**	**Maximum Deviation (%)**	**T_{max} at maximum deviation (°C)**
Coal-KOH blend	10%	2.3	6.4	1140-1200
Coal-KCl blend	10%	2.5	9.6	980-1200
Coal-K_2CO_3 blend	10%	1.4	4.1	1195
Coal-KCH_3CO_2 blend	10%	1.7	8.8	1130-1140

From the TG results obtained for these different potassium compound samples, it was seen that the addition of the potassium compounds to the demineralized coal influenced the mass loss of the demineralized coal. The KOH, KCl and K_2CO_3 compounds decrease the relative reactivity of the demineralized coal. The relative reactivity of the demineralized coal was increased with the addition of KCH_3CO_2 to the coal with maximum increase observed with 10 K-wt% addition. This increase in the relative reactivity might be due to secondary gasification taking place due to reactions taking place between the sample and the decomposition gases. Deviation of the theoretical and experimental TG curves might be due to the anions bound to the potassium metal or demineralization of the coal.

7.2 Mass Spectroscopy (MS)

MS was used to determine the effect that potassium compounds have on the temperature range at which certain gases are evolved and also the temperature at which the maximum evolution of these gases was observed. The MS results that were obtained using the procedures described in Chapter 4 (see paragraph 4.13) are presented in the sections below. It is important to note that only qualitative analyses were done on the MS results for the different samples. Evolution profiles for the different gaseous species determined in this study are derived from the raw coal, demineralized coal and the demineralized coal-alkali blends. The potassium compounds were added to the coal in mass percentages of 1, 4, 5 and 10 K-wt%. Presented in the sections below are the gas species for the different potassium compounds.

7.2.1 H_2 evolution

Presented in the figures 7.2.1.1-7.2.1.5 are the evolution profiles of H_2 (measured at m/z of 2 amu) profiles for the raw and demineralized coal samples, potassium hydroxide blends, potassium chloride blends, potassium carbonate blends and potassium acetate blends. These figures are used to determine the maximum H_2 evolution temperatures for each of the different samples, which are presented in Tables 7.2.1.1 – 7.2.1.5. The temperature at which maximum evolution was taken was the temperature where the MS peak reached its maximum.

7.2.1.1 Raw and demineralized coal

The maximum H_2 evolution temperatures for the raw coal and demineralized coal samples are presented in Table 7.2.1.1. From the table, an increase of 10°C in the maximum H_2 evolution temperature was observed after the coal has undergone demineralization. Figure 7.2.1.1 presents the H_2 evolution profiles for the raw and demineralized coal samples. The increase in temperature at maximum rate of H_2 evolution may be due to the removal of the minerals from the coal sample, which may act as catalysts for the process.

Table 7.2.1.1: Maximum H_2 evolution temperatures for the samples derived from the raw and demineralized coal

Sample	Max evolution temperature (°C)
Raw coal	740
Demineralized coal	750

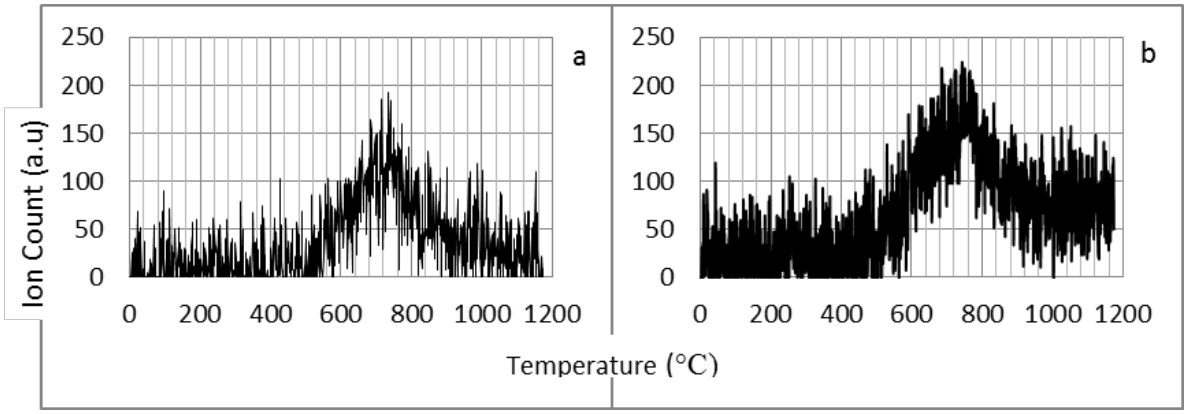

Figure 7.2.1.1: Mass spectra of H_2 for a) the raw coal and b) the demineralized coal

7.2.1.2 Potassium hydroxide

Presented in Table 7.2.1.2 are the maximum evolution temperatures of H_2 for the samples with the different weight percentages of KOH added to the demineralized coal. From these values, it can be seen that with the addition of the KOH to the demineralized coal, a decrease in the H_2 evolution temperatures was observed with the increase in the alkali compound loading. Comparing the H_2 evolution temperatures of the samples with the added alkali compound to that of demineralized coal, a decrease in the temperature can be seen with the addition of the alkali compound. This suggests that KOH promotes the evolution of H_2 during pyrolysis. Figure 7.2.1.2 presents the H_2 evolution profiles for the demineralized coal-alkali blends. From these profiles it can be seen that the temperature at which H_2 evolution started for the samples with the different loadings were the same (around 520°C). Compared to that of the demineralized coal (460°C), an increase was observed. From these observations, KOH decreased the maximum H_2 evolution temperature of the sample, with an observed maximum decrease in the temperature at 10% loading, while increasing the onset of evolution temperature when compared to the demineralized coal. The reactions where H_2 is evolved seem to occur at a faster rate when KOH is added to the coal.

Table 7.2.1.2: Maximum H_2 evolution temperatures for the char samples derived from the demineralized coal-alkali blends with KOH addition

Sample	Loading (wt%)	Max evolution temperature (°C)
Demineralized coal	0	750
KOH - blends	1	720
	4	700
	5	650
	10	640

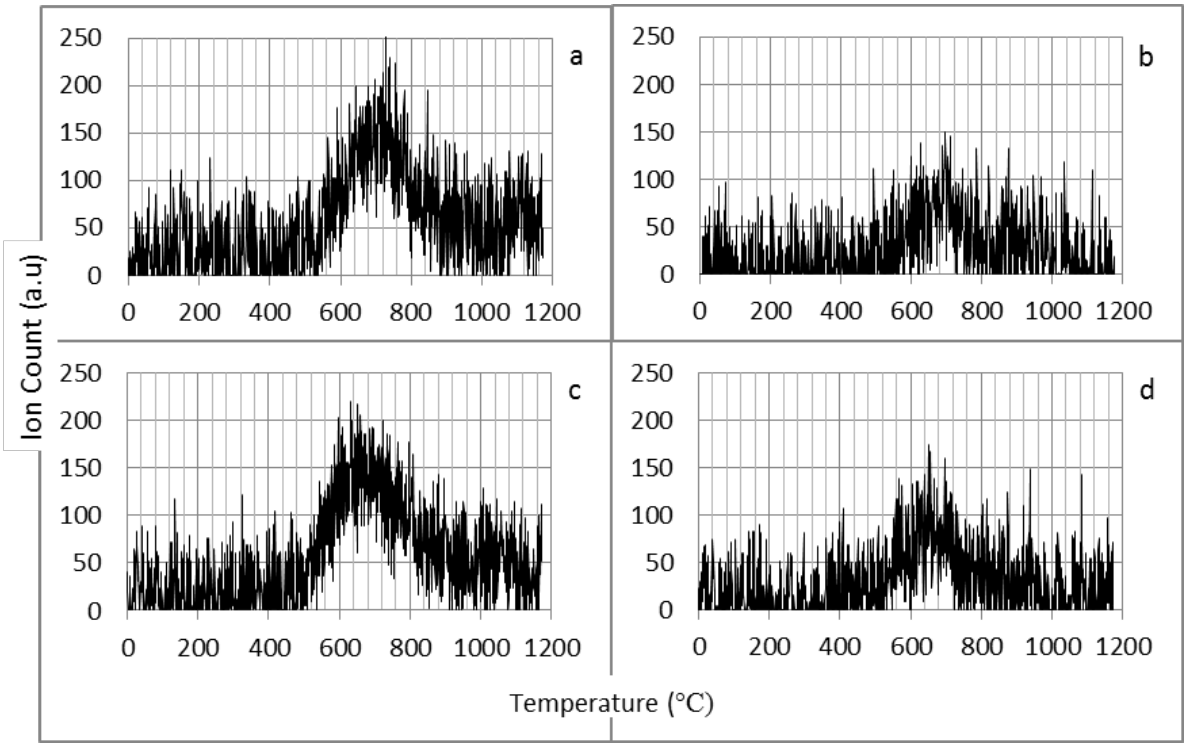

Figure 7.2.1.2: Mass spectra of H_2 for the demineralized coal-alkali blended samples: a) 1% b) 4% c) 5% and d) 10% KOH compound loading

7.2.1.3 Potassium chloride

The maximum H_2 evolution temperatures for the samples with the added KCl compound are presented in Table 7.2.1.3. From these temperature values, it can be seen that there was no significant temperature change with increasing alkali compound loading to the demineralized coal. When compared to that of the demineralized coal, a decrease in the evolution temperature for H_2 was observed. This may suggest that the alkali compound decreased the evolution temperature, but the amount of compound loaded to the demineralized coal did not affect the temperature. The H_2 evolution profiles for the demineralized coal-alkali blends are presented in Figure 7.2.1.3. From these profiles, it can be seen that the temperature at which H_2 evolution started to take place for the samples with the added KCl compound was about 580°C. Compared to that of the demineralized coal (460°C), an increase in the temperature was observed. These results may suggest that the percentage of KCl loaded to the samples does not affect the maximum H_2 evolution temperatures of the samples, but a decrease was observed when compared to the demineralized coal. Also, KCl increases the onset of evolution temperature for the samples with the added alkali compound compared to that of the parent and demineralized coal samples.

Table 7.2.1.3: Maximum H_2 evolution temperatures for the char samples derived from the demineralized coal-alkali blends with KCl addition

Sample	Loading (wt%)	Max evolution temperature (°C)
Demineralized coal	0	750
KCl - blends	1	710
	4	720
	5	710
	10	710

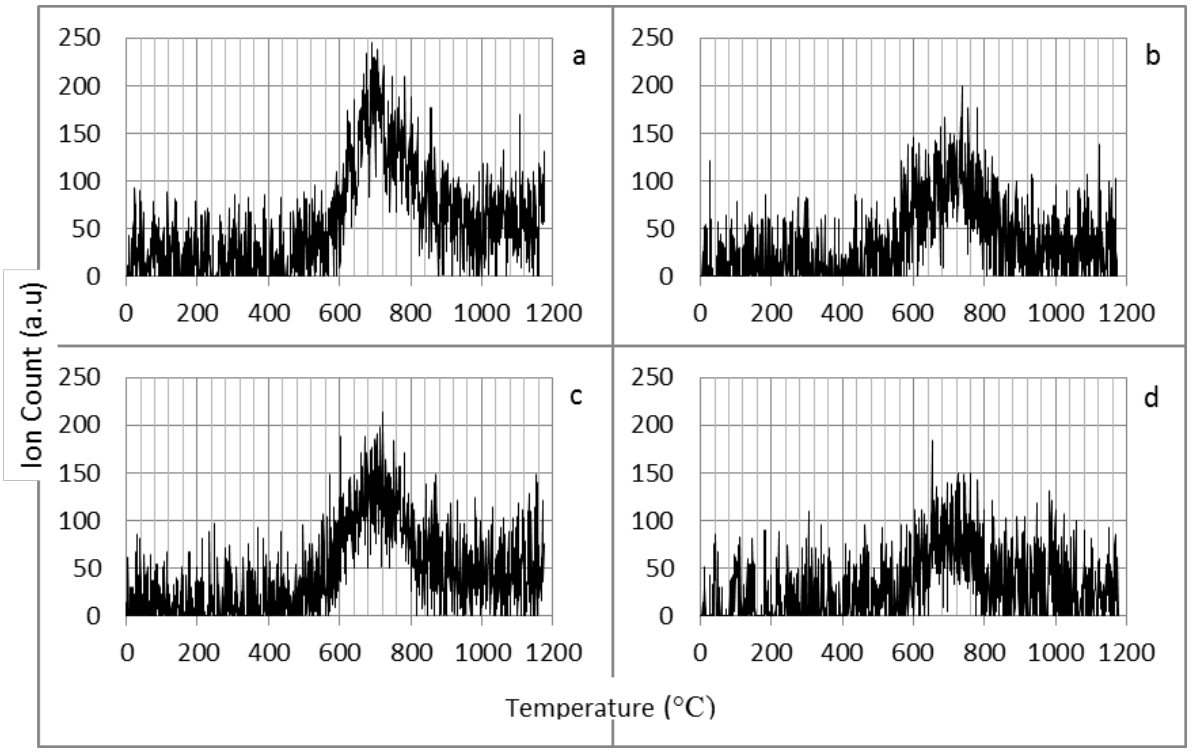

Figure 7.2.1.3: Mass spectra of H_2 for the demineralized coal-alkali blended samples: a) 1% b) 4% c) 5% and d) 10% KCl compound loading

7.2.1.4 Potassium carbonate

The maximum H_2 evolution temperatures for the samples with the added K_2CO_3 are presented in Table 7.2.1.4. From these values in Table 7.2.1.4, it can be seen that a decrease in the maximum H_2 evolution temperature was observed with an increase in alkali compound loading to the demineralized coal. Compared with the demineralized coal sample, a decrease in the H_2 evolution temperature was observed. Figure 7.2.1.4 presents the H_2 evolution profiles for the samples with the added alkali compound. From these profiles it can be seen that no significant change in the onset of evolution temperature was

observed for the demineralized coal-alkali blends, even compared to the demineralized coal sample.

Table 7.2.1.4: Maximum H_2 evolution temperatures for the char samples derived from the demineralized coal-alkali blends with K_2CO_3 addition

Sample	Loading (wt%)	Max evolution temperature (°C)
Demineralized coal	0	750
K_2CO_3 - blends	1	680
	4	650
	5	660
	10	630

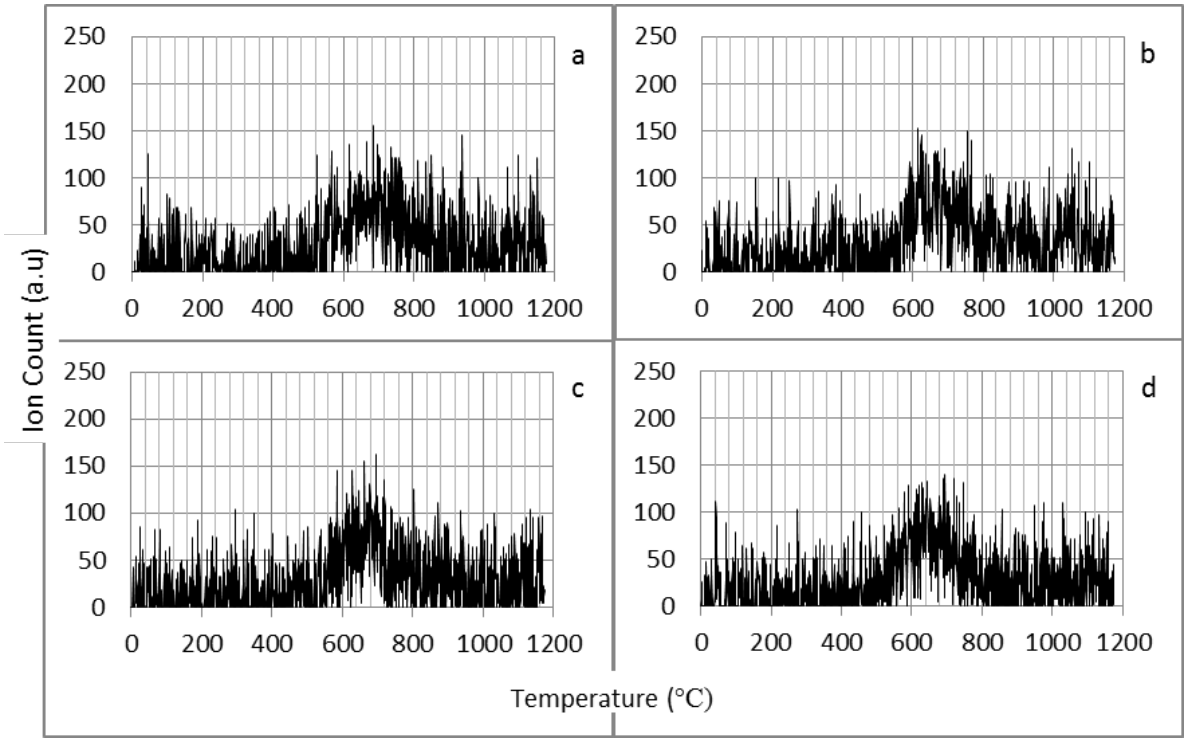

Figure 7.2.1.4: Mass spectra of H_2 for the demineralized coal-alkali blended samples: a) 1% b) 4% c) 5% and d) 10% K_2CO_3 compound loading

7.2.1.5 Potassium acetate

Table 7.2.1.5 presents the maximum H_2 evolution temperatures for the samples with the added KCH_3CO_2. Using the temperatures in the table below, it can be seen that a decrease in the maximum H_2 evolution temperature was observed with increased alkali compound loading to the demineralized coal. When the demineralized coal-alkali blends were compared to that of the demineralized coal sample, an increase in the maximum H_2

evolution temperature was observed for all the samples with the added alkali compound. Presented in Figure 7.2.1.5 are the H_2 evolution profiles for the demineralized coal-alkali blends. From these profiles it can be seen that the onset temperature for evolution of H_2 decreased with an increase in the alkali compound loading. This suggests that potassium acetate promotes the reactions involving the evolution of H_2 and thus evolution started to occur at lower temperatures.

Table 7.2.1.5: Maximum H_2 evolution temperatures for the char samples derived from the demineralized coal-alkali blends with KCH_3CO_2 addition

Sample	Loading (wt%)	Max evolution temperature (°C)
Demineralized coal	0	750
KCH_3CO_2 - blends	1	710
	4	660
	5	650
	10	580

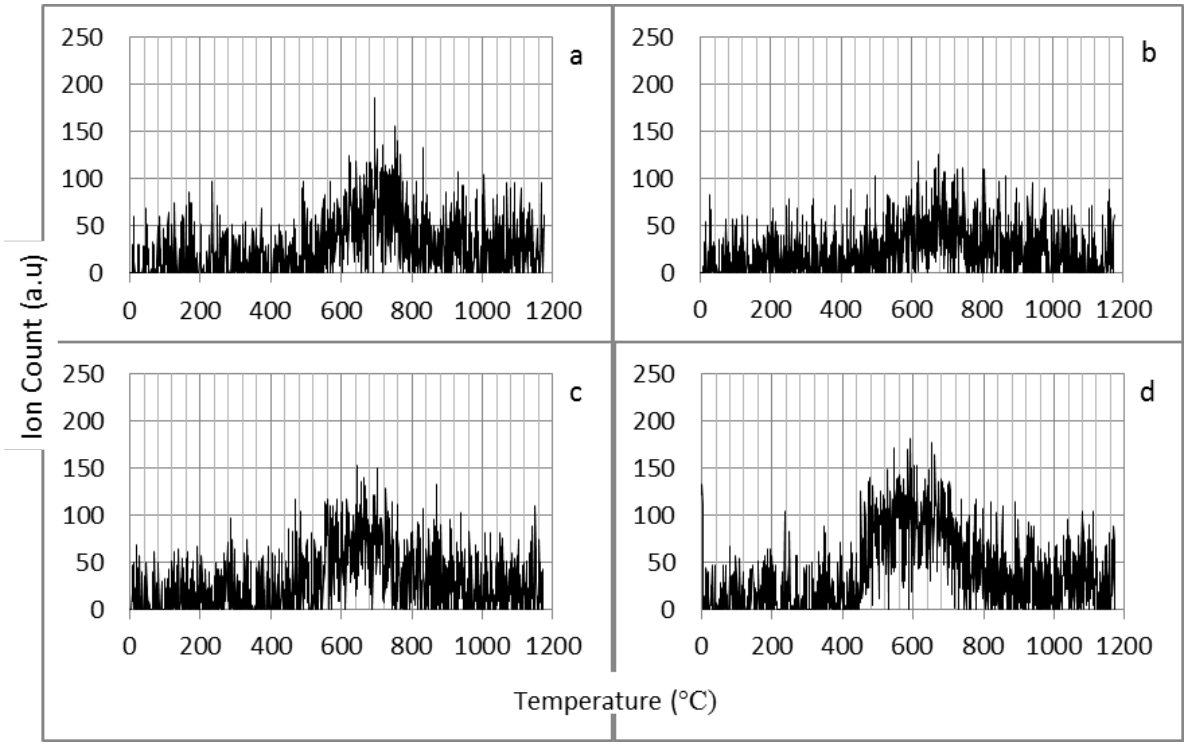

Figure 7.2.1.5: Mass spectra of H_2 for the demineralized coal-alkali blended samples: a) 1% b) 4% c) 5% and d) 10% KCH_3CO_2 compound loading

7.2.2 CH_3^+ evolution

Presented in the figures 7.2.2.1-7.2.2.6are the evolution profiles of CH_3^+ (measured at m/z of 15 amu) for the raw and demineralized coal samples, potassium hydroxide blends, potassium chloride blends, potassium carbonate blends and potassium acetate blends. These figures are used to determine the evolution temperatures at maximum rate of CH_3^+ evolution for each of the different samples, which are presented in Tables 7.2.2.1 – 7.2.2.5.

7.2.2.1 Raw and demineralized coal

Presented in Table 7.2.2.1 are the maximum CH_3^+ evolution temperatures for the raw and demineralized coal samples. From this table it can be seen that a small decrease in the evolution temperature of CH_3^+ was observed after demineralization of the parent coal. From the CH_3^+ evolution profiles presented in Figure 7.2.2.1, it can be seen that the onset of evolution for the raw and demineralized coal samples started at a temperature of 400°C. From these results, it can be seen that demineralization had a small effect on the maximum evolution temperature of CH_3^+ when compared to the parent coal sample, but had no effect on the temperature at which evolution of CH_3^+ started.

Table 7.2.2.1: Maximum CH_3^+ evolution temperatures for the samples derived from the raw and demineralized coal

Sample	Max evolution temperature (°C)
Raw coal	520
Demineralized coal	490

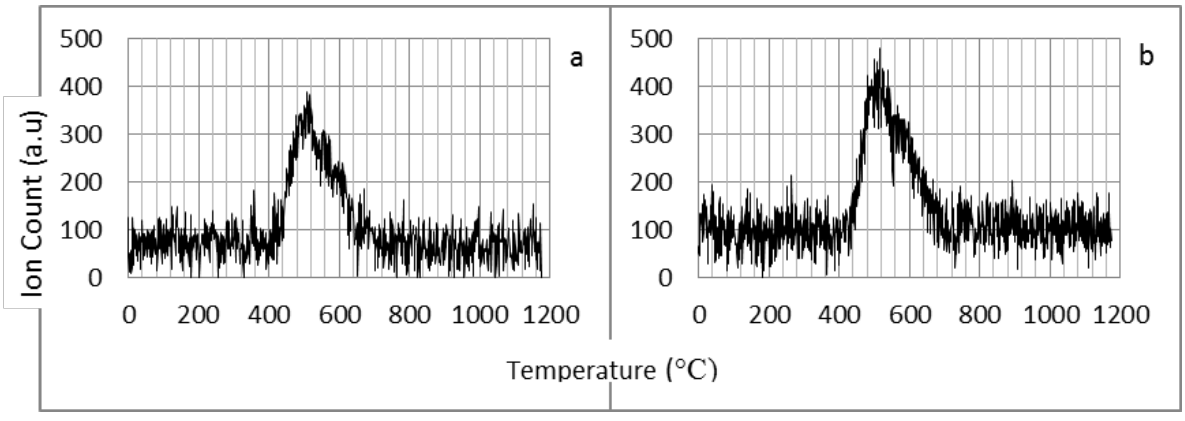

Figure 7.2.2.1: Mass spectra of CH_3^+ for a) the raw coal and b) the demineralized coal

7.2.2.2 Potassium hydroxide

The maximum CH_3^+ evolution temperatures for the demineralized coal-alkali blends with the added KOH are presented in Table 7.2.2.2. These values show that the maximum CH_3^+ evolution temperatures did not change with an increase in alkali compound loading. When CH_3^+ evolution temperatures of the demineralized coal-alkali blends are compared to the CH_3^+ evolution temperature of the demineralized coal sample, no significant change in the temperature was observed. CH_3^+ evolution profiles for the demineralized coal-alkali blends with KOH are presented in Figure 7.2.2.2. These profiles were used to determine the onset of CH_3^+ evolution for the demineralized coal-alkali blends. It was found that evolution for all the samples with the added alkali compounds started at approximately the same temperature of 420°C. Thus it can be said that potassium hydroxide did not influence the evolution of CH_3^+ for the demineralized coal-alkali blended samples.

Table 7.2.2.2: Maximum CH_3^+ evolution temperatures for the char samples derived from the demineralized coal-alkali blends with KOH addition

Sample	Loading (wt%)	Max evolution temperature (°C)
Demineralized coal	0	490
KOH - blends	1	500
	4	500
	5	500
	10	500

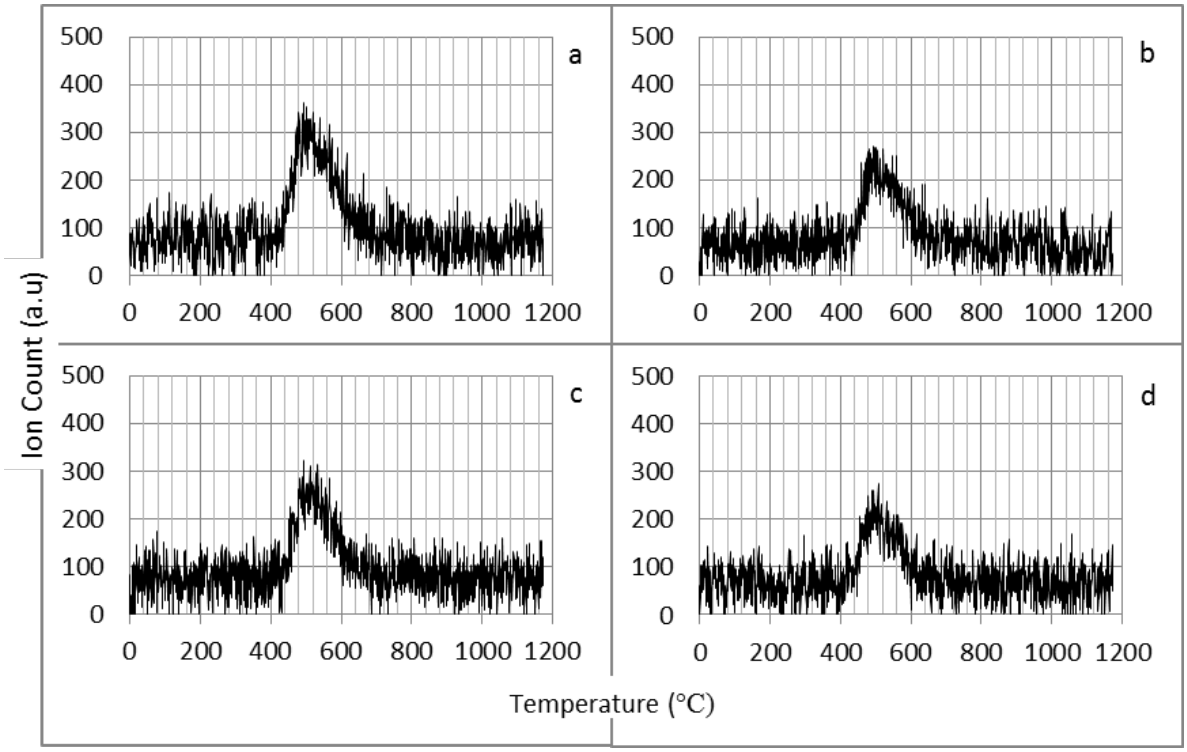

Figure 7.2.2.2: Mass spectra of CH_3^+ for the demineralized coal-alkali blended samples: a) 1% b) 4% c) 5% and d) 10% KOH compound loading

7.2.2.3 Potassium chloride

Presented in Table 7.2.2.3 are the maximum evolution temperatures of CH_3^+ for the demineralized coal-alkali blends with KCl. From these values presented in the table, it can be seen that no significant change in the CH_3^+ evolution temperature was observed for the KCl-blends and demineralized coal. The evolution profiles of CH_3^+ for the demineralized coal-alkali blends are presented in Figure 7.2.2.3. From these profiles it can be seen that the onset of evolution of CH_3^+ was not influenced by the compound loading. Compared to the demineralized coal sample, KCl did not influence the onset of evolution of $CH_3^{+\cdot}$

Table 7.2.2.3: Maximum CH_3^+ evolution temperatures for the char samples derived from the demineralized coal-alkali blends with KCl addition

Sample	Loading (wt%)	Max evolution temperature (°C)
Demineralized coal	0	490
KCl - blends	1	500
	4	500
	5	500
	10	490

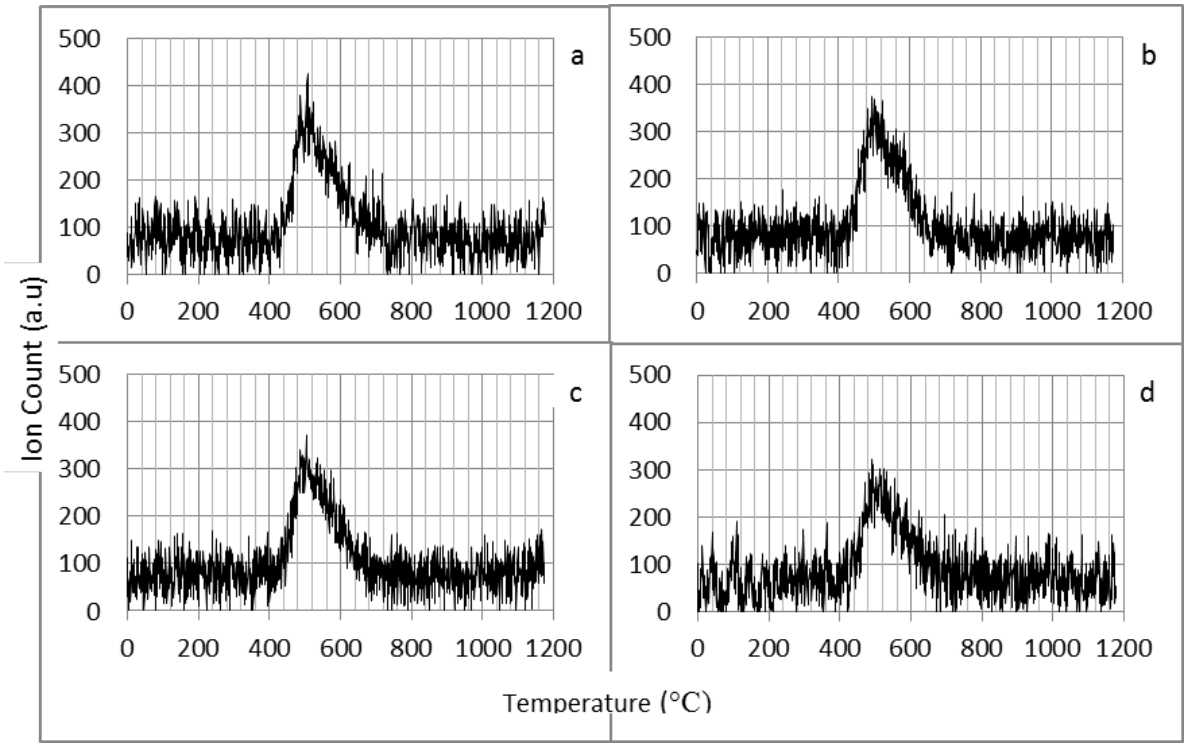

Figure 7.2.2.3: Mass spectra of CH_3^+ for the demineralized coal-alkali blended samples: a) 1% b) 4% c) 5% and d) 10% KCl compound loading

7.2.2.4 Potassium carbonate

Presented in Table 7.2.2.4 are the maximum CH_3^+ evolution temperatures for the samples derived from the demineralized coal-alkali blends with the added K_2CO_3. From the table, it can be seen that no change in the maximum evolution temperature of CH_3^+ was observed for the samples with the added alkali compound. No significant change in the evolution temperature was observed when the samples with the alkali compound were compared to that of the demineralized coal. Considering the CH_3^+ evolution profiles in Figure 7.2.2.4, the onset of evolution for the samples stayed the same (400°C) even with increasing alkali compound loading. The temperature at which evolution of CH_3^+ started for the demineralized coal-alkali blends corresponds to that of the demineralized coal sample, suggesting that no change in the onset temperature was observed after demineralization. From these results it can be seen that K_2CO_3 did not affect the onset of evolution temperatures for the coal samples with the added compound and no change in the maximum CH_3^+ evolution temperature.

Table 7.2.2.4: Maximum CH_3^+ evolution temperatures for the char samples derived from the demineralized coal-alkali blends with K_2CO_3 addition

Sample	Loading (wt%)	Max evolution temperature (°C)
Demineralized coal	0	490
K_2CO_3 - blends	1	500
	4	500
	5	500
	10	500

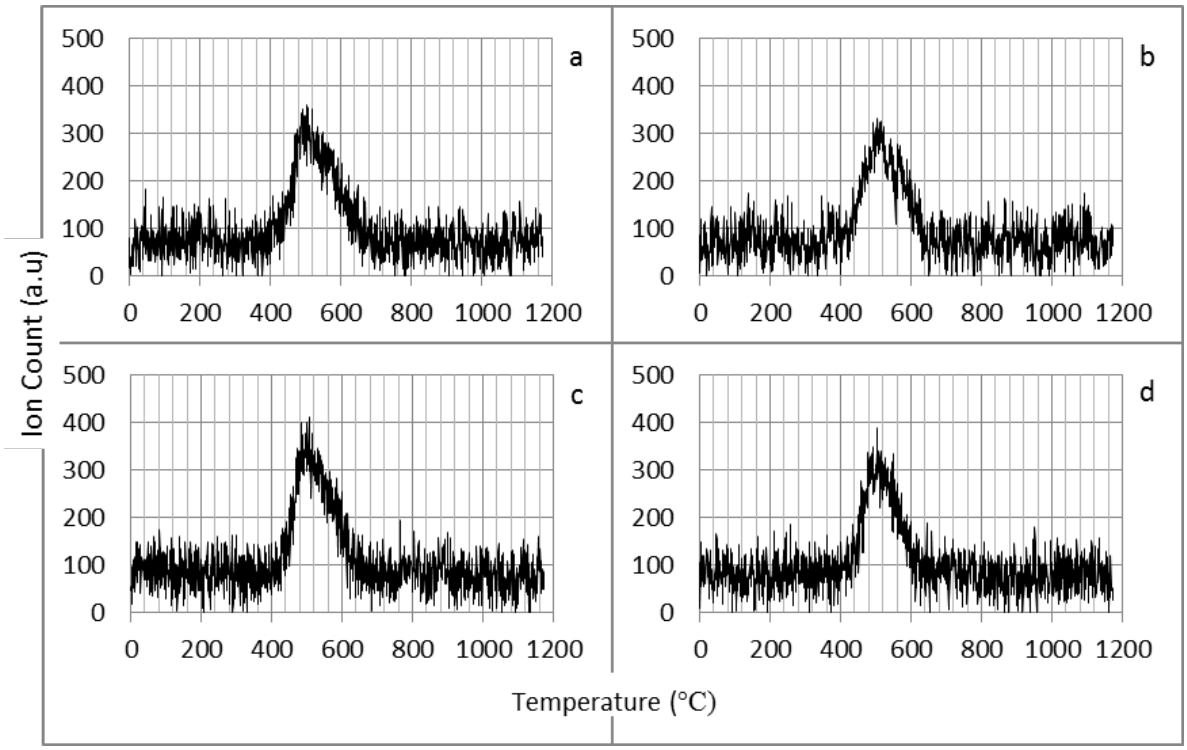

Figure 7.2.2.4: Mass spectra of CH_3^+ for the demineralized coal-alkali blended samples: a) 1% b) 4% c) 5% and d) 10% K_2CO_3 compound loading

7.2.2.5 Potassium acetate

Presented in Table 7.2.2.5 are the maximum CH_3^+ evolution temperatures for the demineralized coal-alkali blends with the added KCH_3CO_2. From the table, a decrease in the CH_3^+ evolution temperature was observed with increased alkali compound loading. When the blends are compared to the demineralized coal, a small increase in the maximum CH_3^+ evolution temperature was observed. From the CH_3^+ evolution profiles presented in Figure 7.2.2.5, the temperature at which CH_3^+ evolution started - (380°C) - for the demineralized coal-alkali blends did not change with an increase in the alkali compound

loading. Thus, with the addition of potassium acetate to the demineralized coal sample, a small increase in the maximum evolution temperature of CH_3^+ was observed with the addition of the alkali compound, followed by a decrease in the evolution temperature as the alkali compound loading increased. This decrease in the CH_3^+ evolution temperature with increased alkali compound loading seems to be due to the decomposition of the alkali compound and the evolution of CH_3^+. Presented in Figure 7.2.2.6 is the CH_3^+ evolution profile for the potassium compound. From this profile it can be seen that the maximum evolution temperature of CH_3^+ for the alkali compound was observed at 480°C.

Table 7.2.2.5: Maximum CH_3^+ evolution temperatures for the char samples derived from the demineralized coal-alkali blends with KCH_3CO_2 addition

Sample	Loading (wt%)	Max evolution temperature (°C)
Demineralized coal	0	490
KCH_3CO_2		480
KCH_3CO_2 - blends	1	520
	4	510
	5	500
	10	470

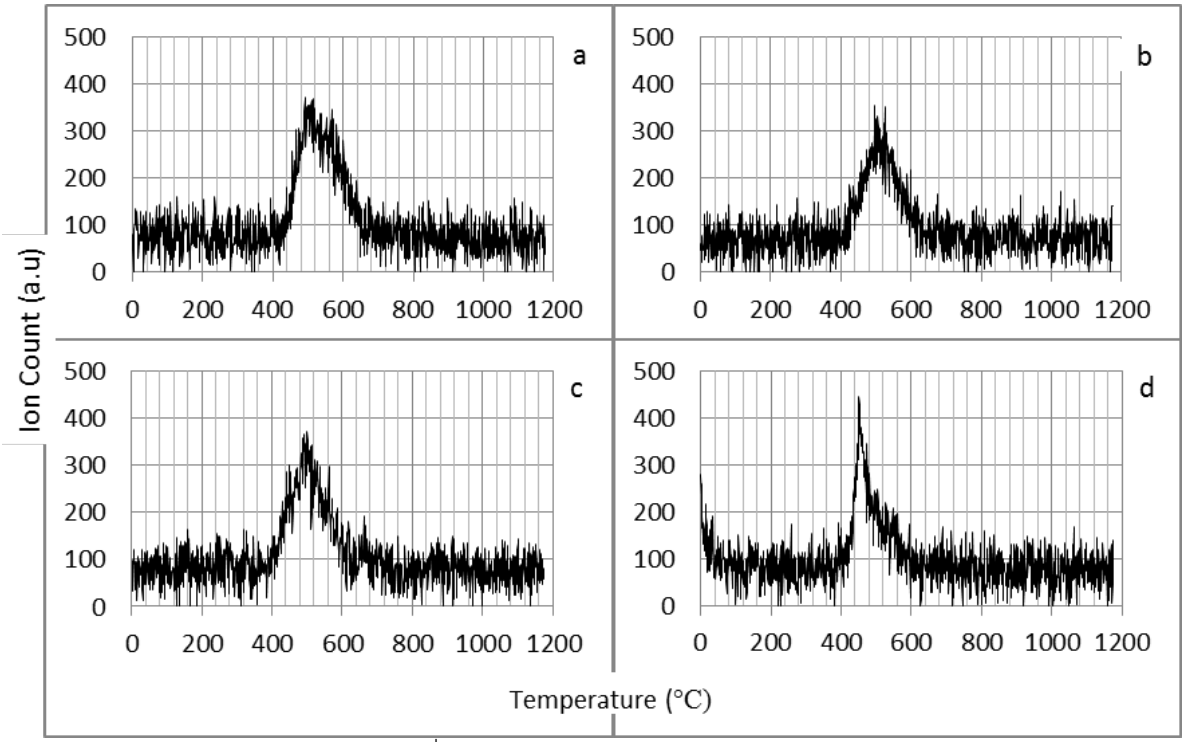

Figure 7.2.2.5: Mass spectra of CH_3^+ for the demineralized coal-alkali blended samples: a) 1% b) 4% c) 5% and d) 10% KCH_3CO_2 compound loading

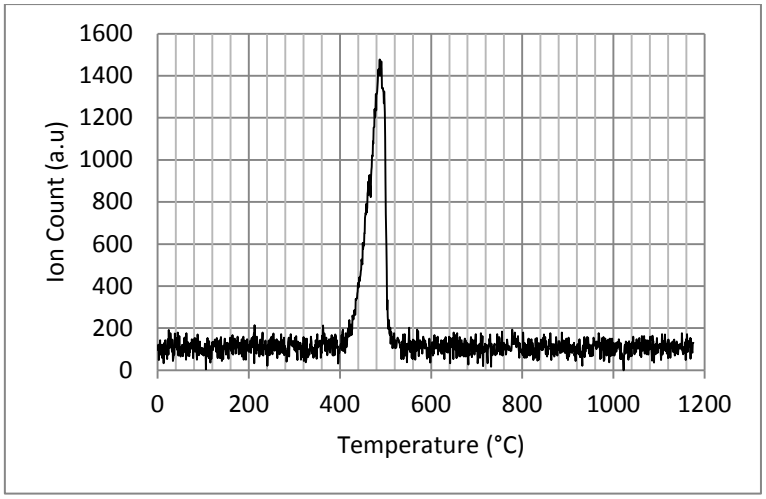

Figure 7.2.2.6: Mass spectra of CH_3^+ for the KCH_3CO_2 compound

7.2.3 CH_4 evolution

Presented in the figures 7.2.3.1-7.2.3.6 are the evolution profiles of CH_4 (measured at m/z of 16 amu) profiles for the raw and demineralized coal samples, potassium hydroxide blends, potassium chloride blends, potassium carbonate blends and potassium acetate blends. These figures are used to determine the maximum evolution temperatures for each of the different samples, which are presented in Tables 7.2.3.1 – 7.2.3.5.

7.2.3.1 Raw and demineralized coal

The maximum CH_4 evolution temperatures for the raw and demineralized coal samples are presented in Table 7.2.3.1. From these values, it can be seen that the temperature of maximum evolution of CH_4 for the raw and demineralized samples did not change. The CH_4 evolution profiles for the samples are presented in Figure 7.2.3.1. From these profiles it can be seen that the onset of CH_4 evolution for the raw and demineralized coal sample started at the same temperature of 380°C. Thus, demineralization of the parent coal did not have an influence on the maximum CH_4 evolution temperature or the temperature at which evolution started.

Table 7.2.3.1: Maximum CH_4 evolution temperatures for the samples derived from the raw and demineralized coal

Sample	Max evolution temperature (°C)
Raw coal	480
Demineralized coal	480

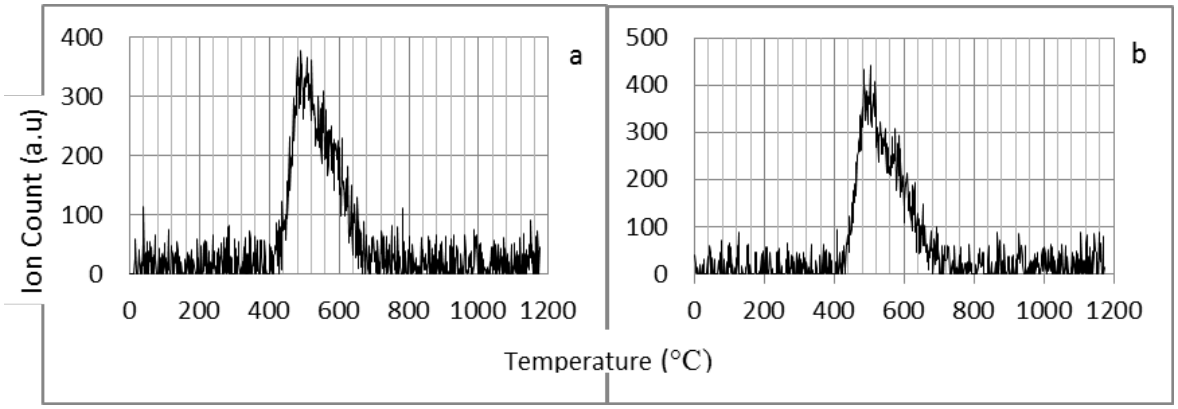

Figure 7.2.3.1: Mass spectra of CH_4 for a) the raw coal and b) the demineralized coal

7.2.3.1 Potassium hydroxide

Presented in Table 7.2.3.2 are the maximum evolution temperatures of CH_4 for the demineralized coal-alkali blends with the added KOH. From these values no change in the CH_4 evolution temperatures was observed with the addition of KOH to the demineralized coal. It was also observed that the alkali compound loading had no influence on the CH_4 evolution temperature for the blended samples. The CH_4 evolution profiles for the demineralized coal-alkali blends are presented in Figure 7.2.3.2. These profiles were used to determine the temperatures at which the onset of CH_4 evolution started for the samples. From these profiles it can be seen that the onset temperature for the blended samples was about 400°C. When compared to the temperature determined for the demineralized coal, a slight increase was observed.

Table 7.2.3.2: Maximum CH_4 evolution temperatures for the char samples derived from the demineralized coal-alkali blends with KOH addition

Sample	Loading (wt%)	Max evolution temperature (°C)
Demineralized coal	0	480
KOH - blends	1	480
	4	480
	5	480
	10	470

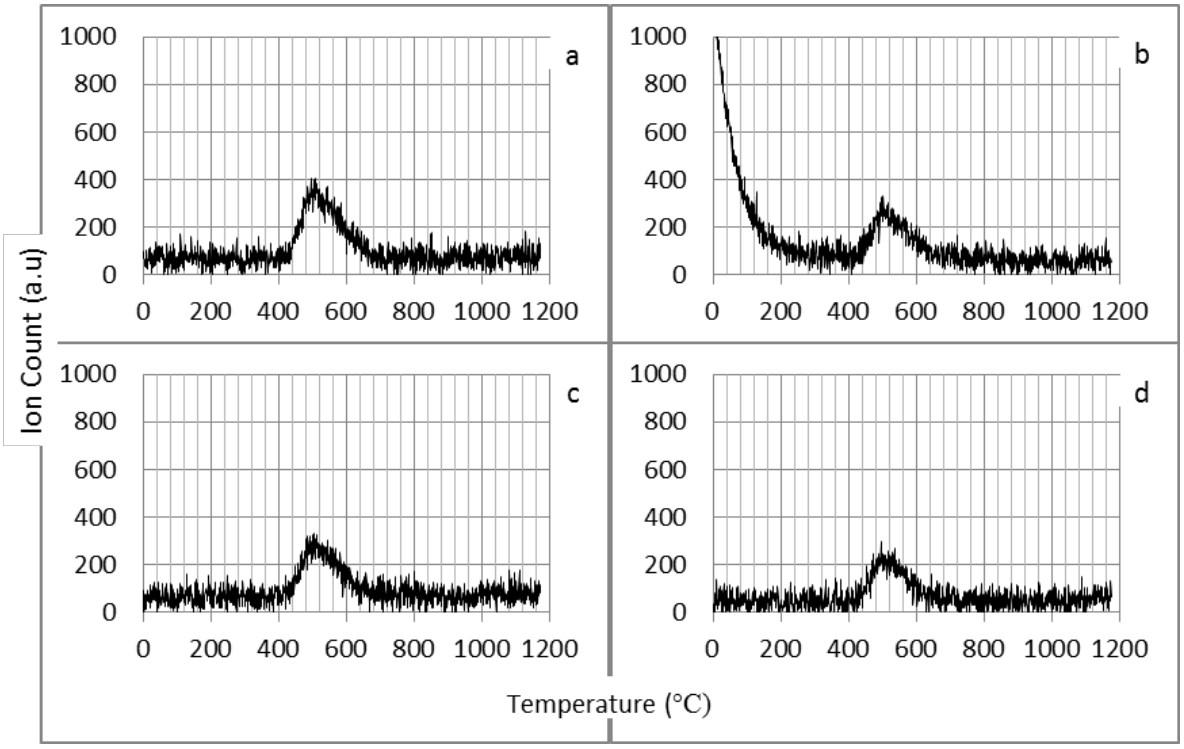

Figure 7.2.3.2: Mass spectra of CH_4 for the demineralized coal-alkali blended samples: a) 1% b) 4% c) 5% and d) 10% KOH compound loading

7.2.3.2 Potassium chloride

Table 7.2.3.3 represents the maximum CH_4 evolution temperatures for the demineralized coal-alkali blends with the added KCl. From these values, it can be seen that the addition of KCl to the demineralized coal did not influence the maximum CH_4 evolution temperature. The compound loading to the demineralized coal had no influence on the evolution temperatures. The CH_4 evolution profiles for the demineralized coal-alkali blends are presented in Figure 7.2.3.3. From these profiles the onset of evolution temperature of CH_4 was determined (380°C) and found that the addition of KCl to the demineralized coal, no change in the onset temperature was observed for the blended samples.

Table 7.2.3.3 Maximum CH_4 evolution temperatures for the char samples derived from the demineralized coal-alkali blends with KCl addition.

Sample	Loading (wt%)	Max evolution temperature (°C)
Demineralized coal	0	480
KCl - blends	1	480
	4	470
	5	470
	10	470

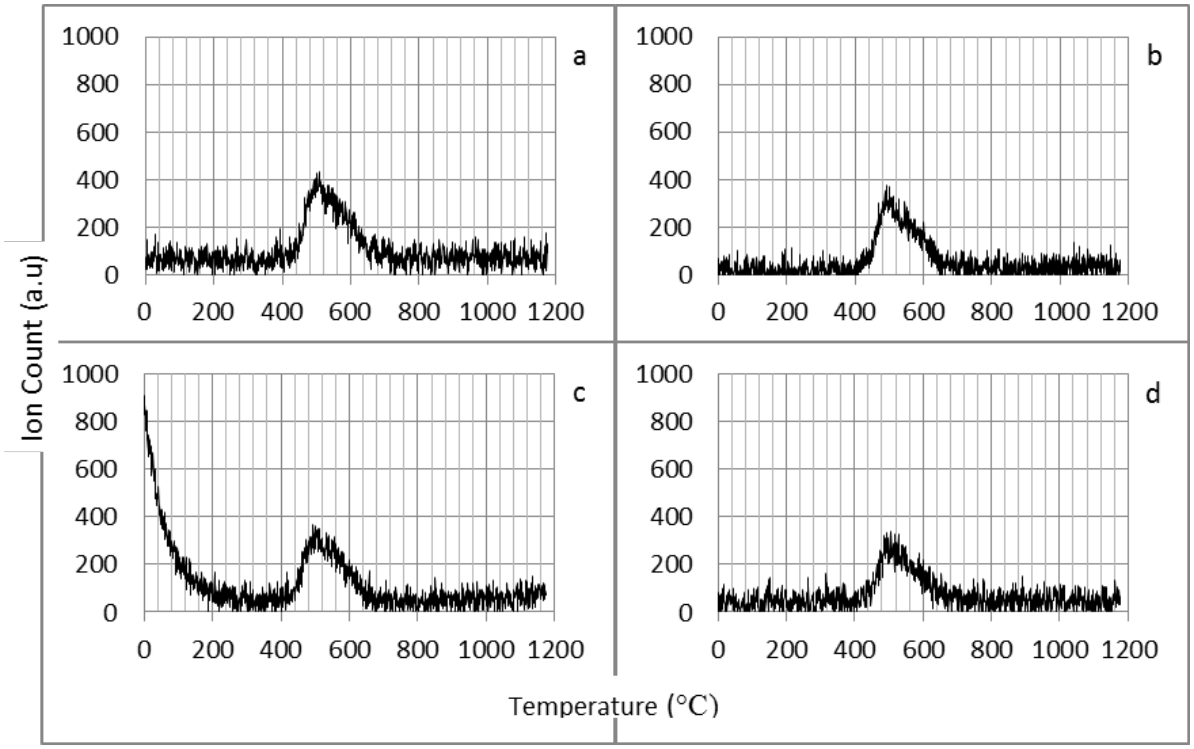

Figure 7.2.3.3: Mass spectra of CH_4 for the demineralized coal-alkali blended samples: a) 1% b) 4% c) 5% and d) 10% KCl compound loading

7.2.3.3 Potassium carbonate

Table 7.2.3.4 presents the maximum evolution temperatures of CH_4 for the demineralized coal-alkali blends with the added K_2CO_3. From the values presented in the table, it can be seen that no change in the CH_4 evolution temperatures for the samples with the alkali compound was observed. No change in the CH_4 evolution temperature was seen when compared to the demineralized coal. The CH_4 evolution profiles for the demineralized coal-alkali blends are presented Figure 7.2.3.4. From these profiles it can be seen that an increase in compound loading did not affect the onset of evolution temperature (380°C).

Table 7.2.3.4 Maximum CH_4 evolution temperatures for the char samples derived from the demineralized coal-alkali blends with K_2CO_3 addition.

Sample	Loading (wt%)	Max evolution temperature (°C)
Demineralized coal	0	480
K_2CO_3 - blends	1	480
	4	480
	5	470
	10	470

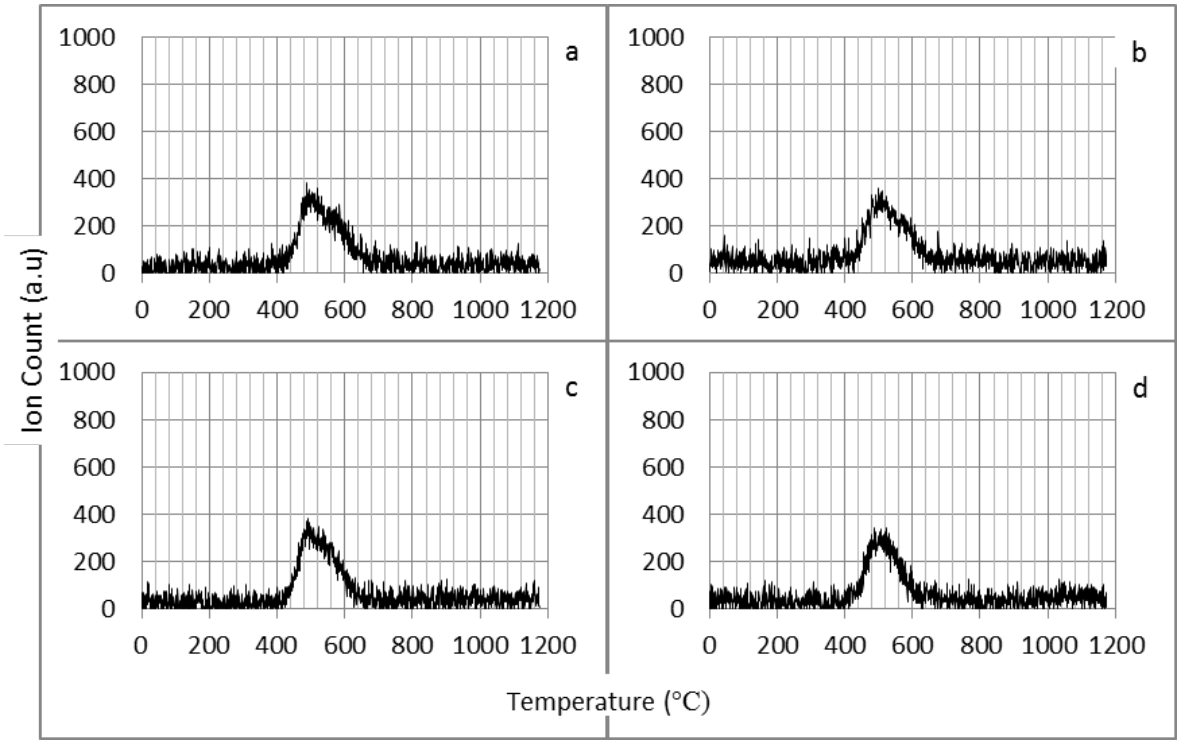

Figure 7.2.3.4: Mass spectra of CH_4 for the demineralized coal-alkali blended samples: a) 1% b) 4% c) 5% and d) 10% K_2CO_3 compound loading

7.2.3.4 Potassium acetate

The maximum CH_4 evolution temperatures for the demineralized coal-alkali blends with the added KCH_3CO_2 are presented in Table 7.2.3.5. Using the temperatures from the table, it can be seen that no change in the CH_4 evolution temperatures were observed for the samples with the added potassium compounds. Figure 7.2.3.5 presents the CH_4 evolution profiles for the demineralized coal-alkali blends. From these profiles it can be seen that the onset of CH_4 evolution temperature (380°C) for the samples with the added potassium compound did not change with an increase in the loading percentage. When compared to the onset temperature of the demineralized coal, no change was observed. Figure 7.2.3.6 presents the evolution curve for the KCH_3CO_2 compound. From this curve it can be seen that the maximum evolution temperature of CH_4 did not change when the compound is added to the demineralized coal.

Table 7.2.3.5: Maximum CH_4 evolution temperatures for the char samples derived from the demineralized coal-alkali blends with KCH_3CO_2 addition

Sample	Loading (wt%)	Max evolution temperature (°C)
Demineralized coal	0	480
KCH_3CO_2		480
KCH_3CO_2 - blends	1	470
	4	470
	5	470
	10	470

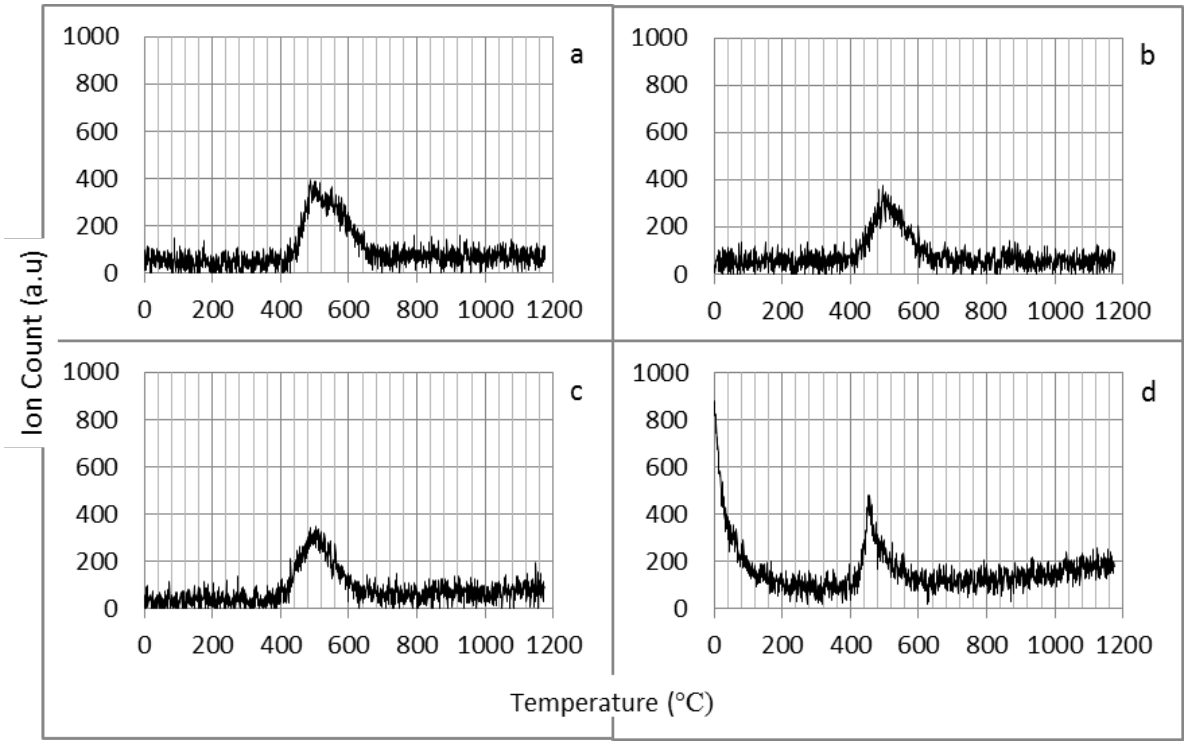

Figure 7.2.3.5: Mass spectra of CH_4 for the demineralized coal-alkali blended samples: a) 1% b) 4% c) 5% and d) 10% KCH_3CO_2 compound loading

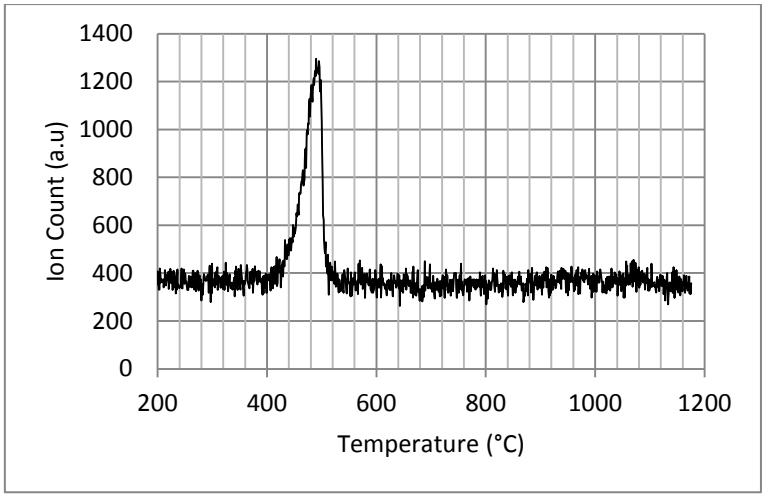

Figure 7.2.3.6 Mass spectra of CH_4 for KCH_3CO_2

7.2.4 CO_2 evolution

Presented in the figures 7.2.4.1-7.2.4.7 are the evolution profiles of CO_2 (measured at m/z of 44amu) for the raw and demineralized coal samples, potassium hydroxide blends, potassium chloride blends, potassium carbonate blends and potassium acetate blends. These figures are used to determine the temperatures at maximum rate of CO_2 evolution for each of the different samples, which are presented in Tables 7.2.4.1 – 7.2.4.2. The temperature at which maximum rate of evolution was taken was the temperature at peak maximum.

7.2.4.1 Raw and demineralized coal

Presented in Figure 7.2.4.1 are the CO_2 evolution profiles for the raw and demineralized coal samples. From these profiles it can be seen that evolution of CO_2 did not occur during the specific temperature range. In Figure 7.2.4.1a evolution of CO_2 seems to occur during the latter part of the heat treatment. From the evolution profile of the raw coal sample, evolution was not completed by the end of the heat treatment. The CO_2 evolution profile of the demineralized coal sample presented in Figure 7.2.4.1b indicated that low amounts of CO_2 are evolved during the heat treatment and evolution has not been completed by the end of the heat treatment. The low amounts of CO_2 evolution seen for the demineralized coal sample may be due to the removal of carbonate containing groups during the demineralization process.

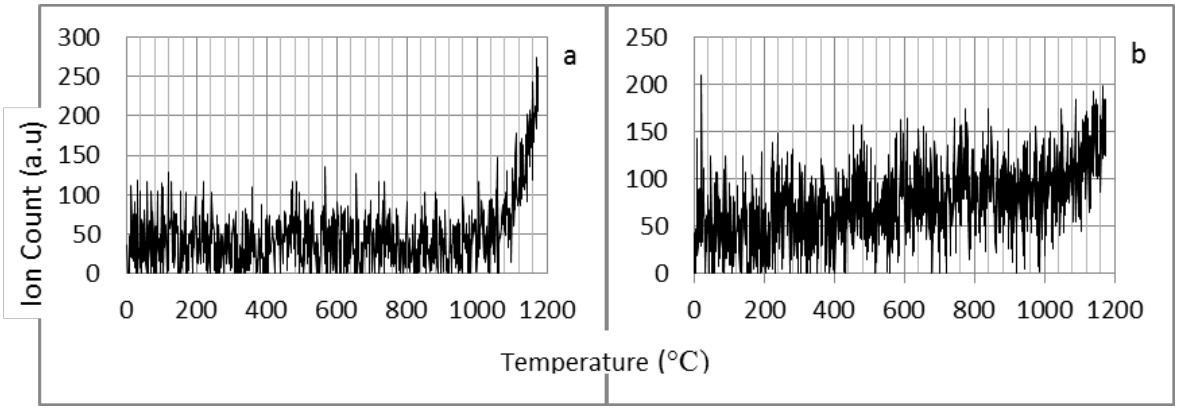

Figure 7.2.4.1: Mass spectra of CO_2 for a) the raw coal and b) the demineralized coal

7.2.4.2 Potassium hydroxide

The evolution profiles of CO_2 for the demineralized coal-alkali blends with the added KOH are presented in Figure 7.2.4.2. From these profiles it can be seen that no significant amount of CO_2 was evolved during the heat treatment and that no temperature range for evolution could be observed. However, non-conclusive increases were observed with an increase in the alkali compound loading. These increases can be seen in the evolution profiles presented in Figure 7.2.4.2.

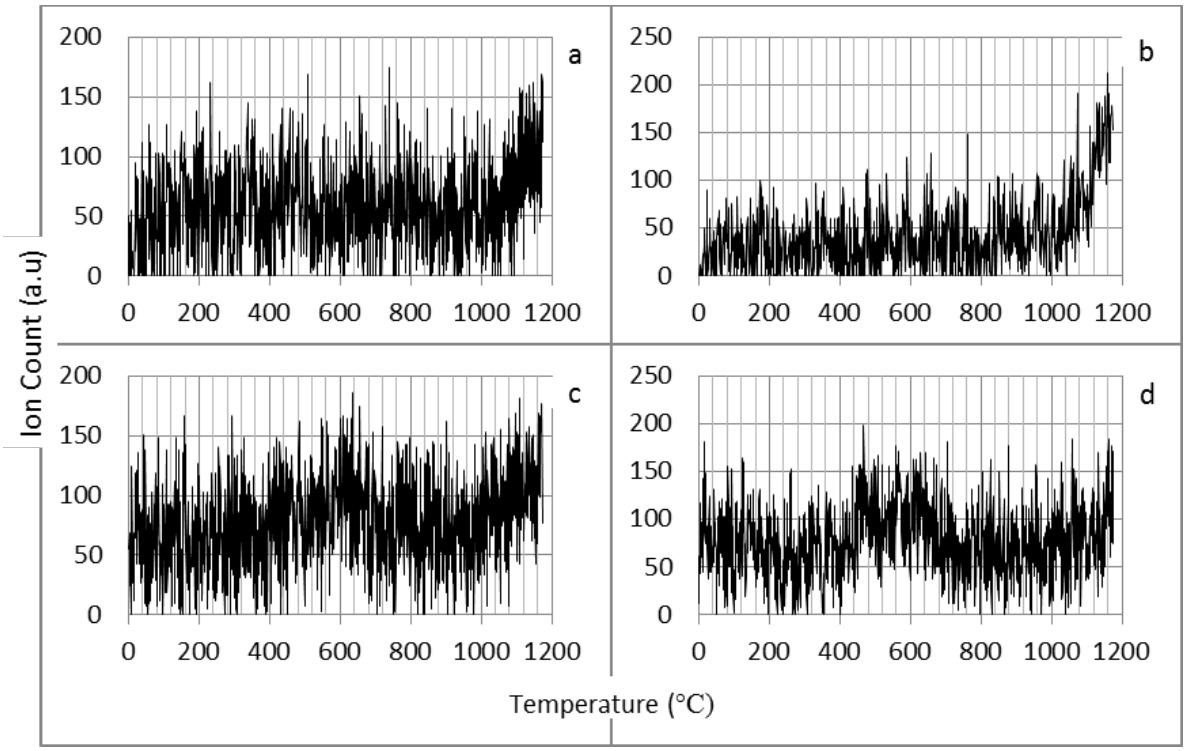

Figure 7.2.4.2: Mass spectra of CO_2 for the demineralized coal-alkali blended samples: a) 1% b) 4% c) 5% and d) 10% KOH compound loading

7.2.4.3 Potassium chloride

The evolution profiles of CO_2 for the demineralized coal-alkali blends with the KCl are presented in Figure 7.2.4.3. From these profiles it can be seen that none to very small amounts of evolution of CO_2 was observed for the samples with the added KCl.

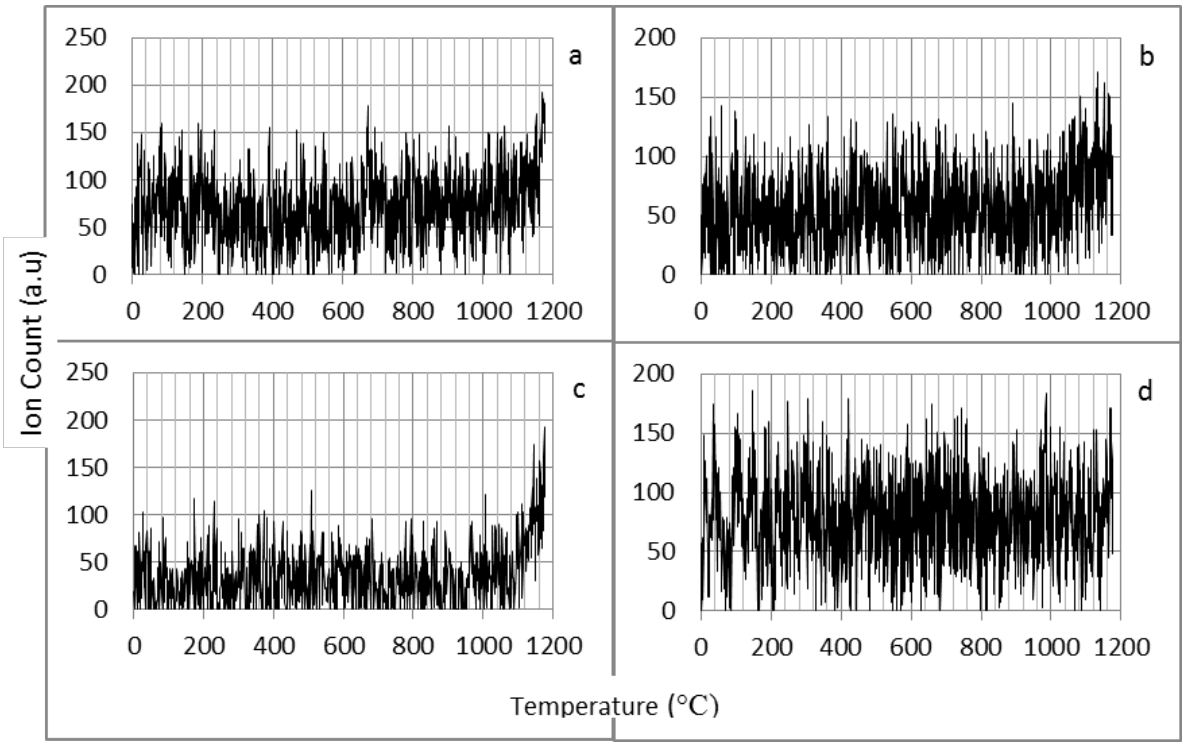

Figure 7.2.4.3: Mass spectra of CO_2 for the demineralized coal-alkali blended samples: a) 1% b) 4% c) 5% and d) 10% KCl compound loading

7.2.4.4 Potassium carbonate

The maximum CO_2 evolution temperatures for the demineralized coal-alkali blends with the K_2CO_3 are presented in Table 7.2.4.1. These curves indicated the possible evolution of very small amounts of CO_2. From the table it can be seen that an increase in the maximum CO_2 evolution temperature was observed with an increase in the alkali compound loading. The CO_2 evolution profiles for the blended samples are presented in Figure 7.2.4.4. Evolution of CO_2 during this heat treatment may be due to the decomposition of the alkali compound. Presented in Figure 7.2.4.5 is the CO_2 evolution profile for the alkali compound, from which it can be seen that evolution of CO_2 started at a temperature of 860°C.

Table 7.2.4.1: Maximum CO_2 evolution temperatures for the char samples derived from the demineralized coal-alkali blends with K_2CO_3 addition

Sample	Loading (wt%)	Max evolution temperature (°C)
Demineralized coal	0	-
K_2CO_3 - blends	1	-
	4	580
	5	610
	10	620

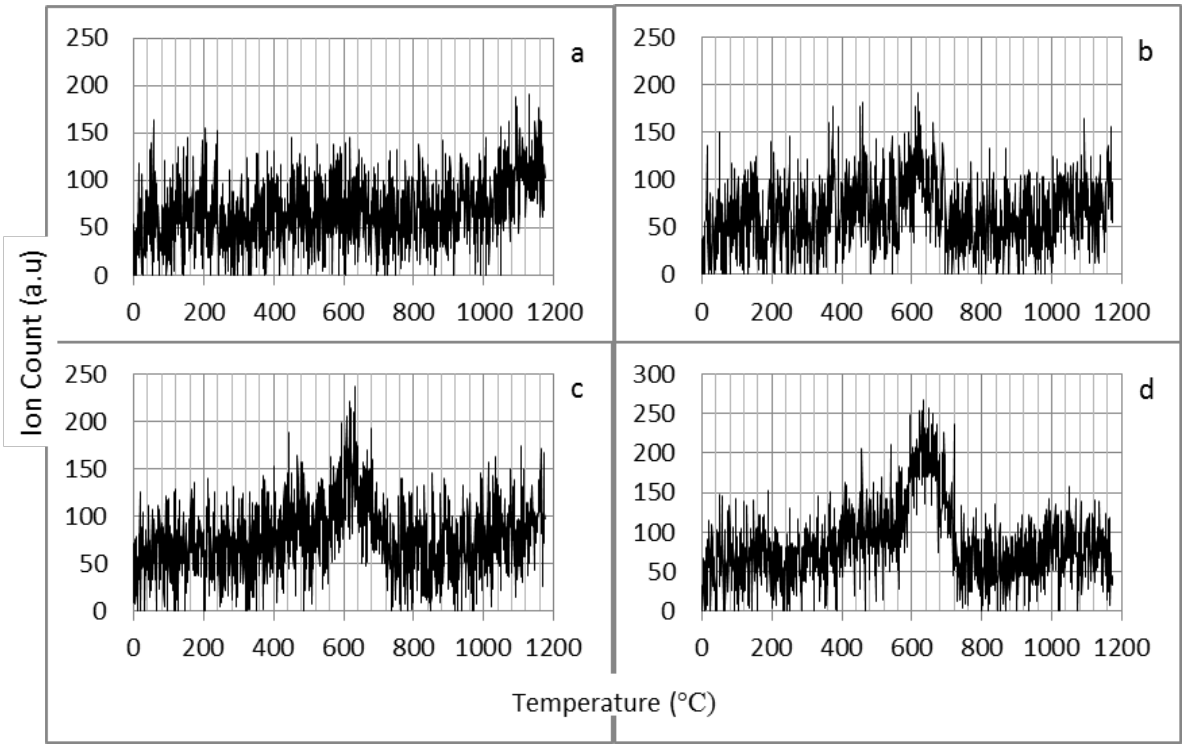

Figure 7.2.4.4: Mass spectra of CO_2 for the demineralized coal-alkali blended samples: a) 1% b) 4% c) 5% and d) 10% K_2CO_3 compound loading

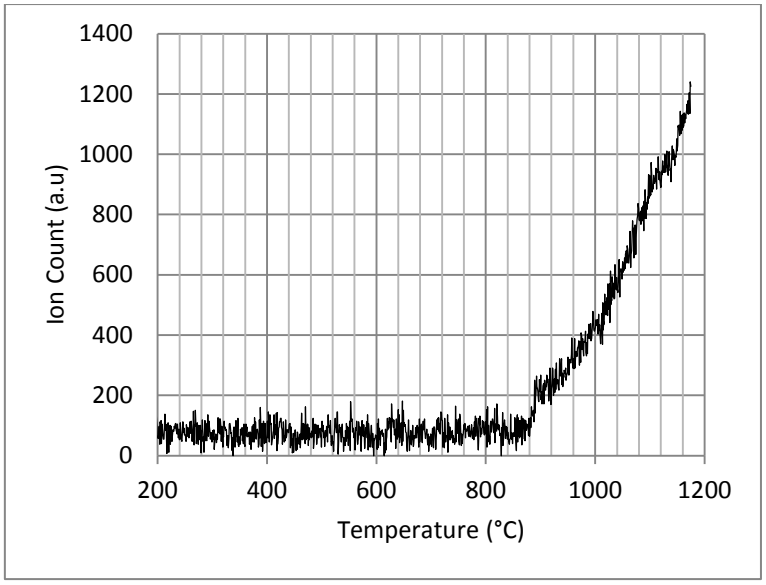

Figure 7.2.4.5: Mass spectra of CO_2 evolution for K_2CO_3

7.2.4.5 Potassium acetate

Presented in Table 7.2.4.2 are the maximum evolution temperatures of CO_2 for the demineralized coal-alkali blends with the added KCH_3CO_2. From these values in the table, it can be seen that no maximum evolution was observed for the blend with 1% alkali addition. For the 4, 5 and 10% blends, a maximum evolution peak can be seen on the evolution profiles. The temperature at which this peak was observed did not change with an increase in the compound loading. Figure 7.2.4.6 presents the CO_2 evolution profiles for the demineralized coal-alkali blends. From these profiles it can be seen that the onset of CO_2 evolution for the blended samples started at the same temperature. This peak has formed due to decomposition of the alkali compound. The CO_2 evolution profile for the KCH_3CO_2 is presented in Figure 7.2.4.7. From this profile it can be seen that the onset of CO_2 evolution for the alkali compound corresponded to that of the blended samples, suggesting that the peaks observed in Figure 7.2.4.6 resulted from alkali compound decomposition. Also observed in the CO_2 evolution profile for the alkali compound was a second peak (temperature range 860-1100°C). This second peak is due to secondary decomposition of the alkali compound.

Table 7.2.4.2: Maximum CO_2 evolution temperatures for the char samples derived from the demineralized coal-alkali blends with KCH_3CO_2 addition

Sample	Loading (wt%)	Max evolution temperature (°C)
Demineralized coal	0	-
KCH_3CO_2		490
		1020
KCH_3CO_2 - blends	1	-
	4	430
	5	440
	10	430

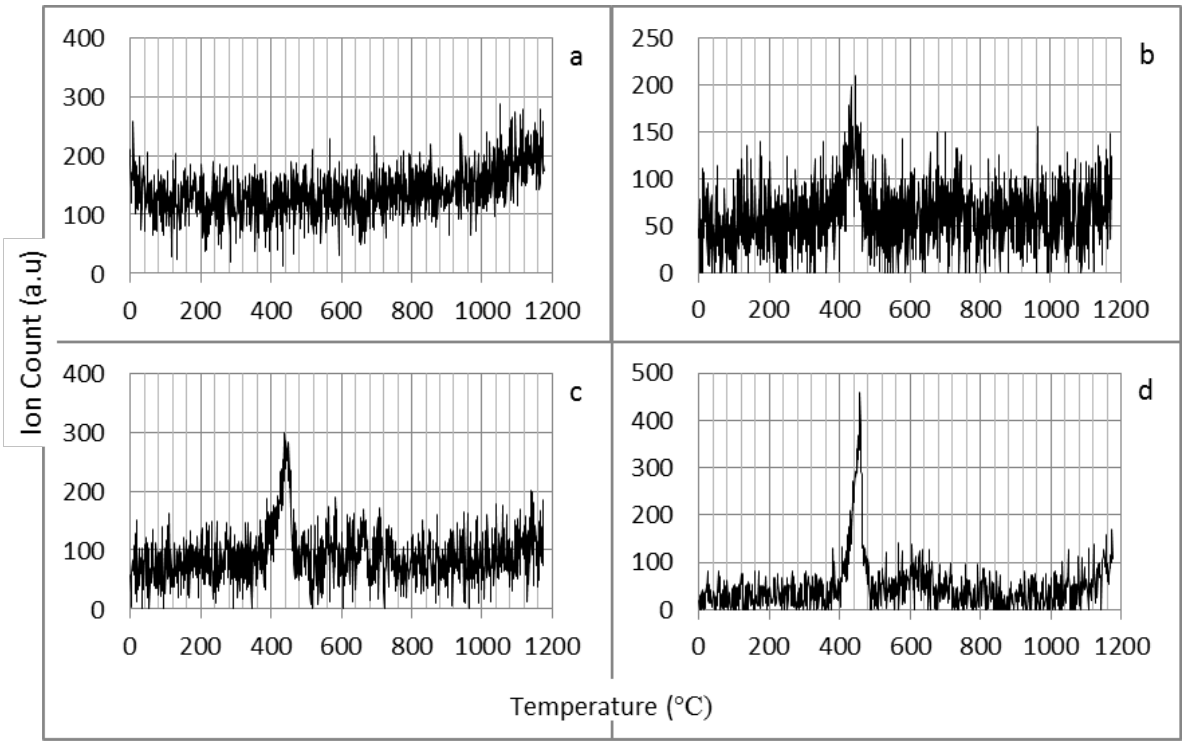

Figure 7.2.4.6: Mass spectra of CO_2 for the demineralized coal-alkali blended samples: a) 1% b) 4% c) 5% and d) 10% KCH_3CO_2 compound loading

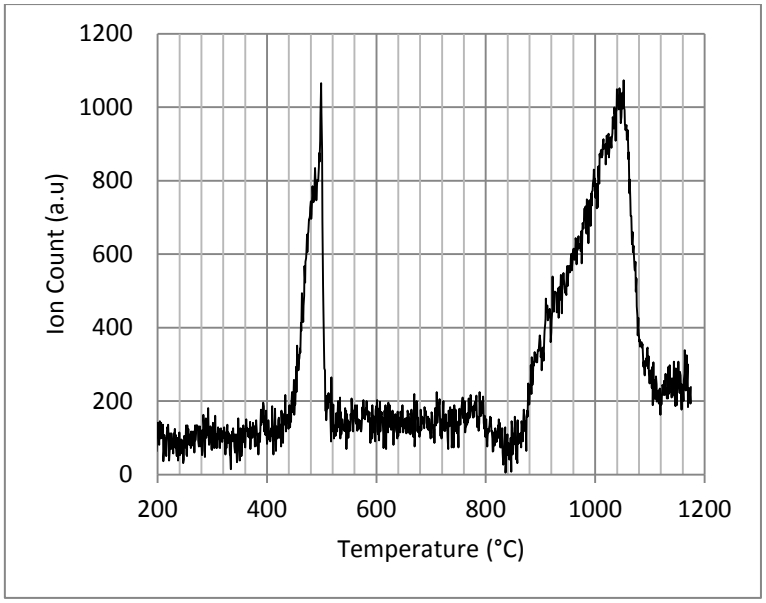

Figure 7.2.4.7: Mass spectra of CO_2 evolution for the KCH_3CO_2

During pyrolysis of the demineralized coal-alkali blended samples, a number of volatiles are evolved, some of which are not considered in this study. A number of these gaseous species has the same mass to ration (m/z) when passing through the mass spectrometer. For the mass ration of 16, other than CH_4, it is possible that the peak on the evolution profile may be partially due to oxygen being evolved as O_2 or H_2O. To determine whether the m/z 16 peak is due to the evolution of O_2/H_2O or CH_4, the CH_4 evolution profiles are compared to that of the CH_3 evolution profiles. After comparison of the profiles, it was found that the temperatures, at which evolution of CH_3 and CH_4 started for the samples, were the same. The maximum evolution temperatures of CH_3 and CH_4 for the different samples were also found to be the same when compared to one another. This indicates that if evolution of O_2/H_2O took place during the heat treatment in this temperature range, that the quantities were too low to influence the peaks observed at m/z 16. This confirms that the peaks observed at m/z 16 are as a result of CH_4 evolution.

From these MS results obtained for the different samples and gaseous species it can be seen that the alkali compounds had an influence on the H_2 (m/z 2) evolution. With the addition of the potassium compounds to the demineralized coal, a decrease in the maximum evolution temperature for H_2 was observed. The highest decreases were observed at maximum alkali compound loading for the KOH, K_2CO_3 and KCH_3CO_2 compounds. Percentage loading for KCl did not influence the temperatures. Thus the effects of the alkali compounds on the maximum evolution temperature are as follows: KCH_3CO_2 > K_2CO_3 > KOH > KCl. For the potassium compounds KOH and KCl, an increase in the onset temperature was observed after addition of the compound to the demineralized coal. K_2CO_3

had no influence on the onset temperature of H_2 and the addition of KCH_3CO_3 showed a decrease in the onset temperature.

The addition of the alkali compounds to the demineralized coal had no influence on the evolution of CH_3^+ or CH_4, m/z 15 and 16 respectively.

Evolution profiles for CO_2 (m/z 44) showed peaks for the blends with the addition of K_2CO_3 and KCH_3CO_2. These peaks may be attributed to the decomposition of the alkali compound and subsequently the evolution of CO_2. An increase in the peak can be seen with increasing alkali compound loading.

Chapter 8

Conclusions and Recommendations

In this chapter, the conclusions made on the experimental results in the previous chapters will be stated. Recommendations on further work will also be given.

8.1 Coal characterization

8.1.1 Demineralization of coal

Proximate analysis done on the parent coal, the demineralized coal and the char of these two samples revealed a high ash content for the parent coal and char (17.7%). Low ash content was found for the demineralized coal (0.6%) and the demineralized char (2.2%). XRF results revealed a decrease in the silica (SiO_2) and alumina (Al_2O_3) minerals after demineralization of the parent coal. These elements are removed during the HF leaching step. The XRD results of the parent and demineralized coal char indicated that quartz (2.5%) and some other minerals where present in the parent coal char. After demineralization only a small amount of quartz (0.2%) was found within the demineralized coal char sample. The CO_2 micropore surface areas increased after demineralization of the parent coal. Charring of the parent and demineralized coal samples decreased the micropore surface area. This decrease in the micropore surface area may be due to the collapsing of the pores during heat treatment of the samples.

Conclusion

- The low amounts of ash and clay minerals in the demineralized coal sample would suggest that the HCl-HF-HCl leaching process was successful in removal of minerals from the coal.

- The decrease in the silica and alumina oxides indicates that the HF leaching step successfully removes most of these compounds from the coal.

- Demineralization of the parent coal increased the CO_2 micropore surface area.

- Charring of the coal samples decreases the CO_2 micropore surface area.

8.1.2 Potassium additions

After the addition of the potassium compounds to the demineralized coal, the samples were submitted to heat treatment (charring). Proximate analysis showed (as expected) an increase in the ash content of the samples with the addition of the potassium compounds. From the XRF analyses an increase in the K_2O content was observed after charring the samples. XRD results indicate that a small percentage of the potassium compound was found in the crystalline structure of the coal, suggesting that not all of the compound decompose to form K_2O.

Conclusion

- The potassium compounds added to the coal decomposed to form K_2O.

- The formation of potassium crystalline structures within the coal formed after heat treatment of the samples with the alkali compound addition.

8.1.3 Free Swelling Indices

Free swelling experiments were done with five potassium compounds and five calcium compounds added to the various coal samples. The alkali compounds used in this study was chosen according to their effectiveness in decreasing the swelling behaviour. These experiments were performed on the raw coal and the demineralized coal with 5 K/Ca-wt% alkali compound additions. From the results obtained from these experiments, it was observed that the potassium compounds had a bigger influence on the swelling behaviour than the calcium compounds. The potassium compounds had swelling indices of 6.6, 8.5, 7.5, 4 and 7 for the compounds KOH, KCl, K_2CO_3, KCH_3CO_2 and $KHCO_2$ respectively,

whereas the calcium compounds had indices of 5, 8, 8, 7 and 8.5 for the compounds $Ca(OH)_2$, $CaCl_2$, $CaCO_3$, $Ca(CH_3CO_2)_2$ and $Ca(HCO_2)_2$ respectively.

Conclusion

- Potassium compounds were more effective in the reduction of swelling behaviour when using the dry mixing method. Decreasing order of effectiveness; KCH_3CO_2 > KOH > K_2CO_3 > $KHCO_2$ > KCl.

- Calcium compounds were less effective than the potassium compounds in reducing the swelling behaviour. The effectiveness of the calcium compounds to decrease influence the swelling behaviour in decreasing order; $Ca(OH)_2$ > $Ca(CH_3CO_2)_2$ > $CaCl_2$ = $CaCO_3$ > $Ca(HCO_2)_2$.

8.2 Thermomechanical analyses and Dilatometry

8.2.1 Thermomechanical analyses

Thermomechanical analysis was the first technique used to determine the influence of potassium compounds on the swelling behaviour of the coal samples used in this study. Data for the raw and demineralized coal samples could not be gathered as a result of their high swelling propensity. With the addition of the different potassium compounds to the demineralized coal, a decrease in the swelling behaviour was observed. The softening temperature and the temperatures at which maximum gaseous evolution takes place during TMA analyses depended on the potassium compound added to the demineralized coal. Compared to the other potassium compounds, KCl exhibited little influence on the swelling behaviour for the sample.

Conclusion

- The ion bound to the potassium influences the amount of swelling observed for the demineralized coal.

- The effectiveness of the potassium compounds to decrease the softening temperature of the samples and also decrease the temperature at which maximum swelling occurs is as follows: KCH_3CO_2 > K_2CO_3 > KOH > KCl.

8.2.2 Dilatometry

Dilatometry was a second technique used to determine the influence that the potassium compounds had on the swelling behaviour of the demineralized coal. From the results it was seen that demineralization decreased the swelling behaviour of the parent coal sample. Upon addition of potassium compounds to the demineralized coal, a further decrease in the swelling behaviour was observed for the samples. The blend with the added KCl showed the least influence on the swelling properties during the experiments. An increase in the softening temperature was observed after demineralization of the parent coal and the addition of the potassium compounds to the demineralized coal.

Conclusion

- Demineralization decreases the swelling behaviour of the coal and increases the softening temperature from 377°C to 397°C.

- Addition of potassium compounds to the demineralized coal decreased the swelling behaviour of the coal.

- Effectiveness of the potassium compounds in decreasing the softening temperature was as follows: $KCH_3CO_2 > K_2CO_3 > KOH > KCl$.

- Effectiveness of the potassium compounds to decrease the dilatation volume of the demineralized coal is as follows: $K_2CO_3 > KOH > KCH_3CO_2 > KCl$.

8.3 Thermogravimetric analyses and Mass Spectroscopy

8.3.1 Thermogravimetric analyses

Thermogravimetric analyses of the demineralized coal-alkali blends were used to determine the influence of the potassium compounds on the mass loss and relative reactivity of the demineralized coal. With the addition of the potassium compounds to the demineralized coal, the mass loss of the coal due to the addition of the potassium compounds were between 25-35%. This mass loss was determined on an alkali compound free basis. From the results it was found that with the addition of KOH, KCl and K_2CO_3 a decrease in the relative reactivity was observed. This decrease continued with an increase in the potassium compound loading. With the addition of KCH_3CO_2 to the demineralized coal, an increase in the relative reactivity was observed. This increase continues with an increase in the potassium compound loading. The increase in the relative reactivity may be due to

secondary gasification taking place within the sample due to the evolution of $(CH_3)_2CO$ (decomposition of KCH_3CO_2).

Conclusion

- Interactions between the alkali compounds and the demineralized coal caused a small increase in the coal mass loss during heat treatment.

- Potassium compounds showed an inhibiting effect on the relative reactivity of the demineralized coal in increasing order; KOH < K_2CO_3 < KCl.

- KCH_3CO_2 increased the relative reactivity of the demineralized coal. Increased compound loading to the coal increased the relative reactivity.

- The evolution of $(CH_3)_2CO$ may influence the relative reactivity of the sample.

8.3.2 Mass spectroscopy

Using a mass spectrometer coupled with a thermo gravimetric analyzer (TG-MS), the different mass fragments were identified. The gaseous species identified in this study were H_2, CH_3, CH_4 and CO_2 for the raw, demineralized and demineralized coal-alkali blends during the pyrolysis process. With the addition of the alkali compounds to the demineralized coal, a decrease in the temperature of maximum evolution for H_2 was observed. This change in temperature was also observed with increasing alkali compound loadings for the KOH, K_2CO_3 and KCH_3CO_2, with the highest decrease observed at maximum (10%) alkali compound loading. Evolution temperatures of CH_3 and CH_4 were not influenced by the addition or percentage loading of the alkali compounds. The evolution of CO_2 was only observed for the raw coal sample at high temperatures and the sample with the addition of K_2CO_3 and KCH_3CO_2 (as expected) for the potassium compounds.

Conclusion

- The alkali compounds (KOH, KCl, K_2CO_3 and KCH_3CO_2) have an influence on the maximum evolution temperature of H_2 during the pyrolysis process. The pyrolysis step wherein H_2 is formed thus seems to be catalyzed.

- Effectiveness of the alkali compounds to decrease the maximum evolution temperature of H_2 during heat treatment are as follows: KCH_3CO_2 > K_2CO_3 > KOH > KCl.

8.4 Conclusion for TG, TMA, Dilatometry and MS

Addition of KOH to the demineralized coal produced the following results:

- Decrease in relative reactivity;
- Decrease in swelling behaviour;
- And a decrease in the maximum evolution temperature of H_2.

Addition of KCl to the demineralized coal produced the following results:

- Decrease in relative reactivity;
- No influence on the swelling behaviour of the coal;
- And no influence on the maximum evolution temperature of H_2.

Addition of K_2CO_3 to the demineralized coal produced the following results:

- Decrease in the relative reactivity;
- Decrease in the swelling behaviour;
- And a decrease in the maximum evolution temperature of H_2.

Addition of KCH_3CO_2 to the demineralized coal produced the following results:

- Increase in relative reactivity;
- Decrease in the swelling behaviour;
- And decrease in the maximum evolution temperatures of H_2.

From these results it can be seen that KCl has no catalytic influence on the relative reactivity of demineralized coal and does not reduce the swelling behaviour of the coal. For the other potassium compounds (KOH, K_2CO_3 and KCH_3CO_2) a decrease in the swelling behaviour and maximum evolution temperature of H_2 was observed with the addition of the potassium compounds in the order as follows: $KCH_3CO_2 > K_2CO_3 > KOH$. The relative reactivity of the demineralized coal was decreased with the addition of KOH and K_2CO_3 to the coal, whereas the addition of KCH_3CO_2 increased the relative reactivity. This increase may be due to $(CH_3)_2CO$ present in the sample as the potassium compound decomposes during heat treatment.

Thus, KCH_3CO_2 was the best potassium compound from these investigated to use in reducing the swelling behaviour of the coal, while increasing the relative reactivity at the same time. KCH_3CO_2 also had a catalytic effect on the evolution temperature of H_2.

8.5 Recommendations

- Further investigations are needed into reactions taking place within the sample after addition of potassium acetate (KCH_3CO_2) to the demineralized coal. This may give insight into how the potassium compound influences the swelling behaviour and reactivity.

- The possible catalytic influence of the organic compound acetone may be investigated.

- Quantitative analyses on the volatiles evolved during heat treatment to determine how much of the volatiles released are as a result of potassium compound decomposition and/or evolution of functional groups from the coal.

- Investigation into the mechanisms controlling the swelling behaviour of a high swelling South African coal.

References

Adánez, J., de Diego, L.F. adn García-Labiano, F. Calcination of calcium acetate and calcium magnesium acetate: effect of the reacting atmosphere. Fuel. 1999, 78, 583-592.

Afzal, M., Ahmad, H. and Mahmood, F. Decomposition kinetics of Metal Acetates. Jour.Chem.Soc.Pak. 1991, 13, 219-222.

Alonso, M.J.G., Borrego, A.G., Alvarez, D. and Menéndez, R. Pyrolysis behaviour of pulverised coals at different temperatures. Fuel. 1999, 78, 1501-1513.

Amarasekera, G., Scarlett, M.J. and Mainwaring, D.E. Micropore size distributions and specific interactions in coals. Fuel. 1995, 74, 115-118.

American Society for Testing and Materials. ASTM D4326: 2012. Standard test for method for major and minor elements in coal and coke ash by x-ray fluorescence. ASTM International.

American Society for Testing and Materials. ASTM D5515 -97(2010)e1: 2010. Standard test method for determination of the swelling properties of bituminous coal using a dilatometer. ASTM International.

Audley, G.J. An evaluation of methods for enhancing the CO_2-reactivity of a caking bituminous coal. Fuel. 1987, 66, 1635-1641

Barriocanal, C., Díez, M.A., Alvarez, R. and Casal, M.D. On the relationship between coal plasticity and thermogravimetric analysis. Journal of Analytical and Applied Pyrolysis. 2003, 67, 23-40.

Basin, A.S., Kaplun, A.B., Meshalkin, A.B. and Uvarov, N.F. The LiCl-KCl Binary System (Physicochemical analysis of inorganic systems). Russian Journal of Inorganic Chemistry. 2008, 53, 1509-1511.

Bauer, H.H., Christian, G.D., O'Reilly, J.E. Instrumental analysis: Techniques and applications. Dordrecht: Kluwer Academic Publishers. 1978, 264p .

Bexley, K., Green, P.D. and Thomas, K.M. Interaction of mineral and inorganic compounds with coal. Fuel. 1986, 65, 47-53.

Bolat, E., Sağlam, S. and Pişkin, S. Chemical demineralization of a Turkish high ash bituminous coal. Fuel Processing Technology. 1998, 57, 93-99.

Bruno, G., Carvani, L. and Passoni G. Correlation between potassium losses and mineral matter composition in catalytic coal steam gasification. Fuel. 1986, 65, 1473-1475.

Formella, K., Leonhardt, P., Sulimma, A., van Heek, K.H. and Jüntgen, H. Interaction of mineral matter in coal with potassium during gasification. Fuel. 1986, 65, 1470-1472.

Gale, T.K., Bartholomew, C.H. and Fletcher, T.H. Decrease in the Swelling and Porosity of Bituminous Coals during Devolatilization at High Heating Rates. Chemical Engineering and Mechanical Engineering Departments, Advanced Combustion Engineering Research Centre. 1994, 94-100.

Green, P.D., Edwards, I.A.S., Marsh, H., Thomas, K.M. and Watson, R.F. Coal thermoplasticity and coke structure as related to gasification. Fuel. 1988, 67, 389-395.

Hang, T., Mathur, M.P., Narain, N.K., Smith, D.N. and Ruether, J.A. Explosive Comminution of Bituminous Coal Using Steam. Energy & Fuels. 1987, 1, 529-534

Jibril, B., Al-Maamari, R.S. and Al-Amri, I. Effects of potassium distributions in carbonizations of bituminous coal. J. Anal. Appl. Pyrolysis. 2009, 85, 529-533.

Jones, J.M., Kubacki, M., Kubica, K., Ross, A.B. and Williams, A. Devolatilisation characteristics of coal and biomass blends. J. Anal. Appl. Pyrolysis. 2005, 74, 502-511.

Khan, M.R.and Jenkins, R.G. Influence of added calcium compounds on swelling, plastic, and pyrolysis behaviour of coal devolatilized at elevated pressures. Fuel. 1986, 65, 1203-1208.

Khan, M.R. and Jenkins, R.G. Influence of K and Ca additives in combination on swelling, plastic and devolatilization properties of coal at elevated pressure. Fuel. 1989, 68, 1336-1030.

Khan, M.R. and Jenkins, R.G. Swelling and plastic properties of coal devolatilized at elevated pressures of H_2 and He. Fuel. 1986, 65, 1291-1299.

Köpsel, R. and Zabawski, H. Catalytic effects of ash components in low rank coal gasification. Fuel. 1990, 69, 275-281.

Lang, R.J. and Neavel, R.C. Behaviour of calcium as a steam gasification catalyst. Fuel. 1982, 61, 620-626.

Lehman, R.L., Gentry, J.S. and Glumac, N.G. Thermal stability of potassium carbonate near its melting point. Thermochimica Acta. 1998, 316, 1-9.

Leonard III, J.W. and Hardinge, B.C. Coal Preparation. Littleton, Colo: Society of Mining, Metallurgy, and Exploration, 1991; 59, 780, 881-883, 888, 898-899, 916, 933-934.

Liu, Q., Hu, H., Zhou, Q., Zhu, S. and Chen, G. Effect of inorganic matter on reactivity and kinetics of coal pyrolysis. Fuel. 2004, 83, 713-718.

Liu, Z. and Zhu, H. Steam gasification of coal char using alkali and alkaline-earth metal catalysts. Fuel. 1986, 65, 1334-1338.

McKee, D.W. Mechanisms of the alkali metal catalysed gasification of carbon. Fuel, 1983, 62, 170-175.

Moore, D.M. and Reynolds Jnr, R.C. X-ray diffraction and the identification and analysis of clay minerals. Oxford: New York. Oxford University Press, 1997; 249, 227-228.

Mulligan, M.J. and Thomas, K.M. Some aspects of the role of coal thermoplasticity and coke struture in coal gasification: The effect of rank, pitch and sodium carbonate on Brabender plastometry parameters. Fuel. 1987, 66, 1289-1298.

Nahas, N.C. Exxon catalytic coal gasification process. Fuel. 1983, 62, 239-241.

Nel, M.V. The influence of coal-associated trace elements on sintering and agglomeration of a model coal mineral mixture. University of North-West: Potchefstroom. RSA. (Dissertation-P.hD). 85 p.

Nishiyama, Y. Catalytic gasification of coals-Features and possibilities. Fuel Processing Technology. 1991, 29, 31-42.

Niu, Y., Tan, H., Wang, X. and Xu, T. Synergistic effect on co-pyrolysis of capsicum stalks and coal. African Journal of Biotechnology. 2011, 10, 174-179.

Oboirien, B.O., Engelbrecht, A.D., North, B.C., du Cann, V.M., Verryn, S. and Falcon, R. Study on the structure and gasification characteristics of selected South African bituminous coals in fluidised bed gasification. Fuel Processing Technology. 2011, 92, 735-742.

Ohtsuka, Y. and Tomita, A. Calcium catalysed steam gasification of Yallourn brown coal. Fuel. 1986, 65, 1653-1657.

Öztaş, N.A. and Yürüm, Y. Pyrolysis of Turkish Zonguldak bituminous coal. Part 1. Effect of mineral matter. Fuel. 2000, 79, 1221-1227.

Pan, W.P. and Serageldin, M.A. Structural characterization of lignite coal and char with $CaCl_2$. Fuel Processing Technology. 1987, 15, 397-409.

Radović, L.R., Walker Jr, P.L. and Jenkins, R.G. Catalytic coal gasification: use of calcium versus potassium. Fuel. 1984, 63, 1028-1030.

Radović, L.R., Walker Jr, P.L. and Jenkins, R.G. Effect of lignite pyrolysis conditions on calcium oxide dispersion and subsequent char reactivity. Fuel. 1983, 62, 209-212.

Radovic, L.R., Steczko, K., Walker Jr, P.L. and Jenkins, R.G. Combined effects of inorganic constituents and pyrolysis conditions on the gasification reactivity of coal chars. Fuel Processing Technology. 1985, 10, 311-326.

Rietveld, H.M. A Profile refinement method for nuclear and magnetic structure. Journal of applied crystallography 2. 1969, 65-71.

Samaras, P., Diamadopoulos, E. and Sakellaropoulos, G.P. The effect of mineral matter and pyrolysis conditions on the gasification of Greek lignite by carbon dioxide. Department of Chemical Engineering and Chemical Process Engineering Research Institute. 1996.

Schobert, H.H. Chemistry of fossil fuels and biofuels. Cambridge university press. 2013, 420-422.

Sentorun, C. and Kücükbyrak, S. The effect of mineral matter on the combustion characteristics of some Turkish lignite samples. Thermochimica Acta. 1996, 287, 139-147.

Seward, R.P. and Martin, K.E. The Melting Point of Potassium Hydroxide. J. Am. Chem. Soc. 1949, 71, 3564-3565.

Silverstein, R.M., Webster, F.X. and Kiemle, D.J. Spectrometric Identification of Organic compounds. John Wiley& Sons, Inc., 2005; 1-38.

Skoog, D.A., Holler, F.J. amd Crouch, S.R. Principles of Instrumental Analysis. Thomson books/cole. 1998; 309-318, 323-326, 439-443, 894-897, 900-905.

Slaghuis, J.H., Ferreira, L.C. and Judd, M.R. Volatile material in coal: effect of inherent mineral matter. Fuel. 1991, 70, 471-473.

Smith, K.L., Smoot, L.D., Fletcher, T.H. and Pugmire, R.J. The Structure and Reaction Processe of Coal. Plenum Press: New York and London, 1994; 169,

Sobolik, J.L., Ludlow, D.K and Hessevick, W.L. Parametric sensitivity comparison of the BET and Dubinin-Radushkevich models for determining char surface area by CO_2 adsorption. Fuel. 1992, 71, 1195-1202.

Solomon, P.R., Fletcher, T.H. and Pugmire, R.J. Progress in coal pyrolysis. Fuel. 1993, 72, 587-597.

Solomon, P.R., Serio, M.A., Despande, G.V. and Kroo, E. Cross-Linking Reactions during Coal Conversion. Energy & Fuels. 1990, 4, 42-54.

South African National Standards. ISO 540: 2008. Hard coal and coke – Determination of ash fusibility. South African Bureau of Standards.

South African National Standards. ISO 562:2010. Hard coal and coke – Determination of volatile matter. South African Bureau of Standards.

South African National Standards. ISO 29541: 2010. Solid mineral fuels – Determination of total carbon, hydrogen and nitrogen content. South African Bureau of Standards.

South African National Standards. ISO 1171:2010. Solid mineral fuels – Determination of ash. South African Bureau of Standards.

South African National Standards. ISO 19579: 2006. Solid mineral fuels – Determination of sulfur by IR spectrometry. South African Bureau of Standards.

South African National Standards. ISO 5925: 2007. Hard coal and coke – Determination of moisture. South African Bureau of Standards.

Speight, J.G. Handbook of Coal Analysis. John Wiley & Sons, Inc., Publication, 2005; 174-175 171, 145-152, 41-64, 67-79

Steel, K.M. and Patrick, J.W. The production of ultra clean coal by chemical demineralisation. Fule. 2001, 80, 2019-2023.

Stutzer, O. and Noé, A.C. Geology of coal. Chicago, Illinois: University of Chicago Press, 1940; 30-34, 15-17.

Suuberg, E.M., Lee, D. and Larsen, J.W. Temperature dependence of crosslinking processes in pyrolysing coals. Fuel. 1985, 64, 1668-1671.

Tamhankar, S.S., Sears, J.T. and Wen, C. Coal pyrolysis at high temperatures and pressures. Fuel. 1984, 63, 1230-1235.

Tomeczek, J. and Palugniok, H. Kinetics of mineral matter transformation during coal combustion. Fuel. 2002, 81, 1251-1258.

Van Heek, K.H. and Mühlen, H.J. Effect of coal and char properties on gasification. Fuel Processing Technology. 1987, 15, 113-133.

Van Krevelen, D.W. and Schuyer, J. Coal Science: Aspects of coal constitution. Amsterdam: Elsevier, 1957; 130-134.

Van Niekerk, D., Pugmire, R.J., Solum, M.S., Painter, P.C. and Mathews, J.P. Structural characterization of vitrinite-rich and inertinite-rich Permian-aged South African bituminous coals. International Journal of Coal Geology. 2008, 76, 290-300.

Veraa, M.J. and Bell, A.T. Effect of alkali metal catalysts on gasification of coal char. Fuel. 1978, 57, 194-200.

Wang, J., Yao, Y., Cao, J. and Jiang, M. Enhanced catalysis of K_2CO_3 for steam gasification of coal char by using $Ca(OH)_2$ in char preparation. Fuel. 2010, 89, 310-317.

Ward, C.R. Analysis and significance of mineral matter in coal seams. International Journal of Coal Geology. 2002, 50, 135-168.

Waugh, A.B. Removal of mineral matter from bituminous coals by aqueous chemical leaching. Fuel Processing Technology. 1984, 9, 217-233.

Wood, B.J., Fleming, R.H. and Wise, H. Reactive intermediate in the alkali-carbonate-catalysed gasification of coal char. Fuel. 1984, 63, 1600-1603.

Yu, J., Lucas, J.A. and Wall, T.F. Formation of the structure of chars during devolatilization of pulverized coal and its thermoproperties: A review. Progress in Energy and Combustion Sciences. 2007, 33, 135-170.

Yuh, S.J. and Wolf, E.E. FTIR studies of potassium catalyst-treated gasified coal chars and carbons. Fuel. 1983, 62, 252-255.

[WEB 1] http://www.wou.edu/las/physci/GS361/Fossil%20fuels/Coal.htm
Date of access: 7 November 2012.
[WEB 2] http://www.nuance.northwestern.edu/KeckII/Instruments/FT-IR/keck-ii%20pages2.html
Date of access 7November 2012
[WEB 3] www.anasys.co.uk/library/tmal/htm
Date of access: 7 November 2012